GAIN-SCHEDULED AIR PATH SYSTEM CONTROL AND COMPRESSOR AIR MASS FLOW ESTIMATION IN DIESEL ENGINES

by

ERCAN ATAM

B.S., Mechanical Engineering, Boğaziçi University, 2002

M.S., Mechanical Engineering, Boğaziçi University, 2005

Submitted to the Institute for Graduate Studies in
Science and Engineering in partial fulfillment of
the requirements for the degree of
Doctor of Philosophy

Graduate Program in Mechanical Engineering
Boğaziçi University

2010

GAIN-SCHEDULED AIR PATH SYSTEM CONTROL AND COMPRESSOR AIR MASS FLOW ESTIMATION IN DIESEL ENGINES

APPROVED BY:

Prof. İ. Emre Köse (Thesis Supervisor)	.....
Assoc. Prof. Hasan Bedir	.....
Prof. Eşref Eşkinat	.....
Prof. Levent Güvenç	.....
Assoc. Prof. Hilmi Luş	.....

DATE OF APPROVAL: 31.05.2010

Dün sabaha karşı kendimle konuştum,

Ben hep kendime çıkan bir yokuştum,

Yokuşun başında bir düşman vardı,

Onu vurmaya gittim, kendimle vuruştum...

(*Ö. A.*)

This thesis is dedicated to the great poet Özdemir Asaf...

ACKNOWLEDGEMENTS

This is the most emotional part of this thesis. After five years of this walk alone, I came to the finish line, eventually. Honestly speaking, it was not easy for me to complete this study. When I look back, sometimes I think that I was lucky that I was able to complete it. God, surely, helped me: otherwise it would not be possible!

The most dominant thank goes to myself!!!. This may seem strange but really, I thank to myself. I am the only one who knows the frustrations, hard times, upsets, hopes and nice moments that I had during this period. Therefore, I am my best friend and the first acknowledgements go to that man.

I am indebt to my family for their endless support during my all education. I will always remember their *"anadolu-type motivations"*. For example, their recent motivating words: "oğlum zorsa, olmuyorsa o kadar uğraşma, kafa yorma, bırak gitsin..." :))

I thank to my Ph.D. advisor Prof. İ. Emre Köse for introducing me to this LPV topic, for his all excellent control lectures, for giving me free time during this study and for many other things I have learned from him. He is very intelligent and in my opinion, he is among the best theoretical control engineers in the Europe. It is a big chance that the mechanical engineering of Boğaziçi university has such a professor.

I thank to Assoc. Prof. Hasan Bedir for being a nice, positive person, for inviting me to his lecture on internal combustion engines and for attending, carefully listening to my progress reports and for always being willing to help.

I thank to Prof. Eşref Eşkinat for participating in my thesis committee and for his nice undergraduate and graduate vibration courses.

I thank to Prof. Levent Güvenç for participating in my thesis committee and providing me a 1 year-scholarship at AUTOCOM center of İstanbul Technical university.

I thank to Assoc. Prof. Hilmi Luş for participating in my thesis committee and for his interesting system identification course that I took in the first year of my Ph.D. study. I have learned many things on system identification by this course.

I thank to all faculty members of mathematics department, especially to Prof. Nilgün Işık for her encouragement "Ercan bitiyor mu, sana ne zaman Dr. Ercan diyecegiz?" and to Prof. Alp Eden for asking me about my Ph.D. thesis when he comes across me . They allowed me to be a research assistant there for many years by which I have learned a lot of mathematics! I also thank my assistant friends during this period, especially to Murat Sağlam, İlker Arslan and Cihan Pehlivan.

I thank to Assist. Prof. Ali Ecder for being a nice person, for being a nice advisor of graduate students, for always helping me when I needed.

I thank to Prof. Kuban Altınel for being a real scientist, always sharing his knowledge with his students and giving incredible optimization lectures of !4! hours per week. In his lectures, he does not only teach optimization but also combines with philosophy. For example, a quotation from him during an e-mail communication: "Ben IE 303'ün başında optimizasyon yaşamdır derim. Gerçekten de sonlu bir zaman aralığını local maximumdan, local maximuma atlayarak globali arayarak geçiririz. Bir ömür globali bulamadan bitebilir. Bazen de buluruz ve local sanıp daha iyisini ararken yitiririz..."

I thank to Assoc. Prof. Yağmur Denizhan for her wonderful nonlinear control course and chaos seminars. She is a perfect scientist and is not just a professor but also a real friend to her students.

I thank to Assist. Prof. Giles Hooker for the academic discussions and collaborations. He is a very gentle person.

Next, I thank to my dear friend Gökhan Tekeli for being a nice friend and for doing nice academic discussions. I should thank to Halil Başẗurk for writing a nice thesis on application of LPV-control theory.

I thank to Assoc. Prof. Leo Liberti for the communications and discussions I had with and for one of his supporting e-mails during one of my bad times. He is not just a big scientist but also a big nice person!

I must not forget to thank to Gamze Can for being a nice friend and the helps she provided. She has a great emotional intelligence.

I thank to Zeynep Şeref for her short, nice lectures on mechanics of materials during Ph.D. qualification examination preparation. She was really an expert on this topic!

Lastly, but not least, I thank to Assist. Prof. Gülay Öke, Dr. Urs Christen, Dr. Umut Genç and Dr. Pietro Belotti.

...And thanks Boğaziçi university! We were together for a very long time (1996-2010). Time is already up and I have to go...

ABSTRACT

GAIN-SCHEDULED AIR PATH SYSTEM CONTROL AND COMPRESSOR AIR MASS FLOW ESTIMATION IN DIESEL ENGINES

In this dissertation, we deal with the independent problems of air path system control and compressor air mass flow estimation in diesel engines. In this regard, the thesis can be divided into two main parts: control and estimation.

In the first part, control part, we consider regulation of the air path system in diesel engines. To that end, an extensively used mean-value engine model in the literature is considered. The underlying nonlinear model is converted into a rational linear parameter-varying (LPV) form and a gain scheduled control approach is used. The main contribution here is that the commonly used simplifying assumptions in the literature (like constant engine speed, use of engine charts, assuming exhaust manifold pressure to be equal to intake manifold pressure plus some constant value, taking constant manifold temperatures, etc.) are avoided and a better engine model with a better subsequent controller design are achieved. As a result, the control system design is covering a wide range of engine operating points.

In the estimation part, we present two different estimation approaches, each having advantages over the other. In the first approach, we develop a general deterministic state estimation method for states appearing linearly in nonlinear systems. The estimation method is based on representation of input-output pairs by a linear moving model and the use of recursive-least squares with an adaptive forgetting factor. The method is on-line applicable and very easy to apply. It is shown that the developed estimation method outperforms the popular extended kalman filter (EKF) method on some case studies. Next, the developed estimation method is used for a diesel engine

model to estimate compressor air mass flow, whose measurement is difficult or unreliable in some situations and therefore its estimation is important in these cases. Again, a comparison with EKF shows the advantage of the developed method.

The second estimation method is based on the use of a state estimation method for affine parameter-dependent linear systems. To use this method, the underlying nonlinear engine model is first transformed into an affine parameter-dependent form and then the method is used. This approach has the advantage of having an asymptotic convergence nature, when compared to the first one. Again, this method is used for compressor air mass flow estimation and the results are compared with those of EKF to demonstrate the superiority of the approach.

ÖZET

DİZEL MOTORLARDA KAZANÇ AYARLAMALI HAVA YOLU SİSTEMİ KONTROLÜ VE KOMPRESÖR HAVA KÜTLESİ KESTİRMESİ

Bu tezde dizel motorlarda hava yolu sistemi kontrolü ve kompresör hava kütlesi kestirmesi problemleriyle uğraştk. Bu anlamda, tez çalışması iki ana kısma ayrılabilir: kontrol ve kestirme.

İlk kısımda, kontrol kısmında, dizel motorlarda hava yolunun düzenlenmesini ele aldık. Bunun için, literatürde sıkça kullanılan ortalama-değerli bir dizel motor modelini kullandık. İlgili model ilk önce doğrusal parametre değişken (DPD) formuna koyuldu ve sonra kazanç ayarlamalı kontrol metodu uygulandı. Bu çalışmanın katkısı şudur: literatürde hava yolu kontrolü yapılırken genelde kolaylaştırıcı varsayımlar yapılmaktadır: örneğin, motor hızının sabit alınması, dizel motor tablolarının kullanımı, egzoz basıncının giriş basıncı artı sabit bir değer olarak kabul edilmesi, manifold sıcaklıklarının sabit alınması, vesaire. Burada bu tür basitleştirici varsayımlardan kaçınılmıştır ve dolayısıyla daha doğru bir motor modeli ve daha geniş operasyonel noktalarda çalışacak kontrol algoritması elde edilmiştir.

Kestirme kısmında iki farklı yöntem sunduk. Karşılıklı olarak düşünüldüklerinde bu iki yöntemin birbirleri üzerinde avantajları mevcuttur. İlk metod, deterministik, doğrusal olmayan diferansiyel denklemlerde doğrusal gözüken durumların kestirilmesi için geliştirilen genel bir metotdur. Metodun dayandığı mantık ölçülebilen durumlardan ve sistem girdilerinden hareketle zamanla hareket eden bir doğrusal modelin saptanması ve model saptanmasında adaptif unutma faktörlü rekursif en küçük kareler yönteminin kullanılmasıdır. Bu metodun temel özelliği çevirimiçi uygulanabilmesi ve uygulama kolaylığı olmasıdır. Akademik-amaçlı oluşturulan örnekler üzerinde metot

ugulandı ve sonuçlar popüler genişletilmiş Kalman filtresi (GKF) ile karşılaştırıldı. Bu karşılaştırmalardan geliştirilen metodun daha iyi sonuç verdiği gözlendi. Daha sonra metot dizel motorlarda bazı durumlarda ölçüm almanın zor olduğu ya da ölçümlere güvenilemediğinde kompresor hava kütlesinin kestirilmesine uygulandı. Tekrar sonuçlar GKF ile karşılaştırıldı ve geliştirilen metodun avantajı görüldü.

İkinci kestirme metodu, ilgin parametre-bağımlı sistemlerde durum kestirmesi için geliştirilmiş olan yöntemi uygulamaya dayanır. Bu yöntemi kullanabilmek için önce varolan doğrusal olmayan dizel motor modeli ilgin parametre-bağımlı forma dönüştürüldü. Bu yöntemin ilk yönteme göre temel avantajı sonuşur yakınsamalı olmasıdır. Bu metot da kompresör hava kütlesinin kestirilmesinde kullanıldı ve yöntemin üstünlüğünü göstermek için kestirme sonuçları GKF ile karşılaştırıldı.

TABLE OF CONTENTS

LIST OF FIGURES

LIST OF TABLES

LIST OF SYMBOLS/ABBREVIATIONS

$A, \mathcal{A}$	State matrices
A_r	Effective exhaust gas recirculation area
$B, \mathcal{B}$	General input matrices
$B_u, \mathcal{B}_u, B_w, \mathcal{B}_w$	Manipulated input and disturbance input matrices
$C, \mathcal{C}$	General output matrices
$C_y, \mathcal{C}_y, C_z, \mathcal{C}_z, C_q, \mathcal{C}_q$	Output matrices
c_p	Specific heat at constant pressure
c_v	Specific heat at constant volume
$D, \mathcal{D}$	Direct feedthrough matrices
G	Nominal plant
K	Controller
N	Engine speed
N_t	Turbocharger speed
P_c	Compressor power
P_t	Turbine power
p_a	Ambient pressure
p_i	Intake manifold pressure
p_{ref}	Reference pressure
p_x	Exhaust manifold pressure
R	Gas constant
T_a	Ambient temperature
T_i	Intake manifold temperature
T_{ref}	Reference temperature
T_x	Exhaust manifold temperature
t	Time
t_s	Sampling period
u	Control input
$\tilde{u}$	Modified control input
V_d	Displacement volume

V_i	Intake manifold volume
V_x	Exhaust manifold volume
v	Process noise
W	Controller design weight
W_{ab}	Air mass flow from location a to location b
W_f	Engine fuel flow rate
w	System disturbance or measurement noise
X, X_{cl}	Lyapunov matrices
x	System state vector
x_c	Controller state vector
x_m	Measured part of the system state vector
x_r	Exhaust gas recirculation valve position
x_{um}	Unmeasured part of the system state vector
x_v	Turbine vane position
Y, Y_{cl}	Inverses of X, X_{cl}, respectively
y	Measured output
z	Controlled output
γ	Constant related to specific heats or $\mathcal{L}_2$-gain
Δ	A specific perturbation block
$\mathbf{\Delta}$	Set of perturbation blocks
Δ_c	Controller scheduling block
η_c, η_t, η_v	Compressor, turbine and volumetric efficiencies
θ	Parameter matrix
μ	Constant related to specific heats
ρ	Time-varying parameter
τ	Turbo lag constant
AFR	Air Fuel Ratio
ANNs	Artificial Neural Networks
AQS	Affine Quadratic Stability

AW	Anti-Windup
ECU	Engine Control Unit
EGR	Exhaust Gas Recirculation
EKF	Extended Kalman Filter
INTLAB	Interval Laboratory
LFR	Linear Fractional Representation
LMI	Linear Matrix Inequality
LPV	Linear Parameter-Varying
LTI	Linear Time-Invariant
NEDC	New European Drive Cycle
PID	Proportional Integral Derivative
PM	Particulate matter
VGT	Variable Geometry Turbine

1. INTRODUCTION AND LITERATURE SURVEY

Internal combustion engines were developed in the late 1800s and, after that time, they became the dominant prime mover technology in the transportation field. In the early years of 1900, most of the automobiles were steam or electrically powered but by 1920, the powering mechanism was replaced by gasoline engines. At the beginning of 2000, almost all motor vehicles were powered by internal combustion engines [1]. Diesel engines are one type of internal combustion engines, which were invented by Rudolf Diesel between 1893-1897 at Augsburg, Germany and become very popular in recent years thanks to their better fuel economy, higher power characteristics and their durability and environmental advantages. These positive facets led to an increasing penetration of diesel engines in the automotive market, for example as seen in Figure 1 for Western Europe. Diesel engines, as all engineering systems, have pros and cons

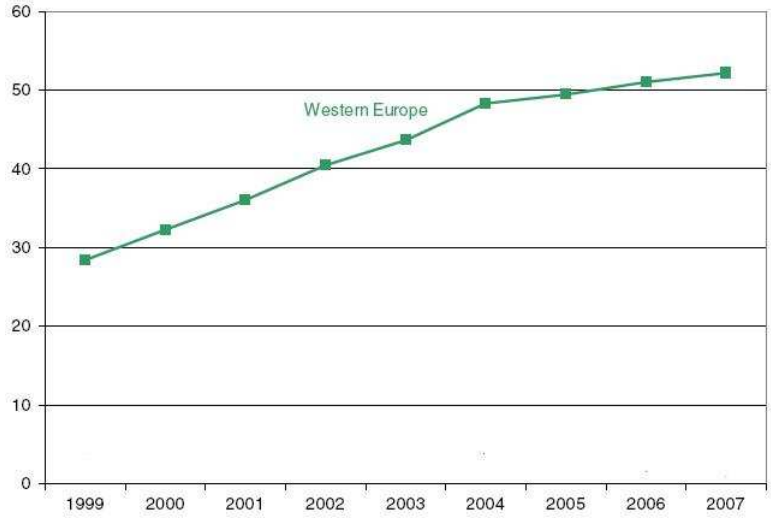

Figure 1.1. Diesel engine market share in Western European market [2]

when compared to their competitors and/or alternatives. Next, we considers these issues.

1.1. Advantages of Diesel Engines

The main factors making diesel engines so popular in automotive industry may be summarized as follows.

- Better fuel economy: This is the most distinguishing property of diesel engines making them superior over gasoline engines. When a light-duty diesel and a gasoline engine of similar power are compared, it is seen that diesel engine consume 30-60 % less fuel, where the percentage changes from the type of vehicle and operating conditions [3]. This better fuel efficiency aspect of diesel engine stems from the high compression ratios and the rich content of diesel fuel. The efficiency of gasoline engines is typically around 25 % while diesel engines can convert over 30 % of the chemical fuel energy into mechanical energy [4]. In terms of fuel cost that means 3 liter per 100 km.
- Higher power rate: For the same speed, the torque production of diesel engines is substantially higher than that of a gasoline engine of the same size. This is due to the high compression ratios during the combustion process. As an example, the Volkswagen 1.9 liter TDI diesel equipped in Jetta with compression ratio 19.5:1 can develop a torque of 114Nm @1900 rpm. On the other hand, the 2.0 liter gasoline engine powered Jetta with compression ratio 10:1 is able to generate only a torque of 89 Nm at a much higher speed of 2600 rmp [3].
- Durability and environmental advantages: The life of a diesel engine is almost twice as that of a gasoline engine due to the increased strength of the parts used, the better lubrication property of the diesel fuel, etc. In a diesel engine, boost pressure is limited only by the strength of the engine components, not by predetonation of the fuel charge as in gasoline engines. Diesel engines have the advantages of lower CO_2, CO and hydrocarbon emissions.

1.2. Disadvantages of Diesel Engines

Although diesel engines have the above advantages, their disadvantages should also be mentioned. A list of disadvantages of diesel engines can be as follows.

- High rate of PM and NO_x emission: The diesel engine particulate matter (PM) is a combustion-generated soot which is a complex chemical structure including many inorganic materials, lubricants, sulfates. These harmful products are of increasing concern as they are small, often less than 2.5 microns in size and are

responsible for a variety of lung related illnesses including asthma, emphysema and bronchitis. The amount of these particulate matter is depended on factors as amount of available oxygen during combustion process, spray formation and oxidation conditions towards the end of the combustion process [5]. On the other hand, oxides of nitrogen (NO_x) are formed when a mix of nitrogen and oxygen is subjected to high temperatures. Emissions of harmful oxides of nitrogen are reduced by recirculating a portion of the exhaust gas back to the intake manifold and this process is known as exhaust gas recirculation. Intermixing the incoming air with recirculated exhaust gas dilutes the mixture with inert gas, lowering the adiabatic flame temperature and reducing the amount of excess oxygen. The exhaust gas also increases the specific heat capacity of the mixture, lowering the peak combustion temperature. Because NO_x formation progresses much faster at high temperatures, EGR serves to limit the generation of NO_x. Legislations are increasing day by day the demands on the lower emissions from the internal combustion engines. Figure 1.2 shows the imposed regulations by European Union and U.S. It is expected that the upcoming standards be more stringent. Therefore, it is necessary to make important technological progress to satisfy these requirements. PM and NO_x minimization requires advanced control

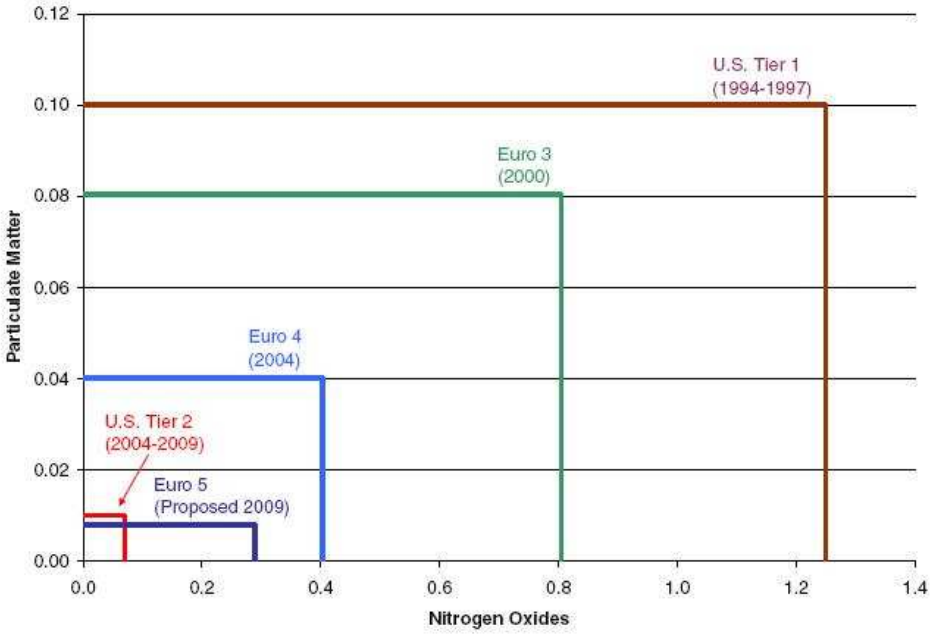

Figure 1.2. Diesel vehicle emissions standards for NO_x and PM in the U.S. and Western Europe (grams per mile) [6, 7, 8]

structures to regulate the air path system and the after-traetment technologies (like PM filters and Selective Catalytic Reduction).

- Vibration and noise problems: Diesel engines are much noisier and tend to vibrate.
- Other disadvantages: They are harder to start in cold weather. In general, many local repair shops either do not have the service personnel or the diesel engine parts. Moreover, diesel engine repair costs more than gasoline engine.

1.3. Turbocharging and EGR

A turbocharged diesel engine with exhaust gas recirculation (EGR) is shown schematically in Figure 1.3. The subscripts "a", "c", "i","e" and "x" are used to represent ambient, compressor, intake manifold, engine cylinder and exhaust manifold locations, respectively. The main function of turbocharging is to use the energy of the exhaust gas and convert it to the mechanical work by passing the gas through the blades of a turbine. The turbine drives a compressor which increases the density of the incoming air, which in turn results in a larger torque output compared to non-turbocharged engines. The power generation of the turbine is increased by turbocharg-

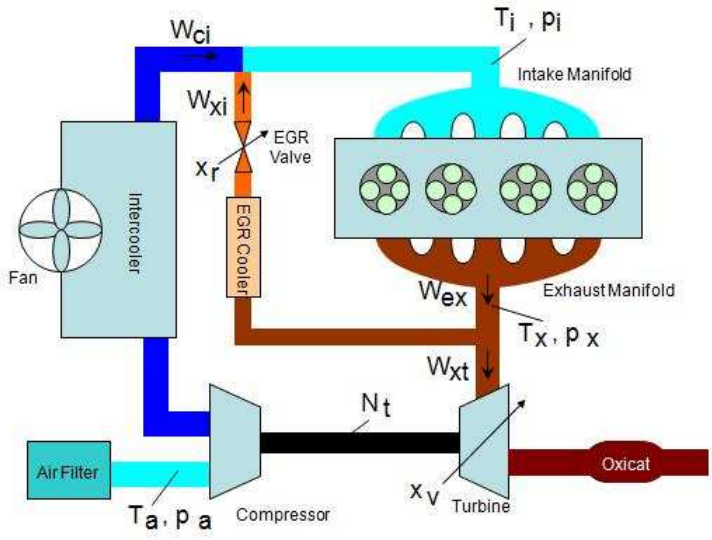

Figure 1.3. Diesel engine flow diagram

ing and it is directly related to exhaust gas pressure-temperature and the amount of flow through turbine blades. In general, in turbocharging a variable geometry turbine

(VGT) technology (Figure 1.4) is used, where the turbo uses little variable vanes to control exhaust flow passing through turbine blades. The vane angles are adjusted by an actuator. The changes in the inlet vane positions can change the power generated by the turbine and hence the transfer of power to the compressor, which in turn affect the power generated by the engine. Emissions of NO_x are reduced by EGR as mentioned

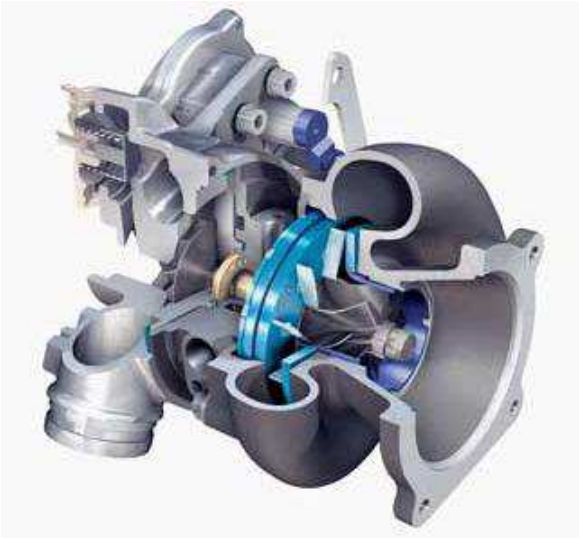

Figure 1.4. VGT [9]

before. As EGR action results in a high level of burned gas fraction, this leads to low in cylinder air to fuel ratio, AFR, and consequently unacceptable smoke generation as Figure 1.5 demonstrates. The negative effect of EGR is from two sides. Firstly, burned gas fraction from the EGR valve replaces some fresh air from the intake manifold and consequently decreases the fresh air mass flows into the cylinders. Secondly, a fraction of the exhaust gas that can be used by the turbine is diverted through the EGR valve to the intake manifold, reducing the turbine power and consequently the flow delivered to the intake manifold through the compressor. As a result, there is an inverse relation between reduction of smoke and NO_x and, therefore, most of the time an optimal AFR is sought to set a compromise between these two harmful products [10].

1.4. Modeling-Identification and Control Problems in Diesel Engines

Modeling and control of diesel engines is a substantial task. The related models can be physics-based or identification-based. The physics-based mean-value models

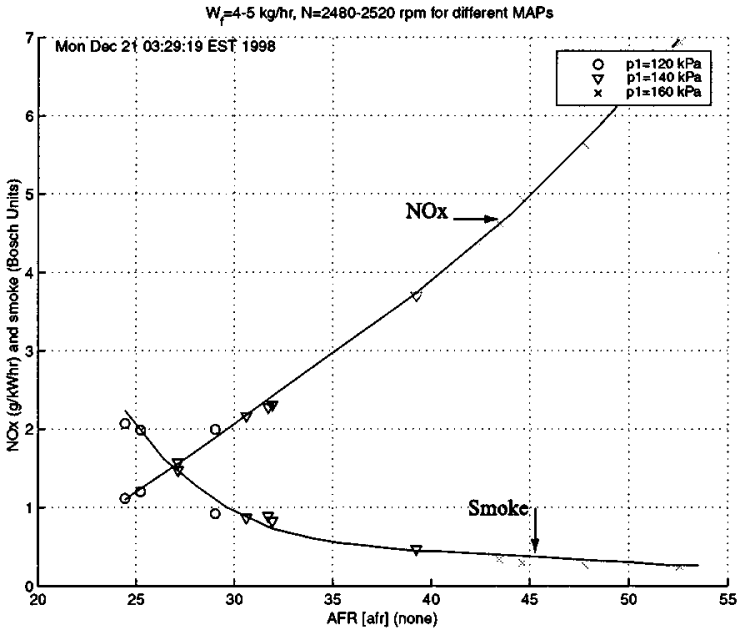

Figure 1.5. NO_x and Smoke versus AFR [10]

are very complicated and contain many tuning parameters to be estimated. A control strategy using these complicated models is not readily available and requires a remarkable effort. On the other hand, linear mean-value models and the associated linear control are not satisfactory for engine control due to the high nonlinearity and availability of feedback interactions between engine components. Therefore, model based control necessities two things at the same time: control oriented modeling of the engine, where the underlying model accurately reflects the engine dynamics, and synthesis of an advanced control strategy for the associated control oriented model.

For the emission control, in particular NO_x control, of diesel engines, the EGR-rate should be controlled. To meet the specified operation requirements, boost pressure or exhaust manifold pressure is, also, controlled. The control of EGR-rate can be achieved by directly controlling EGR air mass flow or indirectly by regulating compressor flow using the VGT-vane and EGR-valve positions.

In general, current production type controllers used in the engine control unit (ECU) try to achieve the above objectives by simple gain scheduled siso-PI(D) controllers or in some cases incorporating feed forward control based on engine maps. The

control strategy is, also, synthesized in a decentralized fashion: EGR-valve and VGT-vane positions are controlled by different, independent controllers. In order to cope with the nonlinearities and to satisfy the required objectives, gains must be scheduled over the entire operation range (over entire speed-load regime). This brings an immense calibration effort and control design is time consuming. In addition, scheduled PI(D) controllers may not be able to satisfy the required objectives since a decentralized control design strategy lacks the coordination between the manipulated inputs. Even, as well-known in the literature, there is no stability guarantee with gain scheduling of designed simple controllers for operating intervals.

In order to reduce both the calibration effort and synthesize controllers with satisfactory performance, advanced modeling-identification and control approaches are required. The next subsections are categorized surveys of the main modeling-identification and control works in the literature generally with a purpose to reduce, model or control harmful emissions from diesel engines.

1.4.1. Neural Networks Based Modeling-Identification and Control

Artificial neural networks (ANNs) have learning capabilities, they bring important benefits by suppressing theoretical difficulties that appear when applying classical techniques to complex systems and they are very flexible with universal approximation capabilities. All these make them a prime candidate tool for many engineering applications including diesel engine modeling-identification and control. In recent years, some researchers used ANNs methods to model, identify and control the internal combustion engine characteristics. For example, in [11] Yuanwang *et al.* analyzed the effect of cetane number on exhaust emissions from engine, in [12] Durna *et al.* studied the effect of specific fatty acid methyl esters present in biofuels on particulate matter emissions, in [13] Lucas *et al.* modeled diesel particulate emission, in [14] Hafner *et al.* designed a diesel engine control system, in [15] Tan and Saif modeled the intake manifold and throttle body processes in an automotive engine, in [16] Roskilly *et al.* on-line modeled and identified a turbocharged medium-speed diesel engine, all using ANNs.

1.4.2. Nonlinear Modeling and Control

Nonlinear modeling and control applications in diesel engines are numerous. The underlying physics in diesel engines naturally brings out nonlinear models. The main difficulty raises in designing nonlinear controllers for the corresponding nonlinear engine models. Nonlinear approaches offer the potential of better coping with the nonlinearities present in diesel engines. The approach of Kao M. and Moskwa J.J in [17] proposes sliding-modes controllers for speed control problem. Several controller classes are considered and compared in this paper using simulations. Feed-forward was proved to be beneficial when a fast transient response is considered and a sliding mode controller is designed to include such a feature. In terms of minimal mean speed error, the best controller is proven to be the sliding mode controller with integral action and gain adaptation. In [10], Stefanopoulou *et al.* considered a direct injected, turbocharged diesel engine with EGR. The objective is to satisfy three conditions; operate the engine with a controller such that driver's torque demand are satisfied, NO_x emissions are minimized and visible smoke creation is avoided. In this study, it is demonstrated that the steady-state optimization of engine emissions results in operating points where EGR and VGT actuators are in effect redundant in their effect on the variables that most directly affect the emissions. To account for the actuator redundancy, a multivariable nonlinear feedback controller based on gain scheduling of linear controllers is proposed and coordination of the two actuators to fully utilize their joint effect on engine emission performance is achieved. In [18], Rajamani considered a turbocharged diesel engine with EGR and VGT . The paper has the same objectives as those of [10]. A feedback linearization approach is used to set AFR and burned gas fraction in the intake manifold to desired values in the presence of variable operating points. Since practically neither of these variables can be measured, an observer based on flow and pressure sensor measurements is developed for their real time estimations.

Lino P. *et al.* in [19] presents a control oriented model and a nonlinear control design for a common rail injection system. First a model is developed, which is tuned in a virtual simulation environment, representing the injection system in details in a reliable replication of reality. Then, a sliding mode control is developed. Both

the model of the injection process and of the control law are validated by a virtual detailed simulation environment. Plianos A. *et al.* in [20] used an optimal nonlinear control strategy based on the analytic solution of a performance index to derive a controller for the diesel engine air path system. The objective of control is to achieve tracking of suitable references (corresponding to low emissions) for the AFR and the fraction of the recirculated exhaust gas. The considered diesel engine is a medium duty Caterpillar 3126B with six cylinders equipped with a variable geometry turbocharger and an exhaust gas recirculation valve. The proposed controller is designed on the reduced third-order mean-value model and implemented as a closed-form nonlinear model predictive control law on the full order model. In order to eliminate steady state offset, integral action is introduced.

1.4.3. Linear Parameter-Varying Based Modeling-Identification and Control

Linear parameter-varying (LPV) models are linear dynamical systems which include external priori unknown but real time measurable parameter(s). If the state is a parameter, then the corresponding model is called a quasi-LPV model. LPV models with the associated LPV control theory will be described in detail in Chapter 2. Mainly, LPV models can be constructed in two ways: identification of an LPV-structure model and first-principles-based LPV models. In the second method, most of the time, the resulting LPV models are of quasi-LPV nature and there is no approximation involved when going from the (simplified) nonlinear model to the quasi-LPV model, i.e. it is just a reformulation. Next, we will list the related work on diesel engines using the mentioned methods.

The recent work of Wei and Re [21] uses physically motivated subsystem models suited for the intake manifold pressure dynamics, exhaust manifold pressure dynamics and the air mass flow dynamics. LPV identification techniques are used to estimate their parameters. A final quasi-LPV model based on the combination of three submodels is determined and used for the controller synthesis to control the air path system.

In fact, in literature, to our knowledge, there are just two studies on control oriented LPV modeling of diesel engines. Song and Grigoriadis in [22] regulated engine speed where a model based LPV approach is applied to address the variable operating conditions of the engine. The closed-loop system has the required stability and optimized load torque rejection performance in the presence of variable transport delays and fuel saturation constraints. Jung and Glover in [23] present a gain scheduled approach using a reduced-order, mean-value diesel engine model to reduce calibration effort which is a significant task encountered in automotive industry. The engine model is put in a quasi-LPV form and scheduling variable is the intake manifold pressure. In addition, a second parameter is introduced to adjust the gain of the controller and hence rendering the controller calibratable. Set points for intake manifold pressure and compressor air mass flow are tracked to control the air path system.

1.5. Estimation Problems in Diesel Engines

Application of control strategies for the achievement of better fuel economy and lower emission in turbocharged diesel engines with exhaust gas recirculation unit requires many flow/temperature or pressure variables to be measured accurately. Sometimes the existing hard conditions prevent the measurement of some of these quantities. In this regard, estimation problems are also very important and challenging in diesel engines. The complicated structure of the engine when combined with some hard existing conditions (like high temperatures, soot coverage on sensors) may induce estimations of some quantities very difficult or unreliable. In addition, some quantities, like oxygen/air fraction in manifolds, load torque on the engine may be physically impossible to measure. Estimation of such quantities are sometimes very important to be used as feedback signals in control strategies to reduce emissions and to increase engine performance. Another reason for estimation is to avoid use of expensive sensors.

Different approaches with different purposes have been used in literature on estimation. Here, we will list just some of them. In [24], Wang uses a Luenberger-like observer for air fraction estimation. In [25], Brahma *et.al* proposes a linear mean-value model, whose structure is motivated by a physics-based nonlinear model. Finally, a

Kalman Filter was designed to predict the torque and NO_x predictions from the manifold pressure and mass air flow measurements. In [26], the authors present a nonlinear sliding mode observer for indicated torque and load torque estimations. Indicated torques were also estimated using ANN [27]. In [28], Desantes *et.al* uses a method known as Δp method for estimating the total air mass admitted by the engine.

1.6. Main Contributions

In the first part of the thesis, we consider a diesel engine model used in a large number of papers for different control methods and purposes [18, 23, 29, 30, 31, 32]. We apply a linear parameter-varying control method to it. In fact, a similar work was done in [23], using the same model. But, there the control problem was to track intake manifold pressure and compressor air mass flow and the LPV-model was simply assumed to be scheduled by the intake manifold pressure and the exhaust pressure was taken to be 2.5 kPa greater than it. This is a huge simplification and it can be rarely encountered for transient situations in real applications. As a result, the effect of scheduling of exhaust manifold pressure on system dynamics is not known. In addition, the LPV-control design procedure was based on a gridding strategy which is computationally difficult.

In this study, we take the state dependent turbine and EGR flow variables as modified control inputs. This idea was considered by [29, 30, 31, 32] when applying different nonlinear controller approaches (like feedback linearization, constructive-lyapunov control, etc.) using the same model. In [29, 30, 31, 32], the engine speed is taken some constant value or engine charts are used and therefore the resulting controller is for the chosen operating point(s). As a result, the controller is not valid for other speed values or engine operating conditions. In addition, fuel flow rate is, also, taken as some fixed set point value. These are clearly restrictive assumptions or simplifications. Our aim is to design a more general controller where we avoid simplifications like the ones in [23] and in [29, 30, 31, 32]. The determined state dependent control flow inputs are divided by the states to obtain the real control inputs. The positiveness of state values makes this idea work. As control performance variables, we track compressor air mass

flow and exhaust manifold pressure, whose set points are expressed in terms of the set points of EGR fraction and AFR ratio in the intake manifold.

The LPV controller design method is based on the approach of [33], where no gridding is necessary. For the control design approach of [33] to work, as a first task, the model is transformed into an equivalent model by a division/multiplication of some terms in the equation with the exhaust manifold pressure state to create exhaust manifold pressure as a state in the associated equations. This is necessary for the feasibility of linear matrix inequalities (LMIs) used in the controller synthesis. In the control part, we first assume manifold temperatures to be constant values which may be encountered in some situations. The resulting model and the associated control system are scheduled on five time-varying parameters. In the second control section, manifold temperatures are furthermore assumed to be time-varying parameters and the number of scheduling parameters is increased from five to seven. The resulting controller is more general to be applied in a wide range of operating points. In the literature, so far in diesel engine air path control no work has included manifold temperatures as parameters. In this regard, this is the first study accomplishing this. The gain-scheduled controller (based on variable manifold temperatures) is compared with a H_∞ controller (based on a linearized engine model) to emphasis that a typical linear controller does not work for the nonlinear engine model.

In the second part of the thesis, we consider compressor air mass flow estimation problem in diesel engines and present two different methods, each having some superior properties compared to the other. We first develop a general deterministic nonlinear state estimation method for states appearing linearly in nonlinear systems. The method is based on fitting an on-line linear moving model to measured states using the input-output measurements. The linear-moving model is identified using a recursive least-squares with an adaptive forgetting factor. An error analysis of the resulting method is also presented. Before application of the method to diesel engine compressor air mass flow estimation, it is applied to some academic-purpose examples to demonstrate the cases where it outperforms the popular and widely used extended kalman filter (EKF). Then, the method is applied to compressor air mass flow estimation, again

with a comparison to EKF to show the effectiveness of the method and the relative poor performance of EKF.

The second estimation method is a linear parameter-varying based approach developed by [34] for estimating state variables in affine LPV models. To apply this approach, the underlying nonlinear diesel engine model is transformed into an equivalent affine parameter-dependent form. The main advantage of this approach when compared to the first one is that the designed observer has an asymptotic convergence nature. Using this method, again estimation of compressor air mass flow is demonstrated and results are compared with EKF.

To sum up, as a contribution in the research area of diesel engine control-estimation problems, we present a more general control strategy and develop/apply two different estimation approaches for compressor air mass flow. The organization of this dissertation is as follows.

Chapter 2: LPV modeling of diesel engines, LPV systems and the LPV control approach of [33] are introduced.
Chapter 3: Application of the control method given in Chapter 2 to LPV-based modeled diesel engine is carried out for tracking of compressor air mass flow and exhaust manifold pressure.
Chapter 4: This chapter is devoted to the development of an identification-based state estimation method, its performance on case studies and then its application to diesel engine compressor air mass flow estimation with a comparison to EKF.
Chapter 5: LPV-based estimation method of [34] and its application to compressor air mass flow estimation with a comparison to EKF are given.
Chapter 6: We conclude with the main findings, contributions of this thesis and the recommendation of some future work.

2. LPV MODELING OF DIESEL ENGINES AND LPV-BASED CONTROL DESIGN THEORY

In this chapter, we will first introduce a physics-based, mean-value, reduced-order diesel engine model describing the air path system dynamics and then convert the underlying model into LPV forms. In LPV-based modeling, we will consider the separate cases of constant and variable manifold temperatures and hence have two different models. Then, we will pass to LPV control design theory with all included details. The developed LPV engine models with the described controller design method will be used in the next chapter for gain scheduled control of the air path system in diesel engines.

2.1. LPV Modeling of Diesel Engines with Constant Manifold Temperatures

Again, consider the schematic flow diagram of a typical turbocharged diesel engine with EGR as shown in Figure 2.1. The related engine variables and their descriptions are provided in Table 2.1. Flow variables are shown with a double subscript which shows the path from the source to the sink location. The dynamics describing the air path system is

$$\dot{p}_i = \frac{RT_i}{V_i}\big(W_{ci} + W_{xi} - W_{ie}\big) + \frac{\dot{T}_i}{T_i}p_i, \tag{2.1a}$$

$$\dot{p}_x = \frac{RT_x}{V_x}\big(W_{ie} + W_f - W_{xi} - W_{xt}\big) + \frac{\dot{T}_x}{T_x}p_x, \tag{2.1b}$$

$$\dot{P}_c = \frac{1}{\tau}\big(-P_c + P_t\big). \tag{2.1c}$$

The first two equations are intake and exhaust manifold pressure state equations, which are obtained simply by differentiating the ideal gas law for each manifold. The third equation is a first order Taylor series approximation for compressor power. Unless manifold temperatures change rapidly, the effect of the terms including the derivatives of the intake and exhaust manifold temperatures on the system are negligible. This is so

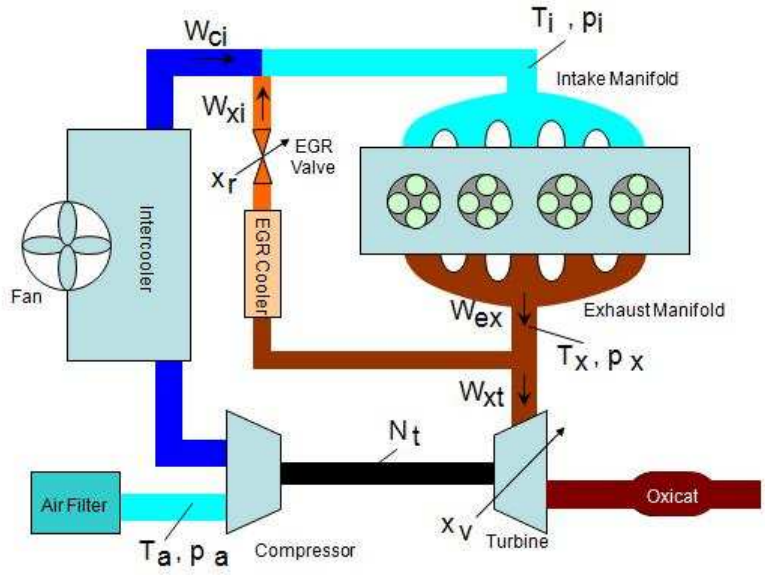

Figure 2.1. Diesel engine flow diagram.

Table 2.1. Engine variables and their descriptions

Symmbol	Description
A_r	Effective EGR flow area
p_i, p_x	Intake and exhaust manifold pressures
T_i, T_x	Intake and exhaust manifold temperatures
p_a, T_a	Ambient pressure and temperature
p_{ref}, T_{ref}	Reference pressure and temperature
N, N_t	Engine and turbo speed
V_i, V_x, V_d	Intake, exhaust manifold volumes and displacement volume
W_{xi}, W_{xt}	EGR and turbine mass flow rate
W_{ci}, W_{ie}, W_f	Compressor, intake-to-engine and fuel mass flow rate
P_c, P_t	Compressor and turbine power
x_v, x_r	VGT vane and EGR valve positions
η_c, η_t, η_v	Compressor, turbine and volumetric efficiencies
R, c_p, c_v	Gas constant and specific heat at constant pressure and volume
τ	Turbo lag constant

because for cases of small-to-moderate temperature changes their contribution orders will be typically small compared to the other terms in the pressure state equations. In this study, the terms including the derivatives of manifold temperatures will be neglected. The expressions for air mass flows and power variables are

$$W_{ci} = \frac{\eta_c}{c_p T_a} \frac{P_c}{\left(\frac{p_i}{p_a}\right)^{\mu} - 1}, \tag{2.2a}$$

$$W_{ie} = \frac{\eta_v V_d N p_i}{120 R T_i}, \tag{2.2b}$$

$$W_{xi} = \frac{A_r(x_r) p_x}{\sqrt{R T_x}} \sqrt{2 \frac{p_i}{p_x} \left(1 - \frac{p_i}{p_x}\right)}, \tag{2.2c}$$

$$W_{xt} = (a(1 - x_v) + b) \left(c \left(\frac{p_x}{p_a} - 1\right) + d\right) \frac{p_x}{p_{ref}} \sqrt{\frac{T_{ref}}{T_x}} \sqrt{2 \frac{p_a}{p_x} \left(1 - \frac{p_a}{p_x}\right)}, \tag{2.2d}$$

$$P_t = W_{xt} c_p T_x \eta_t \left(1 - \left(\frac{p_a}{p_x}\right)^{\mu}\right). \tag{2.2e}$$

A_r in W_{xi} is a quadratic function of x_r:

$$A_r(x_r) = -1.370135 \times 10^{-4} x_r^2 + 3.156976 \times 10^{-4} x_r.$$

A_r is a monotone increasing function of x_r as shown in Figure 2.2 and hence is invertible. This allows us to determine x_r uniquely once A_r is determined.

The constants a, b, c, d in W_{xt} (Table 2.2) and the polynomial coefficients in A_r are taken from [23] for the considered specific engine (related geometric engine model and thermodynamic parameters are given in Appendix D) and for low and medium load-speed signal range of New European Drive Cycle (NEDC). Manifold temperatures are considered as slowly changing parameters and volumetric (η_v), compressor (η_c) and turbine (η_t) efficiencies are taken as constants, all are optimized for the mentioned signal range of NEDC, whose values are presented in Table 2.2 [23]. To make controller

Table 2.2. Constant engine model parameters

T_i (K)	T_x (K)	η_c(%)	η_v(%)	η_t(%)	τ (s)	a	b	c	d
313	509	61	87	76	0.11	-490.4/3600	633.7/3600	0.4	0.6

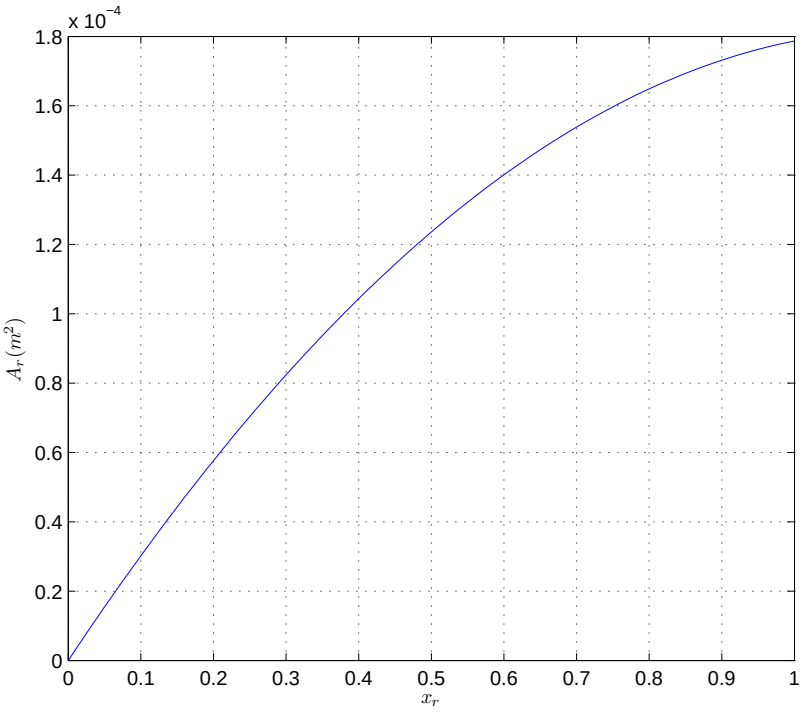

Figure 2.2. A_r versus x_r [23].

design easier, we consider $\tilde{u}_1 := W_{xt}$ and $\tilde{u}_2 := W_{xi}$ as modified inputs. After inserting W_{ci}, W_{ie} and P_t expressions into (2.1), we get

$$\dot{p}_i = -k_3 N p_i + k_1 \frac{P_c}{\left(\frac{p_i}{p_a}\right)^{\mu} - 1} + k_2 \tilde{u}_2, \tag{2.3a}$$

$$\dot{p}_x = l_1 N p_i + l_2 W_f - l_2 \tilde{u}_1 - l_2 \tilde{u}_2, \tag{2.3b}$$

$$\dot{P}_c = -\frac{1}{\tau} P_c + m_1 \tilde{u}_1 \left(1 - \left(\frac{p_a}{p_x}\right)^{\mu}\right), \tag{2.3c}$$

where

$$k_1 := \frac{RT_i\eta_c}{V_i c_p T_a},\ k_2 := \frac{RT_i}{V_i},\ k_3 := \frac{\eta_v V_d}{120 V_i},\ l_1 := \frac{\eta_v V_d T_X}{120 V_x T_i},\ l_2 := \frac{RT_x}{V_x},\ m_1 := \frac{c_p \eta_t T_x}{\tau}.$$

Next, we do the following exogenous parameter definitions and manipulations:

$$\rho_1 := \frac{1}{\left(\frac{p_i}{p_a}\right)^{\mu} - 1},\ \rho_2 = N,\ \rho_3 := 1 - \left(\frac{p_a}{p_x}\right)^{\mu},$$

$$-\frac{1}{\tau}P_c = -\frac{1}{\tau}\frac{P_c}{p_x}p_x = m_2\rho_4 p_x,\ l_1 N p_i = l_1 N\frac{p_i}{p_x}p_x = l_1\rho_5 p_x,$$

where

$$\rho_4 := \frac{P_c}{p_x},\ \rho_5 := \frac{Np_i}{p_x},\ m_2 := -\frac{1}{\tau}.$$

Then, (2.3) becomes

$$\dot{p}_i = -k_3\rho_2 p_i + k_1\rho_1 P_c + k_2\tilde{u}_2, \tag{2.4a}$$

$$\dot{p}_x = l_1\rho_5 p_x + l_2 W_f - l_2\tilde{u}_1 - l_2\tilde{u}_2, \tag{2.4b}$$

$$\dot{P}_c = m_2\rho_4 p_x + m_1\rho_3\tilde{u}_1. \tag{2.4c}$$

The system (2.4) can be written as

$$\begin{pmatrix} \dot{p}_i \\ \dot{p}_x \\ \dot{P}_c \end{pmatrix} = \begin{pmatrix} -k_3\rho_2 & 0 & k_1\rho_1 \\ 0 & l_1\rho_5 & 0 \\ 0 & m_2\rho_4 & 0 \end{pmatrix} \begin{pmatrix} p_i \\ p_x \\ P_c \end{pmatrix} + \begin{pmatrix} 0 & k_2 \\ -l_2 & -l_2 \\ m_1\rho_3 & 0 \end{pmatrix} \begin{pmatrix} \tilde{u}_1 \\ \tilde{u}_2 \end{pmatrix} + \begin{pmatrix} 0 \\ l_2 \\ 0 \end{pmatrix} W_f \tag{2.5}$$

2.2. LPV Modeling of Diesel Engines with Variable Manifold Temperatures

We consider the same model as in Section 2.1, except now manifold temperatures T_i and T_x are also taken as time-varying parameters. This, in turn, results in an improved engine model and hence creating the possibility for a more accurate controller design. To our knowledge, in all diesel engine air path control system designs in the literature, manifold temperatures are taken as some constant values. This is partly due to the fact that taking temperatures as time-varying parameters complicates the model

and the subsequent controller design task. Although manifold temperatures in some operating points can be accepted as slowly-varying parameters and therefore considering them as some optimal constant values (i.e., as optimal model tuning parameters), this is not always valid and there are situations where manifold temperatures change considerably. In this section, we remove the restriction of *"constant manifold temperatures assumption"* and therefore make the designed controller working in a wide range of operating points. The associated LPV model is given as

$$\dot{p}_i = -\hat{k}_3\rho_2 p_i + \hat{k}_1\rho_1\rho_6 P_c + \hat{k}_2\rho_6\tilde{u}_2, \tag{2.6a}$$

$$\dot{p}_x = \hat{l}_1\frac{\rho_5\rho_7}{\rho_6}p_x + \hat{l}_2\rho_7 W_f - \hat{l}_2\rho_7\tilde{u}_1 - \hat{l}_2\rho_7\tilde{u}_2, \tag{2.6b}$$

$$\dot{P}_c = \hat{m}_2\rho_4 p_x + \hat{m}_1\rho_3\rho_7\tilde{u}_1, \tag{2.6c}$$

where

$$\hat{k}_1 := \frac{R\eta_c}{V_i c_p T_a},\ \hat{k}_2 := \frac{R}{V_i},\ \hat{k}_3 := \frac{\eta_v V_d}{120 V_i},\ \hat{l}_1 := \frac{\eta_v V_d}{120 V_x},\ \hat{l}_2 := \frac{R}{V_x},\ \hat{m}_1 := \frac{c_p\eta_t}{\tau}$$

are constants, $\rho_1, \rho_2, \cdots, \rho_5$ are the same as in Section 2.1 and finally $\rho_6 := T_i$, $\rho_7 := T_x$. The system (2.6) can be written as

$$\begin{pmatrix} \dot{p}_i \\ \dot{p}_x \\ \dot{P}_c \end{pmatrix} = \begin{pmatrix} -\hat{k}_3\rho_2 & 0 & \hat{k}_1\rho_1\rho_6 \\ 0 & \dfrac{\hat{l}_1\rho_5\rho_7}{\rho_6} & 0 \\ 0 & \hat{m}_2\rho_4 & 0 \end{pmatrix} \begin{pmatrix} p_i \\ p_x \\ P_c \end{pmatrix} + \begin{pmatrix} 0 & \hat{k}_2\rho_6 \\ -\hat{l}_2\rho_7 & -\hat{l}_2\rho_7 \\ \hat{m}_1\rho_3\rho_7 & 0 \end{pmatrix} \begin{pmatrix} \tilde{u}_1 \\ \tilde{u}_2 \end{pmatrix} + \begin{pmatrix} 0 \\ \hat{l}_2\rho_7 \\ 0 \end{pmatrix} W_f \tag{2.7}$$

Both models (2.5) and (2.7) can be written as

$$\dot{x} = \mathcal{A}(\rho)x + \mathcal{B}_w(\rho)w + \mathcal{B}_u(\rho)u$$

and are special cases of dynamical systems known as LPV systems. When the measured and control outputs (which are introduced in the next chapter) are considered for the underlying engine models, the systems can be put in the form

$$\begin{aligned}\dot{x} =& \mathcal{A}(\rho)x + \mathcal{B}_w(\rho)w + \mathcal{B}_u(\rho)u,\\ z =& \mathcal{C}_z(\rho)x + \mathcal{D}_{zw}(\rho)w + \mathcal{D}_{zu}(\rho)u,\\ y =& \mathcal{C}_y(\rho)x + \mathcal{D}_{yw}(\rho)w + \mathcal{D}_{yu}(\rho)u,\end{aligned}$$

where $x \in R^{n_x}$ is the state vector, $u \in R^{n_u}$ is the manipulated input, $w \in R^{n_w}$ is the disturbance input on the system, $z \in R^{n_z}$ is the controlled output, $y \in R^{n_y}$ is the measured output and $\rho \in R^{n_\rho}$ is the time-varying parameter vector. There exists a large literature on control of such systems [33, 40, 41, 42, 43]. The approaches presented in [40, 41, 42, 43] synthesize parameter dependent controllers and require gridding of the parameter space, which becomes computational very hard if the number of parameters is high (for example, if more than three parameters). In this study, the number of parameters is high, and hence we will use the method of [33] which is for LPV systems in rational form and which does not require gridding. In the next sections, the underlying LPV control theory of [33] will be explained. The interested reader can find more detailed information than presented here in [33] and the references therein.

2.3. Introduction to LPV-Based Control Design: General Framework

Consider the system

$$\begin{aligned}\dot{x} =& \mathcal{A}(\rho)x + \mathcal{B}_w(\rho)w + \mathcal{B}_u(\rho)u,\\ z =& \mathcal{C}_z(\rho)x + \mathcal{D}_{zw}(\rho)w + \mathcal{D}_{zu}(\rho)u,\\ y =& \mathcal{C}_y(\rho)x + \mathcal{D}_{yw}(\rho)w + \mathcal{D}_{yu}(\rho)u,\end{aligned} \tag{2.8}$$

where we assume that the plant is proper so that $\mathcal{D}_{yu}(\rho) = 0$. The parameter vector ρ is "pulled out" from the system such that the system of equations in (2.8) becomes

$$\begin{aligned}
\dot{x} =& Ax + B_p p + B_w w + B_u u, \\
q =& C_q x + D_{qp} p + D_{qw} w + D_{qu} u, \\
z =& C_z x + D_{zp} p + D_{zw} w + D_{zu} u, \\
y =& C_y x + D_{yp} p + D_{yw} w + D_{yu} u, \\
p =& \Delta q,
\end{aligned} \tag{2.9}$$

where $\Delta = \mathbf{diag}\left(\rho_1 I_{n_1}, \rho_2 I_{n_2}, \cdots, \rho_{n_\rho} I_{n_\rho}\right)$. The system in (2.9) can be graphically represented as in Figure 2.3. The control design problem is to find a controller K with

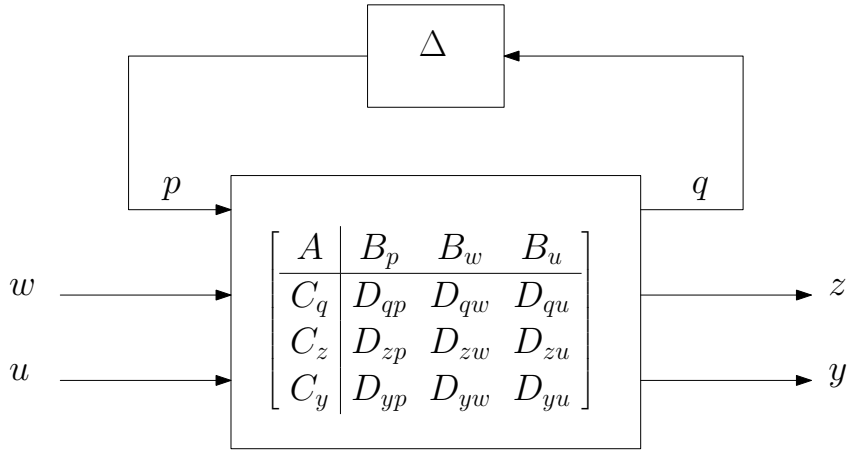

Figure 2.3. General framework

state space equations

$$\begin{aligned}
\dot{x}_c =& A_c x_c + B_{p_c} p_c + B_c y, \\
q_c =& C_{q_c} x_c + D_{q_c p_c} p_c + D_{q_c y} y, \\
u =& C_u x_c + D_{u p_c} p_c + D_{uy} y, \\
p_c =& \Delta_c q_c,
\end{aligned} \tag{2.10}$$

where Δ_c is the controller scheduling function. The controller is required to satisfy the following properties for all admissible parameter trajectories $\rho(t) \in R^{n_\rho}$:

- stabilizes the system
- provides a guaranteed $\mathcal{L}_2$ performance for the closed-loop system from the disturbance channel w to the controlled output channel z. I.e.,

$$\sup_{w \in L_2, w \neq 0} \frac{||z||_2}{||w||_2} \leq \gamma$$

The plant with controller is shown in Figure 2.4.

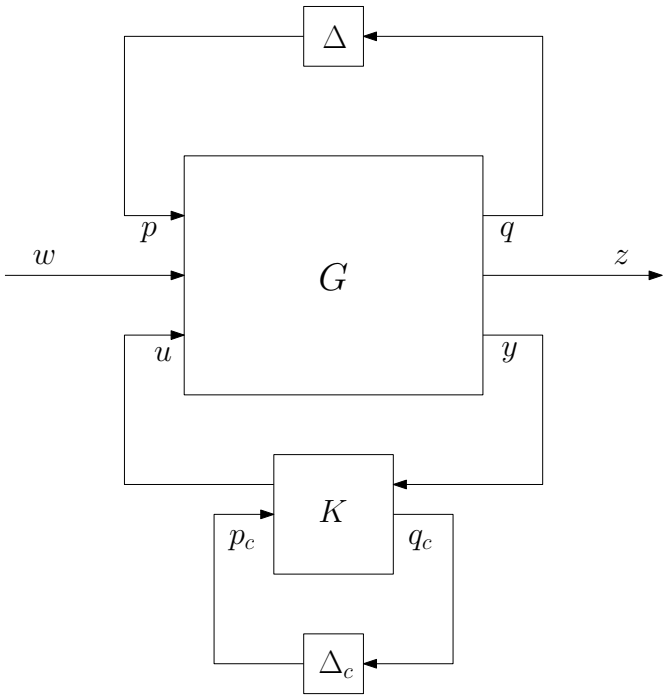

Figure 2.4. Scheduled LTI-plant with scheduled LTI-controller

2.4. Linear Fractional Representations

In Section 2.3, we have assumed that the parameters are "pulled-out" from the system so that we have the system of equations (2.9). In this section, we will give a classical example to demonstrate how to pull-out parameters. We consider the example given in [36], which is a forced mass/spring/damper system as shown in Figure 2.5. The equation of motion of the system is

$$m\ddot{\xi} + c\dot{\xi} + k\xi = F. \tag{2.11}$$

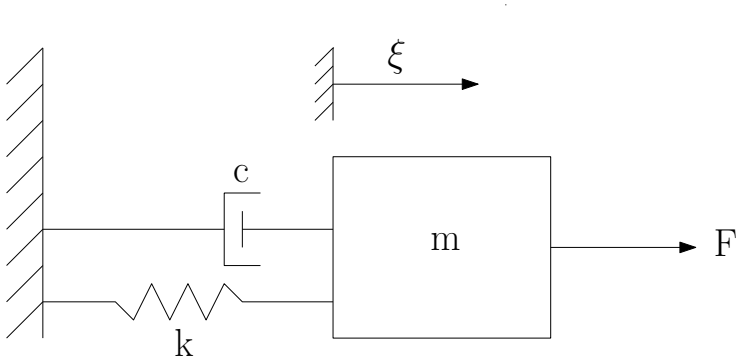

Figure 2.5. Uncertain mass-spring-damper system

Suppose that the physical parameters m, c, k are not known exactly but it is known that they lie in a range centered about some nominal values. In particular, suppose that

$$m = m_0(1 + 0.1\delta_m),\ c = c_0(1 + 0.2\delta_c),\ k = k_0(1 + 0.3\delta_k)$$

Here, the perturbations δ_m, δ_c, δ_k are unknown but they lie in the interval $[-1, 1]$. With a simple algebra, one can show that

$$\frac{1}{m} = \frac{1}{m_0} - \frac{0.1\delta_m}{m_0}\left(1 + 0.1\delta_m\right)^{-1}.$$

Next, we select the states of the dynamical system (2.11) as $x_1 = \xi$, $x_2 = \dot{\xi}$, resulting in,

$$\dot{x_1} = x_2, \tag{2.12a}$$

$$\begin{aligned}
\dot{x_2} &= -\frac{c}{m}x_2 - \frac{k}{m}x_1 + \frac{F}{m} \\
&= \left(-\frac{c}{m_0}x_2 - \frac{k}{m_0}x_1 + \frac{F}{m_0}\right)\left(1 - 0.1\delta_m\left(1 + 0.1\delta_m\right)^{-1}\right) \\
&= \left(-\frac{c_0 + 0.2c_0\delta_c}{m_0}x_2 - \frac{k_0 + 0.3k_0\delta_k}{m_0}x_1 + \frac{F}{m_0}\right)\left(1 - 0.1\delta_m\left(1 + 0.1\delta_m\right)^{-1}\right) \\
&= -\frac{c_0}{m_0}x_2 - \frac{k_0}{m_0}x_1 + \frac{F}{m_0} - \frac{1}{m_0}\left(0.2c_0\delta_c x_2 + 0.3k_0\delta_k x_1\right) \\
&\quad + \frac{0.1}{m_0}\Big(-\left(1 + 0.2\delta_c\right)c_0x_2 - \left(1 + 0.3\delta_k\right)k_0x_1 + F\Big)\left(-\delta_m\left(1 + 0.1\delta_m\right)^{-1}\right).
\end{aligned} \tag{2.12b}$$

Now, we make the following definitions

$$q_k := 0.3k_0x_1, \tag{2.13a}$$

$$p_k := \delta_k q_k, \tag{2.13b}$$

$$q_c := 0.2c_0x_2, \tag{2.13c}$$

$$p_c := \delta_c q_c, \tag{2.13d}$$

$$q_m := \left(-\left(1+0.2\delta_c\right)c_0x_2 - \left(1+0.3\delta_k\right)k_0x_1 + F\right)\left(1+0.1\delta_m\right)^{-1}, \tag{2.13e}$$

$$p_m := \delta_m q_m. \tag{2.13f}$$

Next, observe that $\left(1+0.1\delta_m\right)^{-1} = 1 - 0.1\delta_m\left(1+0.1\delta_m\right)^{-1}$. Then, q_m and x_2 become

$$q_m = -k_0x_1 - c_0x_2 + F - p_k - p_c - 0.1p_m. \tag{2.14}$$

$$\dot{x}_2 = -\frac{k_0}{m_0}x_1 - \frac{c_0}{m_0}x_2 - \frac{1}{m_0}p_k - \frac{1}{m_0}p_c - \frac{0.1}{m_0}p_m. \tag{2.15}$$

Equations (2.12a, 2.15, 2.13a, 2.13c, 2.14) can be written more compactly as

$$\begin{pmatrix} \dot{x}_1 \\ \dot{x}_2 \\ \hdashline q_k \\ q_c \\ q_m \end{pmatrix} = \underbrace{\left(\begin{array}{cc:cccc} 0 & 1 & 0 & 0 & 0 & 0 \\ -\frac{k_0}{m_0} & -\frac{c_0}{m_0} & \frac{1}{m_0} & -\frac{1}{m_0} & -\frac{1}{m_0} & -\frac{0.1}{m_0} \\ \hdashline 0.3k_0 & 0 & 0 & 0 & 0 & 0 \\ 0 & 0.2c_0 & 0 & 0 & 0 & 0 \\ -k_0 & -c_0 & 1 & -1 & -1 & -0.1 \end{array}\right)}_{\mathrm{M}} \begin{pmatrix} x_1 \\ x_2 \\ \hline F \\ p_k \\ p_c \\ p_m \end{pmatrix}, \tag{2.16a}$$

$$\begin{pmatrix} p_k \\ p_c \\ p_m \end{pmatrix} = \Delta \begin{pmatrix} q_k \\ q_c \\ q_m \end{pmatrix}, \tag{2.16b}$$

$$\Delta = \begin{pmatrix} \delta_k & 0 & 0 \\ 0 & \delta_c & 0 \\ 0 & 0 & \delta_m \end{pmatrix}. \tag{2.16c}$$

We have

$$\begin{pmatrix} \dot{x}_1 \\ \dot{x}_2 \end{pmatrix} = \mathcal{F}_l(M, \Delta) \begin{pmatrix} x_1 \\ x_2 \\ F \end{pmatrix},$$

where $\mathcal{F}_l(M, \Delta)$ is defined in Appendix C. The state-space matrices corresponding to the LTI-part of the system (2.16a, 2.16b) and (2.16c) are given as

$$A = \begin{pmatrix} 0 & 1 \\ -\frac{k_0}{m_0} & -\frac{c_0}{m_0} \end{pmatrix}, B_p = \begin{pmatrix} 0 & 0 & 0 \\ -\frac{1}{m_0} & -\frac{1}{m_0} & -\frac{0.1}{m_0} \end{pmatrix}, B_u = \begin{pmatrix} 0 \\ \frac{1}{m_0} \end{pmatrix},$$

$$C_q = \begin{pmatrix} 0.3k_0 & 0 \\ 0 & 0.2c_0 \\ -k_0 & -c_0 \end{pmatrix}, D_{qp} = \begin{pmatrix} 0 & 0 & 0 \\ 0 & 0 & 0 \\ -1 & -1 & -0.1 \end{pmatrix}, D_{qu} = \begin{pmatrix} 0 \\ 0 \\ 1 \end{pmatrix}.$$

A second way of obtaining LFR form is as follows. First, obtain a block-diagram for the equation of motion of the system (2.11) as shown in Figure 2.6. Next, isolate the uncertain parameters $\delta_c, \delta_k, \delta_m$, and denote their inputs and outputs as q_c, q_k, q_m and p_c, p_k, p_m as shown in Figure 2.7. With all δ's taken out, writing the transfer function from the "system states + system inputs + p_k, p_c, p_m" to "derivative of system states + q_k, q_c, q_m" will give the matrix M in (2.16a). This transfer function can easily be computed using Matlab command "**linmod**". Δ will be a block-diagonal matrix, where the size of each block is equal to the number of times the associated uncertain parameter appears in Figure 2.7.

In addition to the two methods presented above for LFR representations, a third way is to use the software developed by Hecker-Varga-Magni [37]. This software is freely available and it is accompanied with an excellent user manual.

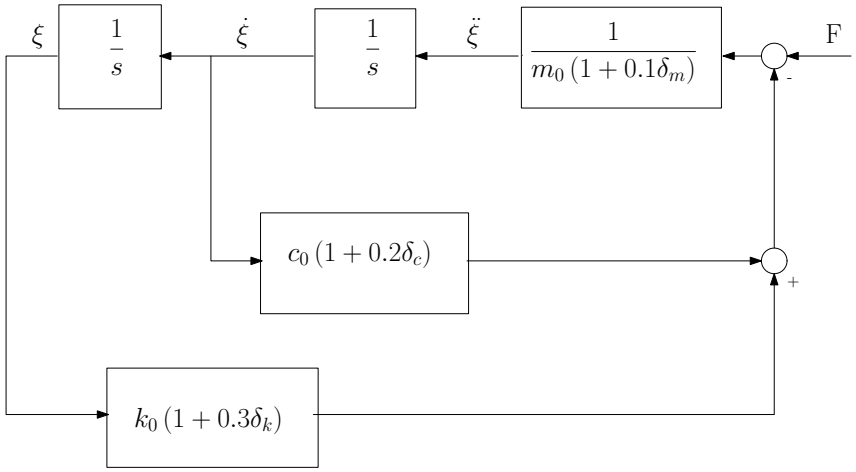

Figure 2.6. Block diagram for uncertain mass-spring-damper system

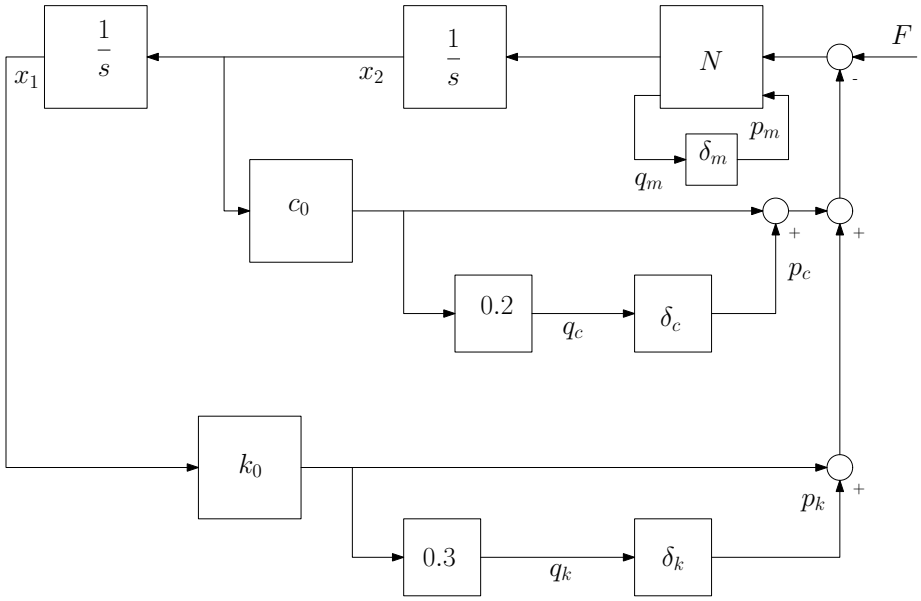

Figure 2.7. Uncertain mass-spring-damper system with uncertain parameters

2.5. LPV Controller Synthesis

Before presenting the control synthesis algorithm of [33], we need the following concepts regarding uncertainty sets and their characterizing multipliers.

Definition 2.1. *The uncertainty set* Δ *is said the be generated by (or is the convex hull of)* $\Delta_1, \Delta_2, \cdots, \Delta_N$ *if*

$$\Delta = \left\{ \sum_{i=1}^{N} \alpha_i \Delta_i : \alpha_i \geq 0, \sum_{i=1}^{N} \alpha_i = 1 \right\}.$$

Definition 2.2. *The multiplier set $\mathcal{P}$ and the corresponding dual multiplier set $\widetilde{\mathcal{P}}$ associated with Δ are defined as*

$$\mathcal{P} := \left\{ \begin{pmatrix} Q & S \\ S^T & R \end{pmatrix} : Q \prec 0, \begin{pmatrix} \Delta_j \\ I \end{pmatrix}^T \begin{pmatrix} Q & S \\ S^T & R \end{pmatrix} \begin{pmatrix} \Delta_j \\ I \end{pmatrix} \succ 0, \ \textit{for } j = 1 : N \right\}.$$

$$\widetilde{\mathcal{P}} := \left\{ \begin{pmatrix} \widetilde{Q} & \widetilde{S} \\ \widetilde{S}^T & \widetilde{R} \end{pmatrix} : \widetilde{R} \succ 0, \begin{pmatrix} I \\ -\Delta_j^T \end{pmatrix}^T \begin{pmatrix} \widetilde{Q} & \widetilde{S} \\ \widetilde{S}^T & \widetilde{R} \end{pmatrix} \begin{pmatrix} I \\ -\Delta_j^T \end{pmatrix} \prec 0, \ \textit{for } j = 1 : N \right\}.$$

In general, Δ can include dynamic components, time-varying or constant parameters, can be full block or diagonal block. When Δ is a block diagonal matrix whose blocks consist of time-varying scalar functions $\bar{\rho}_i(t)$ with $||\bar{\rho}_i(t)|| \leq 1$, the multiplier sets

$$\mathcal{P}_{sub} = \left\{ \begin{pmatrix} Q & S \\ S^T & R \end{pmatrix} : Q \prec 0, S = -S^T, R = -Q \right\}.$$

$$\widetilde{\mathcal{P}}_{sub} = \left\{ \begin{pmatrix} \widetilde{Q} & \widetilde{S} \\ \widetilde{S}^T & \widetilde{R} \end{pmatrix} : \widetilde{R} \succ 0, \widetilde{S} = -\widetilde{S}^T, \widetilde{Q} = -\widetilde{R} \right\}.$$

are subsets of $\mathcal{P}$ and $\widetilde{\mathcal{P}}$, respectively, hence, characterizing the uncertainty in the system [38]. Full block multipliers can be used to decrease conservatism for block diagonal uncertainties [39]. In this study, it will be be satisfactory to use the sets $\mathcal{P}_{sub}$ and $\widetilde{\mathcal{P}}_{sub}$ when synthesizing LPV controllers.

2.5.1. Stability and Performance Analysis of LPV Systems

Next, we consider the following LPV system, which includes the controller dynamics in case of forced systems.

$$\begin{aligned}\dot{x} =& \mathbf{A}x + \mathbf{B}_p p + \mathbf{B}_w w \\ q =& \mathbf{C}_q x + \mathbf{D}_{qp} p + \mathbf{D}_{qw} w \\ z =& \mathbf{C}_z x + \mathbf{D}_{zp} p + \mathbf{D}_{zw} w \\ p =& \Delta q \end{aligned} \tag{2.17}$$

Then, we have the following analysis theorem regarding the stability and performance of (2.17).

Theorem 2.1. *[33] Consider the system (2.17). Let $\gamma > 0$. Then, the LPV system (2.17) is stable with a $\mathcal{L}_2$-gain less than γ if there exist $X = X^T \succ 0$ and $P \in \mathcal{P}$ such that*

$$\left(\begin{array}{c} * \\ * \\ \hdashline * \\ * \\ \hdashline * \\ * \end{array}\right)^T \left(\begin{array}{cc:cc:cc} 0 & X & 0 & 0 & 0 & 0 \\ X & 0 & 0 & 0 & 0 & 0 \\ \hdashline 0 & 0 & Q & S & 0 & 0 \\ 0 & 0 & S^T & R & 0 & 0 \\ \hdashline 0 & 0 & 0 & 0 & -\gamma I & 0 \\ 0 & 0 & 0 & 0 & 0 & \gamma^{-1} I \end{array}\right) \left(\begin{array}{ccc} I & 0 & 0 \\ \mathbf{A} & \mathbf{B}_p & \mathbf{B}_w \\ \hdashline 0 & I & 0 \\ \mathbf{C}_q & \mathbf{D}_{qp} & \mathbf{D}_{qw} \\ \hdashline 0 & 0 & I \\ \mathbf{C}_z & \mathbf{D}_{zp} & \mathbf{D}_{zw} \end{array}\right) \prec 0. \tag{2.18}$$

The performance is characterized by

$$\sup_{w \in \mathcal{L}_2, w \neq 0} \frac{||z||_2}{||w||_2} \leq \gamma,$$

where $\mathcal{L}_2$ is the set of square integrable functions which is defined as

$$\mathcal{L}_2 := \left\{ x(t) \in \mathbb{R}^n : \int_{-\infty}^{\infty} x(t)^T x(t) dt < \infty \right\}$$

and

$$||x||_2 := \left(\int_{-\infty}^{\infty} x(t)^T x(t) dt \right)^{1/2}.$$

2.5.2. Scheduled Closed-Loop System

After closing the control input-measured output channel in Figure 2.4, we obtain the scheduled closed-loop system shown in Figure 2.8 in the following state-space form.

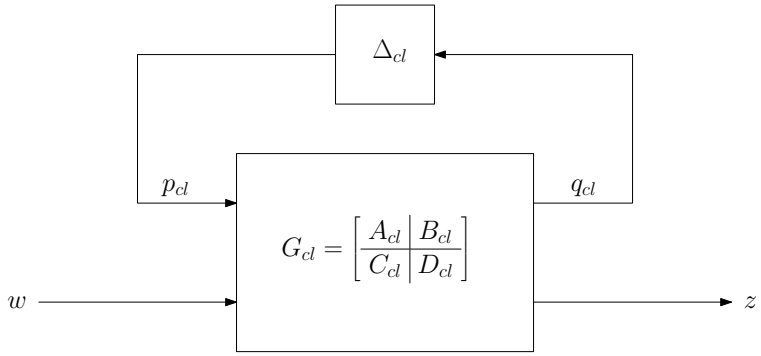

Figure 2.8. Scheduled closed-loop system

$$\begin{aligned} \dot{x}_{cl} &= A_{cl} x_{cl} + B_{p_{cl}} p_{cl} + B_w^{cl} w, \\ q_{cl} &= C_{q_{cl}} x_{cl} + D_{q_{cl} p_{cl}} p_{cl} + D_{q_{cl} w} w, \\ z &= C_z^{cl} x_{cl} + D_{z p_{cl}} p_{cl} + D_{zw}^{cl} w, \\ p_{cl} &= \Delta_{cl} q_{cl}, \end{aligned} \tag{2.19}$$

where

$$p_{cl} = \begin{pmatrix} p \\ p_c \end{pmatrix}, \; q_{cl} = \begin{pmatrix} q \\ q_c \end{pmatrix}, \Delta_{cl} = \begin{pmatrix} \Delta & 0 \\ 0 & \Delta_c \end{pmatrix}. \tag{2.20}$$

In the above notation, note that the subscript and superscript "cl" (meaning closed-loop) is used whenever necessary to prevent confusion with the previously defined matrices. The scheduled closed loop system matrices in (2.19) are

$$\left(\begin{array}{c|c|c} A_{cl} & B_{p_{cl}} & B_w^{cl} \\ \hline C_{q_{cl}} & D_{q_{cl}p_{cl}} & D_{q_{cl}w} \\ \hline C_z^{cl} & D_{zp_{cl}} & D_{zw}^{cl} \end{array}\right) = \left(\begin{array}{cc|cc|c} A & 0_{n_xn_x} & B_p & 0_{n_xn_p} & B_w \\ 0_{n_xn_x} & 0_{n_xn_x} & 0_{n_xn_p} & 0_{n_xn_p} & 0_{n_xn_w} \\ \hline C_q & 0_{n_qn_x} & D_{qp} & 0_{n_xn_p} & D_{qw} \\ 0_{n_qn_x} & 0_{n_qn_x} & 0_{n_xn_p} & 0_{n_qn_p} & 0_{n_qn_w} \\ \hline C_z & 0_{n_zn_x} & D_{zp} & 0_{n_zn_p} & D_{zw} \end{array}\right)$$

$$+\left(\begin{array}{c|cc} B_u & O_{n_xn_q} & 0_{n_xn_x} \\ 0_{n_xn_u} & 0_{n_xn_q} & I_{n_x} \\ \hline D_{qu} & 0_{n_qn_q} & 0_{n_qn_x} \\ 0_{n_qn_x} & I_{n_q} & 0_{n_qn_x} \\ \hline D_{zu} & 0_{n_zn_q} & 0_{n_zn_x} \end{array}\right)\left(\begin{array}{ccc} D_{uy} & D_{up_c} & C_u \\ D_{q_cy} & D_{q_cp_c} & C_{q_c} \\ B_c & B_{p_c} & A_c \end{array}\right)\left(\begin{array}{cc|cc|c} C_y & 0_{n_yn_x} & D_{yp} & 0_{n_yn_p} & D_{yw} \\ 0_{n_pn_x} & 0_{n_pn_x} & 0_{n_yn_p} & I_{n_p} & 0_{n_pn_w} \\ 0_{n_xn_x} & I_{n_x} & 0_{n_xn_p} & 0_{n_xn_p} & 0_{n_xn_w} \end{array}\right) \tag{2.21}$$

2.5.3. Controller Synthesis Procedure

In this subsection, we will describe the controller design algorithm based on Linear Matrix Inequalities (LMIs), which are introduced in Appendix A.

2.5.3.1. Existence LMIs. Consider the system (2.9) and let

$$P = \begin{pmatrix} Q & S \\ S^T & R \end{pmatrix}, \quad \widetilde{P} = \begin{pmatrix} \widetilde{Q} & \widetilde{S} \\ \widetilde{S}^T & \widetilde{R} \end{pmatrix}$$

be two multiplier sets in $\mathcal{P}_{sub}$ and $\widetilde{\mathcal{P}}_{sub}$, respectively. Let X, Y be matrices of dimension $n_x \times n_x$. Finally, let Φ and Ψ be orthonormal basis matrices for kernels of $[B_u^T \quad D_q^T \quad D_{zu}^T]$ and $[C_y \quad D_{yp} \quad D_{yw}]$, respectively. The following theorem states the existence conditions for the scheduled controller of the form (2.10).

Theorem 2.2 ([33]). *Let $P \in \mathcal{P}_{sub}, \widetilde{P} \in \widetilde{\mathcal{P}}_{sub}$. Assume that there exist $X = X^T \in$*

$\mathbb{R}^{n_x \times n_x}$, $Y = Y^T \in \mathbb{R}^{n_x \times n_x}$ *and a scalar* $\gamma > 0$ *such that*

$$\begin{pmatrix} \left(\star\right)_\perp^T \left(\star\right)^T \left(\begin{array}{c|c|c|c} 0 & 0 & X & 0 \\ \hline 0 & P & 0 & 0 \\ \hline X & 0 & 0 & 0 \\ \hline 0 & 0 & 0 & -\gamma I \end{array}\right) \left(\begin{array}{ccc} A & B_p & B_w \\ \hline C_q & D_{qp} & D_{qw} \\ \hline 0 & I & 0 \\ \hline I & 0 & 0 \\ \hline 0 & 0 & I \end{array}\right) \begin{pmatrix} C_y^T \\ D_{yp}^T \\ D_{yw}^T \end{pmatrix}_\perp & \star \\ \begin{pmatrix} C_z & D_{zp} & D_{zw} \end{pmatrix} \begin{pmatrix} C_y^T \\ D_{yp}^T \\ D_{yw}^T \end{pmatrix}_\perp & -\gamma I \end{pmatrix} \prec 0 \tag{2.22a}$$

$$\begin{pmatrix} \left(\star\right)_\perp^T \left(\star\right)^T \left(\begin{array}{c|c|c|c} 0 & 0 & Y & 0 \\ \hline 0 & \widetilde{P} & 0 & 0 \\ \hline Y & 0 & 0 & 0 \\ \hline 0 & 0 & 0 & \gamma I \end{array}\right) \left(\begin{array}{ccc} I & 0 & 0 \\ \hline 0 & I & 0 \\ \hline -B_p^T & -D_{qp}^T & -D_{zp}^T \\ \hline -A^T & -C_q^T & -C_z^T \\ \hline 0 & 0 & I \end{array}\right) \begin{pmatrix} B_u \\ D_{qu} \\ D_{zu} \end{pmatrix}_\perp & \star \\ \begin{pmatrix} B_w^T & D_{qw}^T & D_{zw}^T \end{pmatrix} \begin{pmatrix} B_u \\ D_{qu} \\ D_{zu} \end{pmatrix}_\perp & \gamma I \end{pmatrix} \succ 0 \tag{2.22b}$$

$$\begin{pmatrix} Y & I \\ I & X \end{pmatrix} \succ 0 \tag{2.22c}$$

$$\begin{pmatrix} R & I \\ I & \widetilde{R} \end{pmatrix} \succ 0 \tag{2.22d}$$

Then, there exists a controller of the form (2.10) which stabilizes the system and pro-

vides $\mathcal{L}_2$*-gain* $< \gamma$.

Here, we adopted the following notational convention. When we write

$$\begin{bmatrix} A & \star \\ B^T & C \end{bmatrix},$$

we mean $\star = B$. Instead of showing the actual content of a matrix, use of such a convention is very useful for compactness purposes.

2.5.3.2. Extended Multiplier and Extended Lyapunov Matrix Construction. The controller construction requires an extended multiplier and an extended Lyapunov matrix, which are required for the performance and stability analysis of the closed loop system (Section 2.5.1). After determination of $P, \widetilde{P}, X$ and Y from Theorem (2.22), the extended multiplier, P_{cl}, for closed loop system is given as

$$P_{cl} = \begin{pmatrix} \widetilde{P}_{cl_{11}} & 0 & \widetilde{P}_{cl_{12}} & 0 \\ 0 & \gamma^{-1}I & 0 & 0 \\ \widetilde{P}_{cl_{12}}^T & 0 & \widetilde{P}_{cl_{22}} & 0 \\ 0 & 0 & 0 & -\gamma I \end{pmatrix},$$

where

$$\widetilde{P}_{cl} = \begin{pmatrix} \widetilde{P}_{cl_{11}} & \widetilde{P}_{cl_{12}} \\ \widetilde{P}_{cl_{12}}^T & \widetilde{P}_{cl_{22}} \end{pmatrix} = P_{perm}^T \begin{pmatrix} P & T \\ T^T & T^T E T \end{pmatrix} P_{perm},$$

where

$$T := [T_1 \quad T_2],\ P_{perm} := \begin{pmatrix} I & 0 & 0 & 0 \\ 0 & 0 & I & 0 \\ 0 & I & 0 & 0 \\ 0 & 0 & 0 & I \end{pmatrix}.$$

Here, T_1, T_2 are a basis for the positive eigenspaces of

$$\left[E - Z\left(Z^T P Z\right)^{-1} Z^T\right] \text{ and } \left[E - Z_\perp \left(Z_\perp^T P Z_\perp\right)^{-1} Z_\perp^T\right], \text{respectively,}$$

where

$$E = \left(P - \widetilde{P}^{-1}\right)^{-1}, Z = \begin{pmatrix} I_\rho \\ 0 \end{pmatrix}.$$

As to extended Lyapunov matrix,

$$X_{cl} = \begin{pmatrix} X & X_{cl_{12}} \\ X_{cl_{12}}^T & X_{cl_{22}} \end{pmatrix},$$

where

$$X_{cl_{12}} = I, \quad X_{cl_{22}} = (X - Y^{-1})^{-1}.$$

2.5.3.3. $\Delta_c(\Delta)$ Construction.

$$\Delta_c(\Delta) = -W_{22} + (W_{21}\ V_{21}) \begin{pmatrix} U_{11} & * \\ W_{11} + \Delta & V_{11} \end{pmatrix}^{-1} \begin{pmatrix} U_{12} \\ W_{12} \end{pmatrix}, \tag{2.23}$$

where

$$U := P_{cl_{11}} - P_{cl_{12}} P_{cl_{22}}^{-1} P_{cl_{12}}^T, V := -P_{cl_{22}}^{-1} \text{ and } W := P_{cl_{22}}^{-1} P_{cl_{12}}^T.$$

2.5.3.4. Controller Construction. In this part, we first need to define some necessary terms. The closed-loop system in (2.19) or (2.21) can be written as

$$G := \left[\begin{array}{c|c} A_{cl} & B_{cl} \\ \hline C_{cl} & D_{cl} \end{array}\right],$$

where

$$B_{cl} := \begin{pmatrix} B_{p_{cl}} & B_w^{cl} \end{pmatrix}, C_{cl} = \begin{pmatrix} C_{q_{cl}} \\ C_z^{cl} \end{pmatrix}, D_{cl} = \begin{pmatrix} D_{q_{cl}p_{cl}} & D_{q_{cl}w} \\ D_{zp_{cl}} & D_{zw}^{cl} \end{pmatrix}.$$

Next, we have

$$\left(\begin{array}{c|c} A_{cl} & B_{cl} \\ \hline C_{cl} & D_{cl} \end{array}\right) = \left(\begin{array}{c:cc} \widetilde{A} & \widetilde{B}_p & \widetilde{B}_w \\ \hdashline \widetilde{C}_q & \widetilde{D}_{qp} & \widetilde{D}_{qw} \\ \widetilde{C}_z & \widetilde{D}_{zp} & \widetilde{D}_{zw} \end{array}\right) + \left(\begin{array}{c} \widetilde{B}_u \\ \hdashline \widetilde{D}_{qu} \\ \widetilde{D}_{zu} \end{array}\right) K \left(\begin{array}{c:cc} \widetilde{C}_y & \widetilde{D}_{yp} & \widetilde{D}_{yw} \end{array}\right)$$

$$=: U_A + U_B K U_C,$$

where the "$\widetilde{\cdot}$" terms are clear from a comparison with (2.21). Next, let

$$\Pi := \begin{pmatrix} 0 & 0 & X_{cl} & 0 \\ 0 & P_{cl_{11}} & 0 & P_{cl_{12}} \\ X_{cl} & 0 & 0 & 0 \\ 0 & P_{cl_{12}}^T & 0 & P_{cl_{22}} \end{pmatrix}$$

$$\Phi := \begin{pmatrix} U_A & U_B \\ I & 0 \end{pmatrix}^T \Pi \begin{pmatrix} U_A & U_B \\ I & 0 \end{pmatrix}$$

$$\Gamma := \begin{pmatrix} -U_C^T & 0 \\ 0 & I \end{pmatrix}^T \Phi^{-1} \begin{pmatrix} -U_C^T & 0 \\ 0 & I \end{pmatrix}$$

Then, the controller matrices are given by

$$K = V_2^{-T} V_1^T,$$

where

$$\begin{pmatrix} V_1 \\ V_2 \end{pmatrix}$$

is a basis for the positive eigenspace of Γ.

2.6. Comments on LPV Modeling of Diesel Engines

In LPV modeling of diesel engines given by (2.4) and (2.6), the first thing to notice is that both models could be obtained with a smaller number of parameters. For example, we could obtain a LPV model in case of constant manifold temperatures by just considering N, $\dfrac{1}{(p_i/p_a)^\mu - 1}$, $1-(p_a/p_x)^\mu$ as time-varying parameters and in case of variable manifold temperatures, we could consider additionally T_i and T_x as parameters so that in the first case we would have a LPV system with three parameters and in the second one a system with five parameters. Therefore, the immediate question that will arise is that why P_c/p_x and Np_i/p_x were considered as additional parameters, which increased the number of parameters from three to five in the first case and from five to seven in the second case.

Before answering the above question, it is helpful to know that in real application of LPV controllers it is better to have a small number of time-varying parameters as much as possible because first of all, as the number of parameter increases, the underlying controller may require more sensors for measurement of the parameters and this is a disadvantage from cost considerations. Secondly, as the number of parameter

increases, the size of Δ may increase and this may introduce computational costs and even delays due to computations, especially in the scheduling function for the controller (See 2.23) since it is necessary to take on-line inversions. Therefore, in general, the objective is to have a LPV-model with a small number of time-varying parameters.

In this study, the above suggested LPV models with a smaller number of parameters did not work. I.e., the controller existence conditions given in (2.22) did not produce any feasible solution. In fact, not only these selections of parameters but also many other possible parameter selections either did not give a feasible solution or a solution but working in a very small range of parameters and hence not satisfactory. In the LPV models presented here, note that the selected extra parameters P_c/p_x and Np_i/p_x are not obvious at all; i.e., they are created artificially. Luckily, this set of parameters resulted in a feasible solution for a very wide range of parameter values (See Chapter 3) and subsequently achievement of controllers working in a wide range of operating points and having satisfactory results.

To summarize, the non-unique LPV representation of a system may produce conservative solutions or even infeasible solutions. Therefore, optimal time-varying parameter selection brings an additional freedom in LPV-based control systems [44]. As to this optimization, there is nothing available except a trial-error mechanism.

3. GAIN-SCHEDULED AIR PATH CONTROL IN DIESEL ENGINES

In this chapter, we consider regulation of the air path system in diesel engines. To that end, the LPV-control method described in Chapter 2 will be applied. The considered diesel engine model is the physics-based derived, third order mean-value model considered in [18, 23, 29, 30, 31, 32]. As mentioned before, in [18, 29, 30, 31, 32] either engine speed is taken as some constant value or engine charts are used when control method is nonlinear control (especially feedback linearization). Moreover, the gain scheduled approach of [23] assumes exhaust manifold pressure to be 2.5 kPa greater than intake manifold pressure for LPV control method. As another point, in all studies in the literature, manifold temperatures are considered as slowly-varying parameters which may not be the case in some situations. Now, we will extend the air path system control in diesel engines in two directions. Firstly, we will control the air path system by tracking the exhaust manifold pressure and compressor air mass flow and in doing this we will not do any simplifying assumption or the use of any engine chart. Next, we will furthermore take manifold temperatures as time-varying parameters so that a more accurate engine model and control system are obtained. Finally, the designed gain-scheduled controller based on variable manifold temperatures is compared to a H_∞ controller (which is based on a linearized engine model) to show the inadequacy of a linear controller under variable engine operating points.

We start the chapter with the selection of performance variables and their relations with variables that are directly related to emissions.

3.1. Selection of Control Performance Variables

As mentioned before, to control emissions from diesel engines AFR and EGR fraction in the intake manifold (EGR_f) must be controlled by regulating them to set

points which are determined from the static engine data

$$\overline{AFR} = \overline{AFR}(N, W_f),\ \overline{EGR}_f = \overline{EGR}_f(N, W_f)$$

Since it is not possible to measure AFR and EGR_f physically, we will transform the set points of these quantities into set points for measurable variables, namely, among many possibilities, to set points of compressor air mass flow W_{ci} and exhaust manifold pressure p_x. As a result, the control problem will boil down to regulation of W_{ci} and p_x. Next, we will show this transformation.

Lean combustion in diesel engines (the situation that the cylinder mixture contains more air than that of stoichiometric) results in a non-exact burning process. I.e., the engine combustion products include extra air which subsequently flow to exhaust and intake (via EGR) manifolds. The dynamics of fractions of burned gases in the intake and exhaust manifolds are given by [46] as

$$\dot{F}_i = \frac{W_{xi}\left(F_x - F_i\right) - W_{ci}F_i}{m_i}, \tag{3.1a}$$

$$\dot{F}_x = \frac{W_e\left(F_e - F_x\right)}{m_x}, \tag{3.1b}$$

where m_i, m_x are masses of gases in the intake, exhaust manifolds, respectively and

$$F_e = \frac{\alpha W_f + F_i W_{ie} + W_f}{W_e},$$

where $W_e = W_{ie} + W_f$ and α is the stoichiometric ratio, namely which is equal to 14.6.

AFR and EGR_f are given as

$$\mathrm{AFR} = \frac{\left(1 - F_1\right) W_{ie}}{W_f}, \tag{3.2a}$$

$$\mathrm{EGR}_f = \frac{W_{xi}}{W_{ci} + W_{xi}}. \tag{3.2b}$$

Solving W_{ie} from (3.2a) and inserting into the expression for F_e, we obtain

$$F_e = \frac{(1 - F_1)(\alpha + 1) + F_1 \mathrm{AFR}}{1 - F_1 + \mathrm{AFR}}. \tag{3.3}$$

Next, using the steady-state values of F_1 and F_2 from (3.1a-3.1b) and using (3.3), we obtain

$$W_{ci} = \frac{(1 - F_1)(\alpha + 1 - F_1)}{F_1(1 - F_1 + \mathrm{AFR})} W_{xi}, \tag{3.4}$$

Next, solving F_1 from (3.2a), using the fact that at steady-state $W_{ie} = W_{ci} + W_{xi}$ and (3.4), we get

$$W_{ci} = W_f \frac{\alpha(W_{ci} + W_{xi}) + \mathrm{AFR} W_f}{(W_{ci} + W_{xi} - \mathrm{AFR} W_f)(W_f + W_{ci} + W_{xi})} W_{xi}. \tag{3.5}$$

Now, solving for W_{xi} from (3.2b), inserting into (3.5), solving the resulting quadratic equation for W_{ci} and considering the set points for AFR and EGR_f, we obtain the corresponding set point for W_{ci}:

$$\begin{aligned} \overline{W}_{ci} = \frac{W_f}{2} \Bigg[& \left(\overline{\mathrm{AFR}} - 1\right)\left(1 - \overline{\mathrm{EGR}}_f\right) - \alpha \overline{\mathrm{EGR}}_f \\ & + \sqrt{\left(\left(\overline{\mathrm{AFR}} - 1\right)\left(1 - \overline{\mathrm{EGR}}_f\right) - \alpha \overline{\mathrm{EGR}}_f\right)^2 + 4\overline{AFR}\left(1 - \overline{\mathrm{EGR}}_f\right)} \Bigg]. \end{aligned} \tag{3.6}$$

Finally, solving for W_{xi} from (3.2b), considering the set points for AFR and EGR_f and using (3.6), we have

$$\overline{W}_{xi} = \frac{\overline{\mathrm{EGR}}_f}{1 - \overline{\mathrm{EGR}}_f} \overline{W}_{ci}. \tag{3.7}$$

Now using (2.2c), $\overline{p}_x$ corresponding to $\overline{W}_{xi}$ and $\overline{W}_{ci}$ is determined as

$$\overline{p}_x = p_i - \frac{R T_x^\star \overline{W}_{xi}^2}{2 A_r^2 p_i}, \tag{3.8}$$

where $T_x^\star$ is the optimal engine parameter when manifold temperatures are considered as slowly time-varying parameters (which is the case in this section) or is the real time-varying exhaust manifold temperature (see the next section). In addition, as we observe from (2.2c), A_r is always nonzero when $\overline{W}_{xi}$ is always nonzero. As a result, the set point values of AFR and EGR_f are expressed in terms of the set point values of p_x and W_{ci} given by (3.6) and (3.8).

3.2. Gain Scheduled Air Path Control with Constant Manifold Temperatures

The LPV diesel engine model with constant manifold temperatures (Section 2.1) was

$$\dot{p}_i = -k_3\rho_2 p_i + k_1\rho_1 P_c + k_2\tilde{u}_2, \tag{3.9a}$$

$$\dot{p}_x = l_1\rho_5 p_x + l_2 W_f - l_2\tilde{u}_1 - l_2\tilde{u}_2, \tag{3.9b}$$

$$\dot{P}_c = m_2\rho_4 p_x + m_1\rho_3\tilde{u}_1, \tag{3.9c}$$

where $\rho_1 = \dfrac{1}{(p_i/p_a)^\mu - 1}$, $\rho_2 = N$, $\rho_3 = 1 - \left(\dfrac{p_a}{p_x}\right)^\mu$, $\rho_4 = \dfrac{P_c}{p_x}$, $\rho_5 = \dfrac{Np_i}{p_x}$.

We assume $p_i \in [103,\, 160]\,\text{kPa}$, $p_x \in [105,\, 170]\,\text{kPa}$, $P_c \in [150,\, 2000]\,\text{W}$ and $N \in [1000,\, 2500]\,\text{rpm}$. Therefore, we take the corresponding range of parameters as $\rho_1 \in [6.82,\, 92.5]$, $\rho_2 \in [1000,\, 2500], \rho_3 \in [0.016,\, 0.143], \rho_4 \in [0.88,\, 19.04]$, $\rho_5 \in [911.5,\, 2500]$ (assuming $p_x - p_i \in [0,\, 10]$ kPa, which is a situation occurring in real applications). To put the model in (3.9) into the framework of Figure 2.3 for controller design phase, we use lfr-toolbox and obtain $\Delta = \mathbf{diag}\,(\bar{\rho}_1, \bar{\rho}_2, \cdots, \bar{\rho}_5)$ where $\bar{\rho}_i$, i=1:5, are parameters normalized about the mean of each ρ_i.

As air path control variables, we choose to track exhaust manifold pressure (p_x) and compressor air mass flow (W_{ci}). The tracking configuration is shown in Figure 3.1. Note that the designed LPV controller is applied in an anti-windup (AW) form. The AW method used is the one developed in [45] and is described in Appendix E. Using

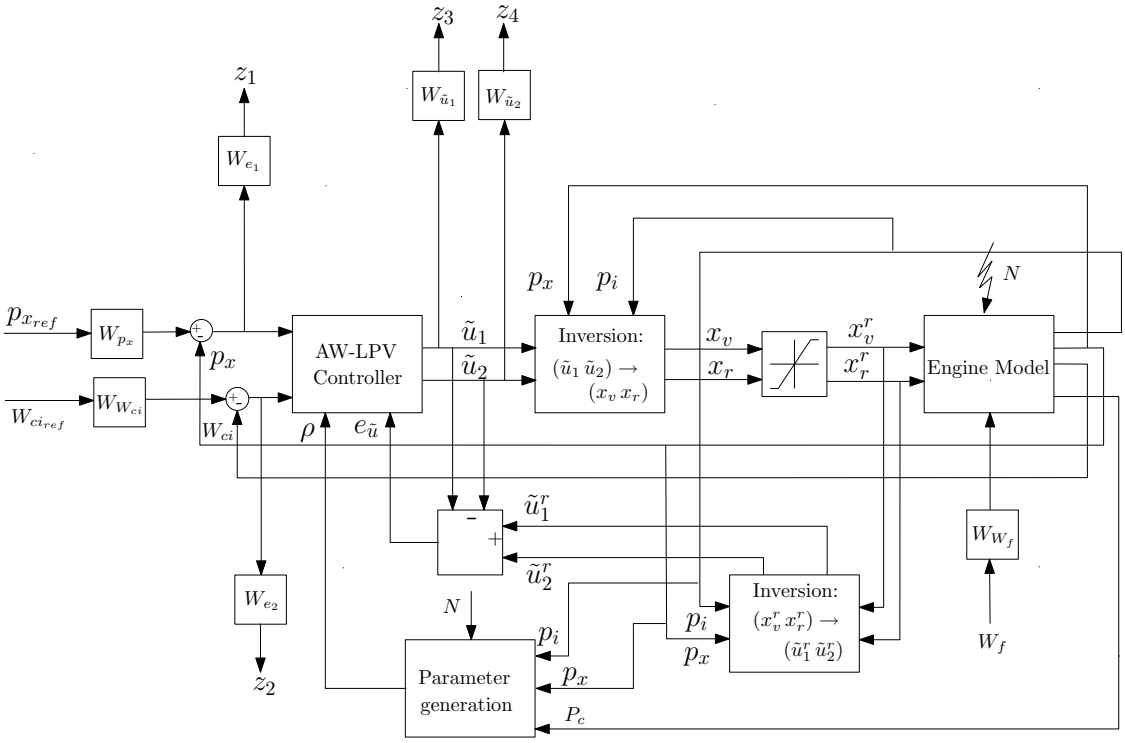

Figure 3.1. Closed-loop system with inversion mappings, AW and weights.

manifold pressures, determined modified control inputs are inverted to obtain VGT vane and EGR valve positions, which are, then, passed through the saturation block to guarantee achievement of physically meaningful control inputs (which are called real process inputs). The possible negative effect of saturation block is compensated by first inverting the the real process inputs to obtain the corresponding modified real process control inputs and then feeding the difference between modified control inputs and modified real process inputs to the AW-LPV controller. The AW-LPV controller is also scheduled by $\rho = [\rho_1,\, \rho_2,\, \rho_3,\, \rho_4,\, \rho_5]^T$. Fuel rate, W_f, is considered as disturbance on the system. Although for tracking of p_x and W_{ci} it is necessary just to measure p_x and W_{ci}, from definition of scheduling parameters and inversion mappings, all states p_i, p_x and P_c are necessarily measured.

Weight selection, which involves trail and error most of the time, is an important task and strongly affects the performance of the controller. The chosen frequency

weights are as follows.

$$W_{p_x} = W_{W_{ci}} = \frac{6.283}{s+6.283},\ W_{W_f} = 1,\ W_{e_1} = \frac{300}{s+0.01},$$
$$W_{e_2} = \frac{600}{s+0.01},\ W_{\tilde{u}_1} = W_{\tilde{u}_2} = 1.$$

Next, tracking of some $W_{ci} - p_x$ set points, the associated process control inputs and the states $P_c - p_i$ are shown in the following cases. The obtained $\mathcal{L}_2$-gain of the controlled closed-loop system, γ, is 76. In all cases, the initial conditions are $p_i(0) =$ 103 kPa, $p_x(0) = 109$ kPa and $P_c(0) = 150$ W.

3.2.1. Case I

In the first case study, we will track set points consisting of one step. The fuel flow rate and engine speed are consisting of two steps. The corresponding plots are shown through Figures 3.2-3.5.

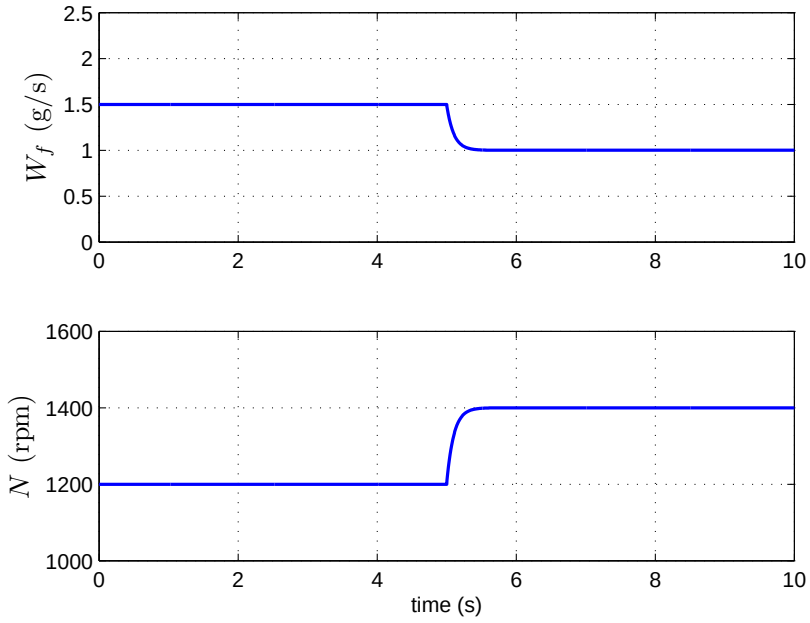

Figure 3.2. Fuel flow rate and engine speed

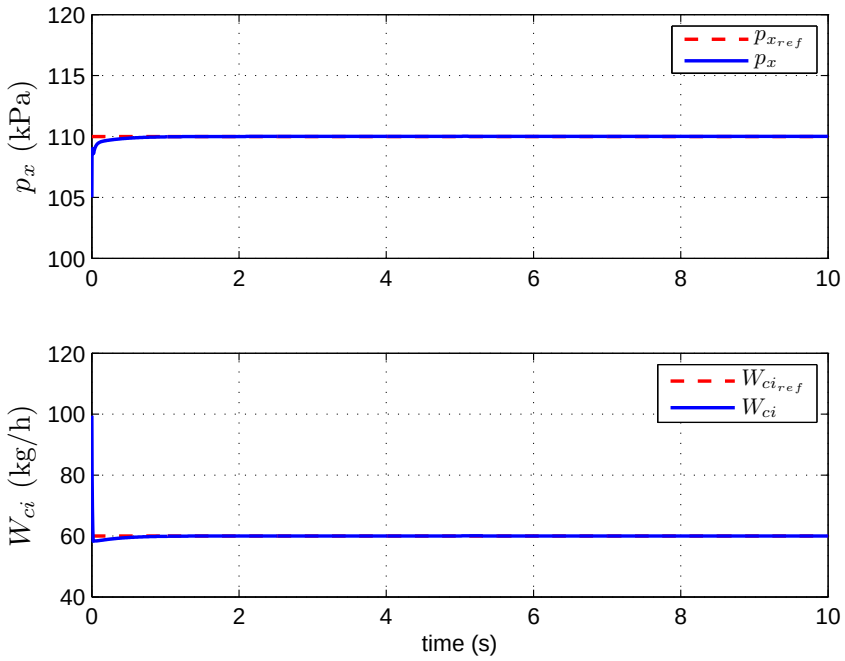

Figure 3.3. Exhaust manifold pressure, compressor air mass flow references and the corresponding system response

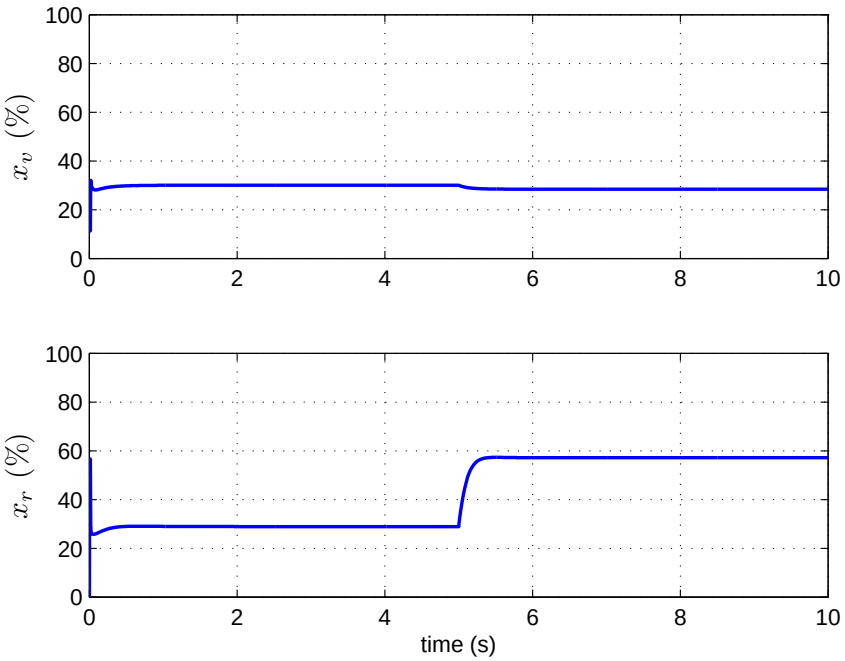

Figure 3.4. Vgt vane and egr valve positions

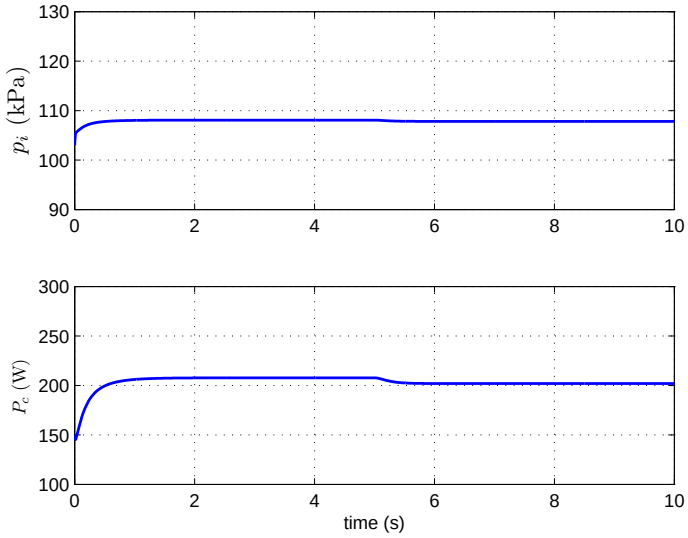

Figure 3.5. Intake manifold pressure and compressor power

3.2.2. Case II

In the second case study, we will track set points such that p_x consists of three steps step and W_{ci} consists of one step. The fuel flow rate and engine speed are taken as one step signals. The corresponding plots are shown through Figures 3.6 and 3.9.

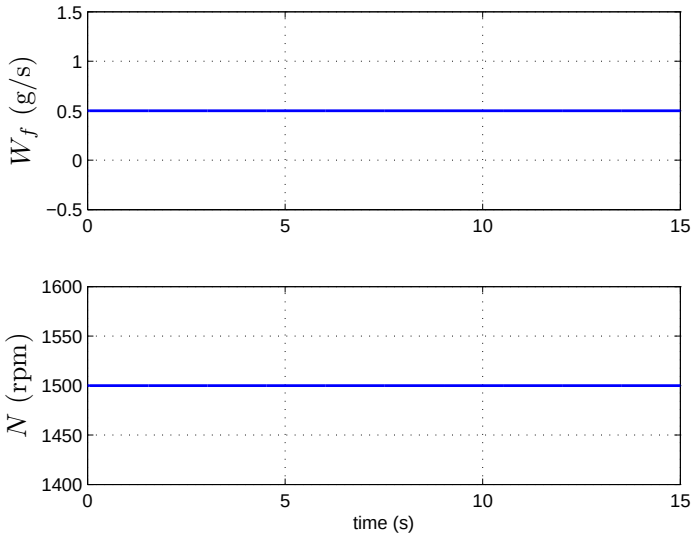

Figure 3.6. Fuel flow rate and engine speed

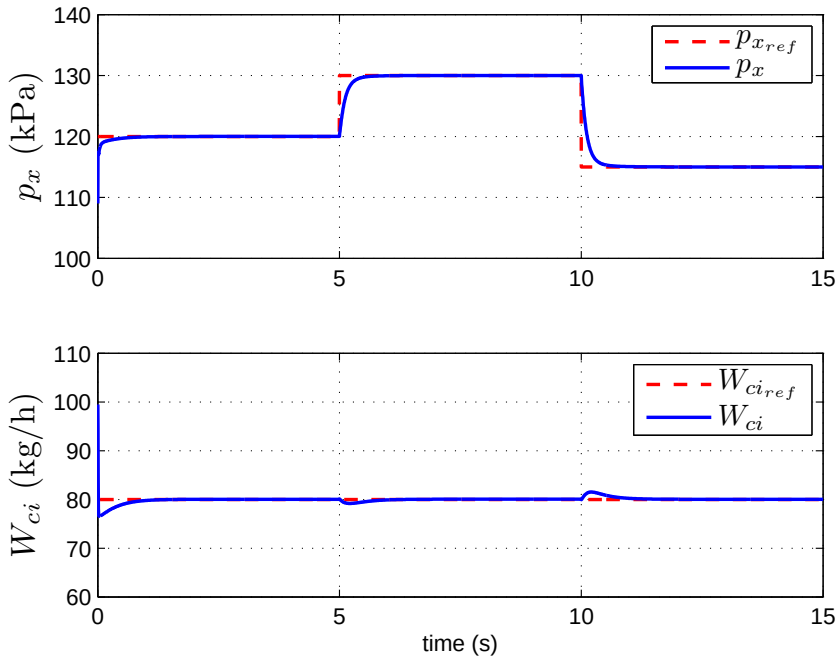

Figure 3.7. Exhaust manifold pressure, compressor air mass flow references and the corresponding system response

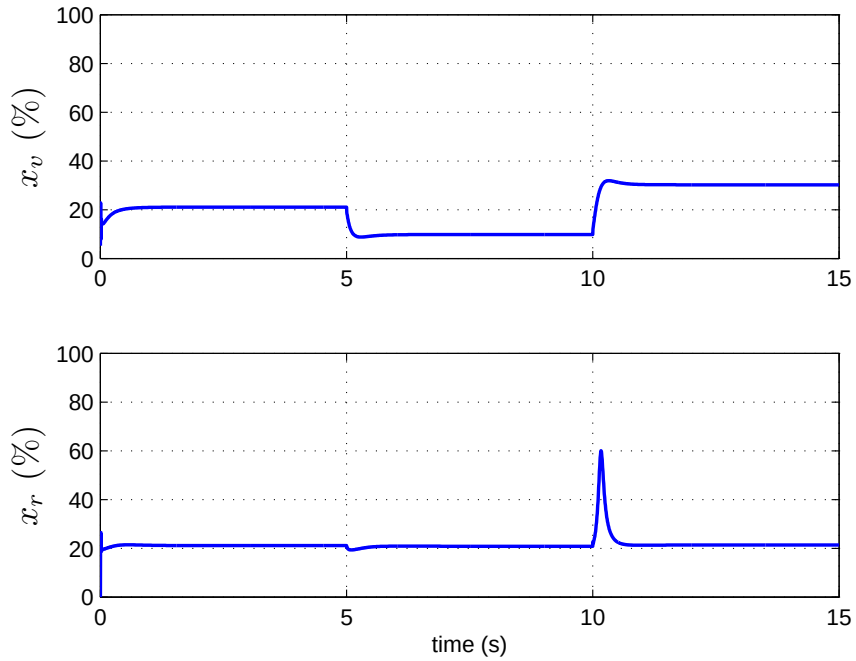

Figure 3.8. Vgt vane and egr valve positions

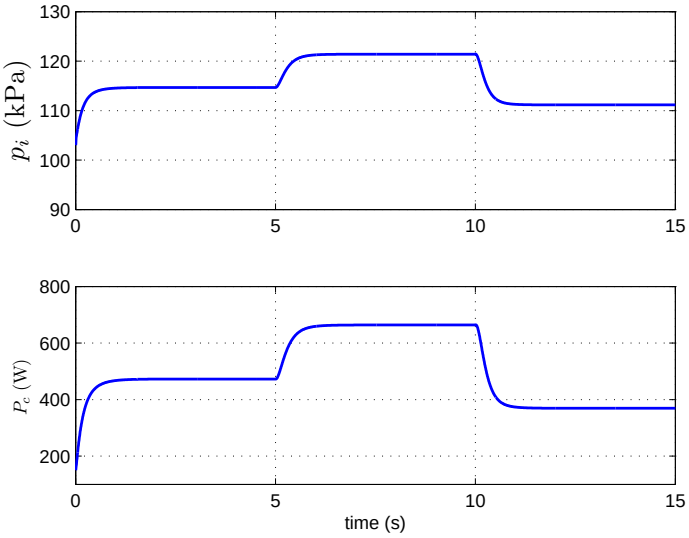

Figure 3.9. Intake manifold pressure and compressor power

3.2.3. Case III

In the third case study, we will track set points such that p_x consists of one step but W_{ci} consists of three steps. The fuel flow rate and engine speed are taken sinusoidal signals. The corresponding plots are shown through Figures 3.10 and 3.13.

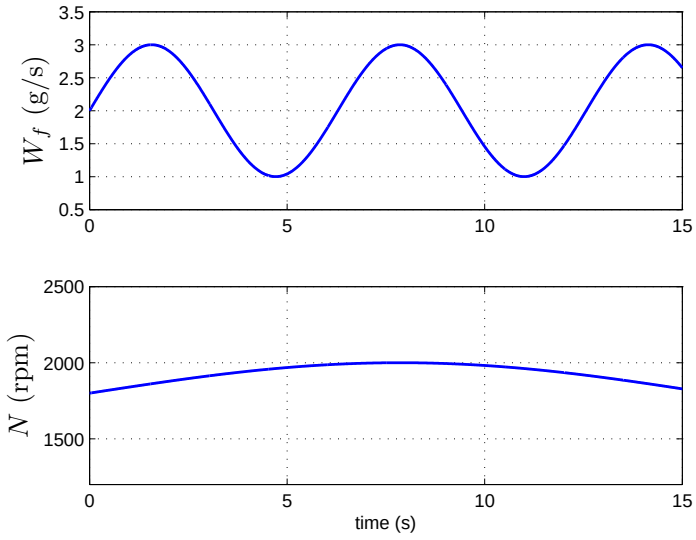

Figure 3.10. Fuel flow rate and engine speed

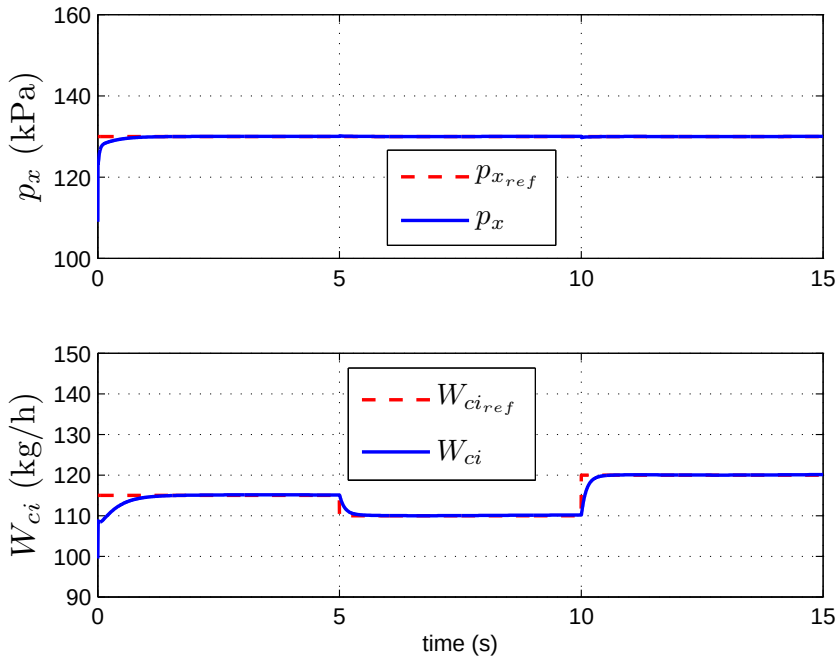

Figure 3.11. Exhaust manifold pressure, compressor air mass flow references and the corresponding system response.

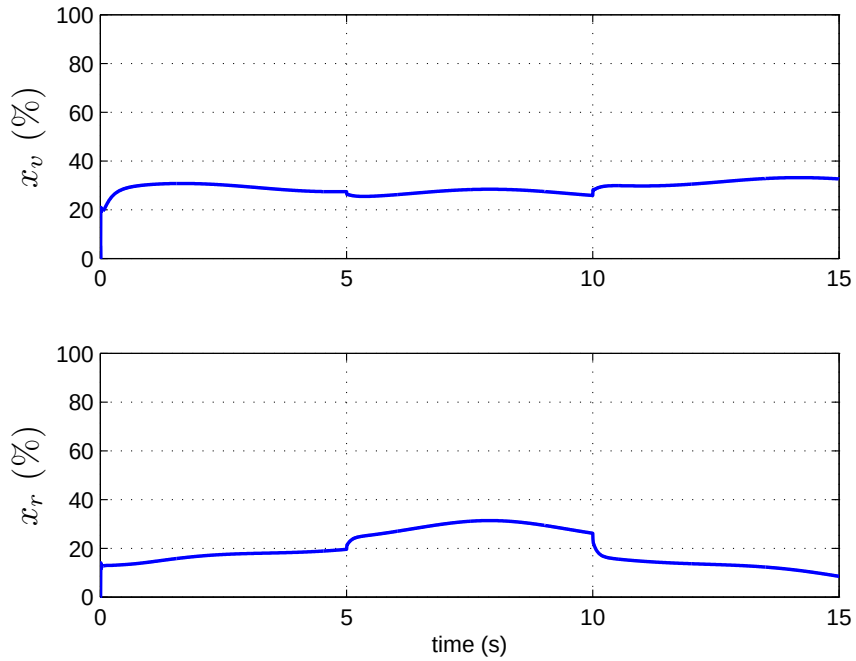

Figure 3.12. Vgt vane and egr valve positions

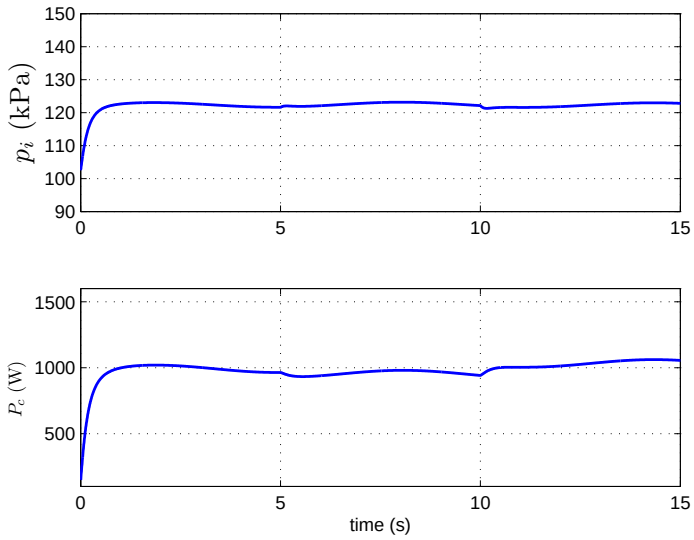

Figure 3.13. Intake manifold pressure and compressor power

3.2.4. Case IV

In the last case study, we will track set points such that p_x and W_{ci} are sinusoids. The fuel flow rate and engine speed consist of one step. The corresponding plots are shown through Figures 3.14 and 3.17.

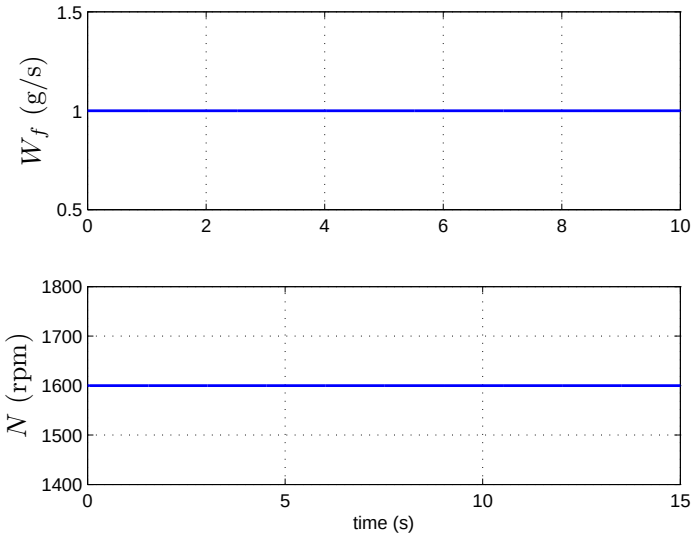

Figure 3.14. Fuel flow rate and engine speed

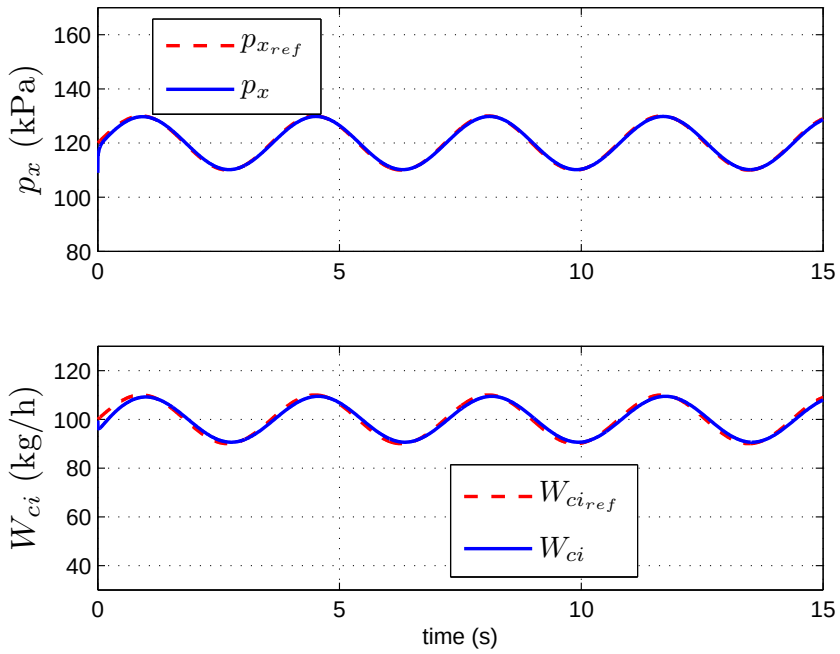

Figure 3.15. Exhaust manifold pressure, compressor air mass flow references and the corresponding system response

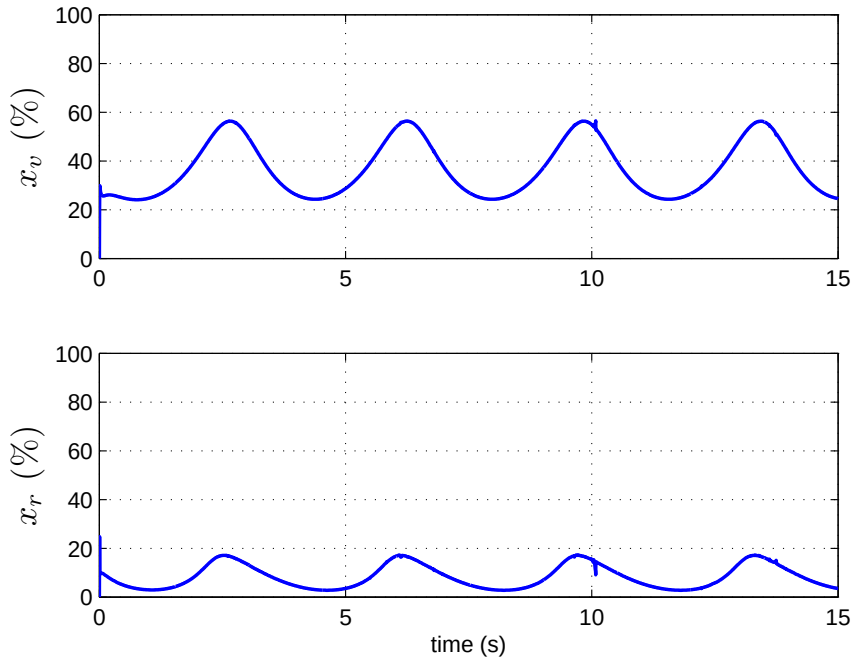

Figure 3.16. Vgt vane and egr valve positions

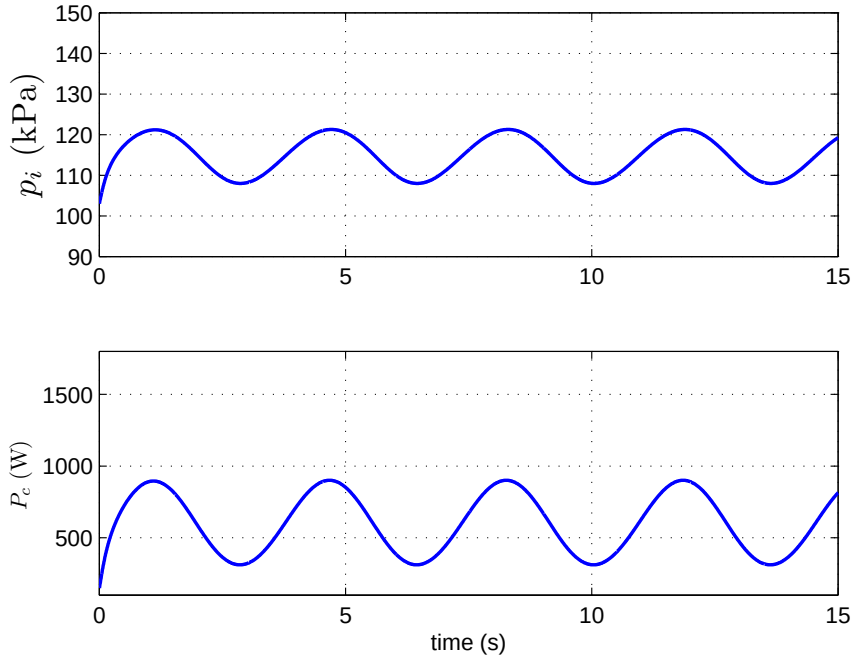

Figure 3.17. Intake manifold pressure and compressor power

3.3. Gain Scheduled Air Path Control with Variable Manifold Temperatures

The LPV diesel engine model with variable manifold temperatures (Section 2.2) was

$$\dot{p}_i = -\hat{k}_3\rho_2 p_i + \hat{k}_1\rho_1\rho_6 P_c + \hat{k}_2\rho_6\tilde{u}_2, \tag{3.10a}$$

$$\dot{p}_x = \hat{l}_1\frac{\rho_5\rho_7}{\rho_6}p_x + \hat{l}_2\rho_7 W_f - \hat{l}_2\rho_7\tilde{u}_1 - \hat{l}_2\rho_7\tilde{u}_2, \tag{3.10b}$$

$$\dot{P}_c = \hat{m}_2\rho_4 p_x + \hat{m}_1\rho_3\rho_7\tilde{u}_1, \tag{3.10c}$$

where $\rho_i, i = 1:5$ are as in the previous section and $\rho_6 = T_i$, $\rho_7 = T_x$. We assume that intake and exhaust manifold temperatures vary in $300 - 350$ K and $350 - 700$ K, respectively. I.e., $\rho_6 \in [300, 350]$ and $\rho_7 \in [350, 700]$. Again to put the model into (3.10) in the framework of Figure 2.3 for controller design phase, we use lfr-toolbox and obtain $\Delta = \mathbf{diag}\,(\bar{\rho}_1, \bar{\rho}_2, \bar{\rho}_3, \bar{\rho}_4, \bar{\rho}_5, \bar{\rho}_6 I_2, \bar{\rho}_7 I_2)$. W_f is again taken as a disturbance

signal. The weight set is now as follows

$$W_{p_x} = W_{W_{ci}} = \frac{6.283}{s+6.283},\ W_{W_f} = 1,\ W_{e_1} = \frac{60}{s+0.01},$$
$$W_{e_2} = \frac{120}{s+0.01},\ W_{\tilde{u}_1} = W_{\tilde{u}_2} = 1.$$

The controller implementation is in the same way as in Figure 3.1, except now two more parameters are added and in the inversion mappings T_x is also used. Next, we consider two case studies for the illustration of the performance of the more general controller designed in this part. The obtained $\mathcal{L}_2$-gain of the closed system in this case is 217.5 and the initial conditions are the same as before.

3.3.1. Case I

In this case study, fuel flow rate consists of one step, engine speed is a sinusoid, manifold temperatures and $p_x - W_{ci}$ references consist of three steps. The corresponding plots are shown through Figures 3.18 and 3.21.

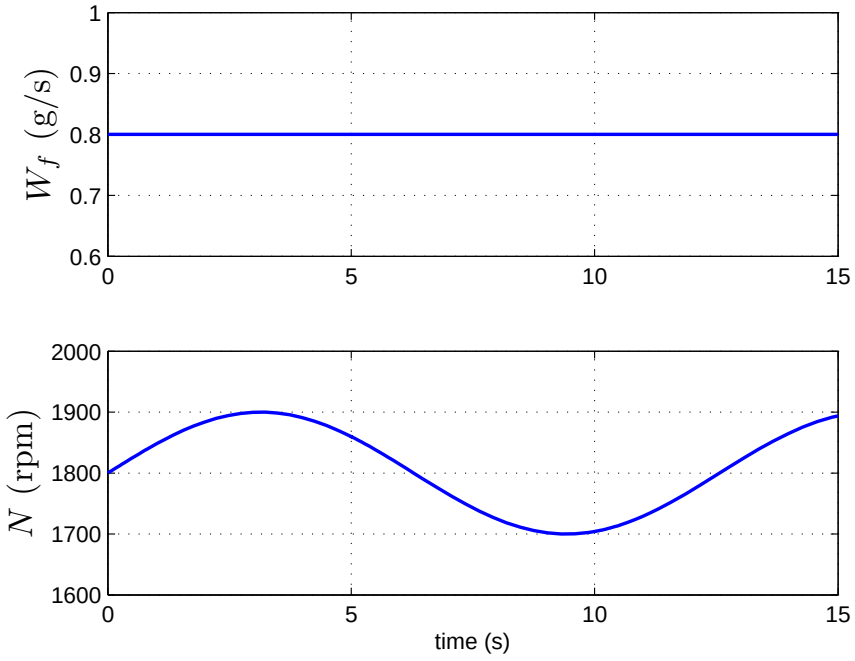

Figure 3.18. Fuel flow rate and engine speed

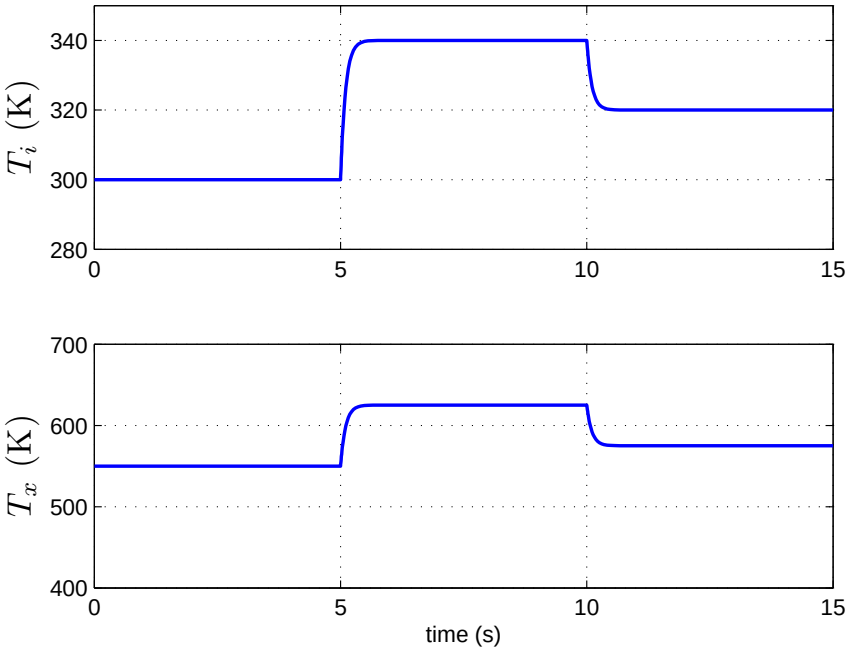

Figure 3.19. Intake and exhaust manifold temperatures

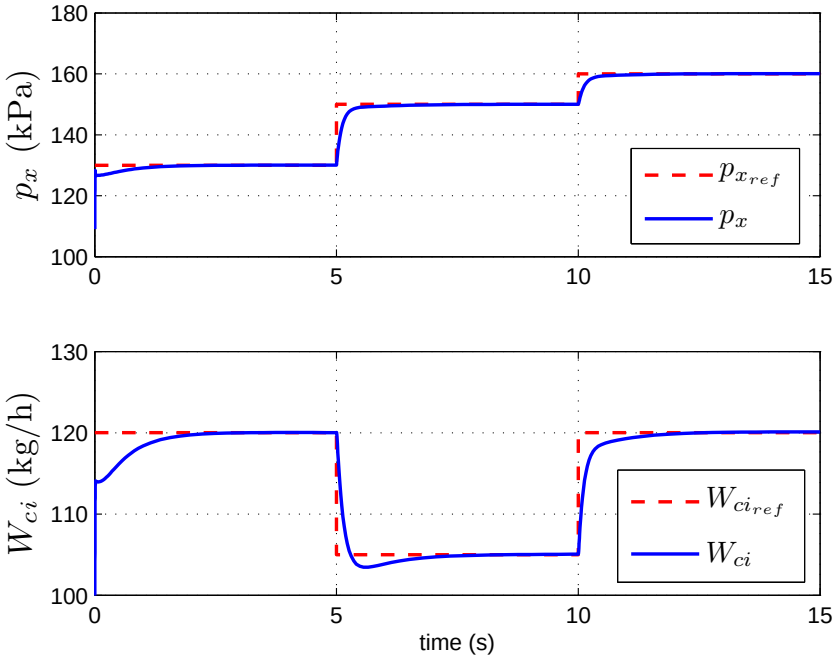

Figure 3.20. Exhaust manifold pressure, compressor air mass flow references and the corresponding system response

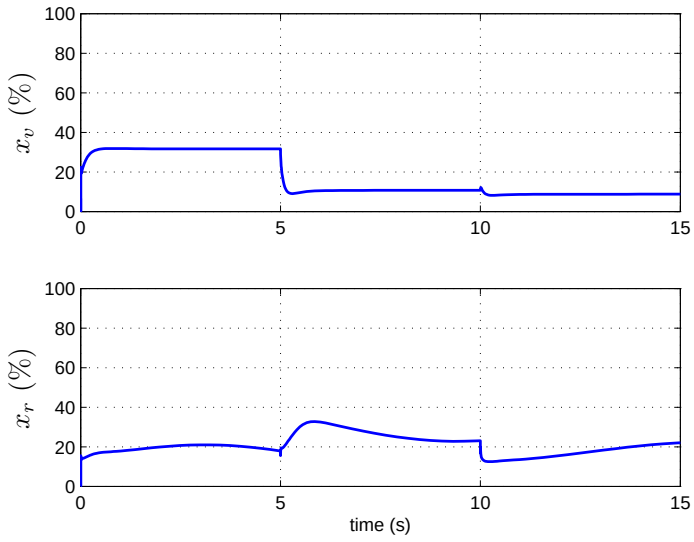

Figure 3.21. Vgt vane and egr valve positions.

3.3.2. Case II

In the second case study, fuel flow rate and manifold temperatures are sinusoids engine speed and $p_x - W_{ci}$ references consist of three steps. The corresponding plots are shown through Figures 3.22 and 3.25.

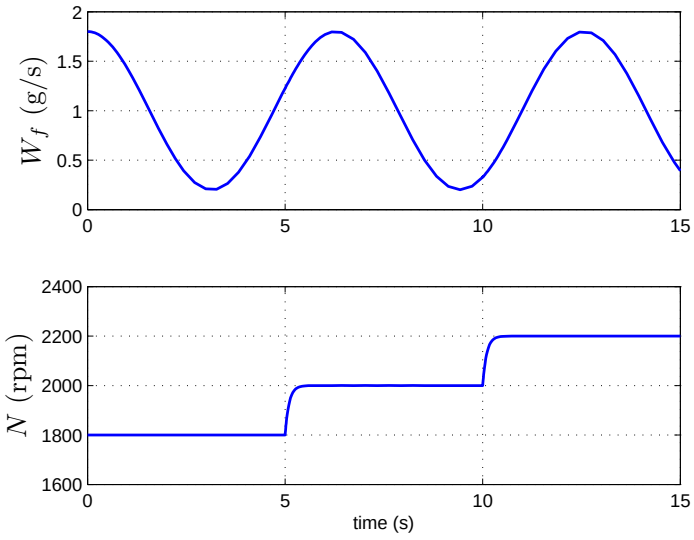

Figure 3.22. Engine speed and fuel flow rate

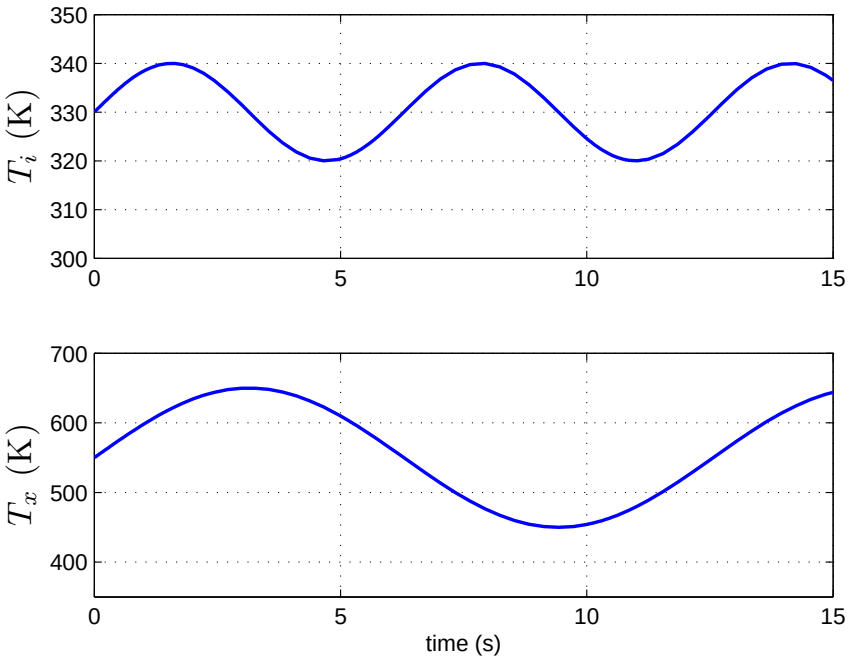

Figure 3.23. Intake and exhaust manifold temperatures

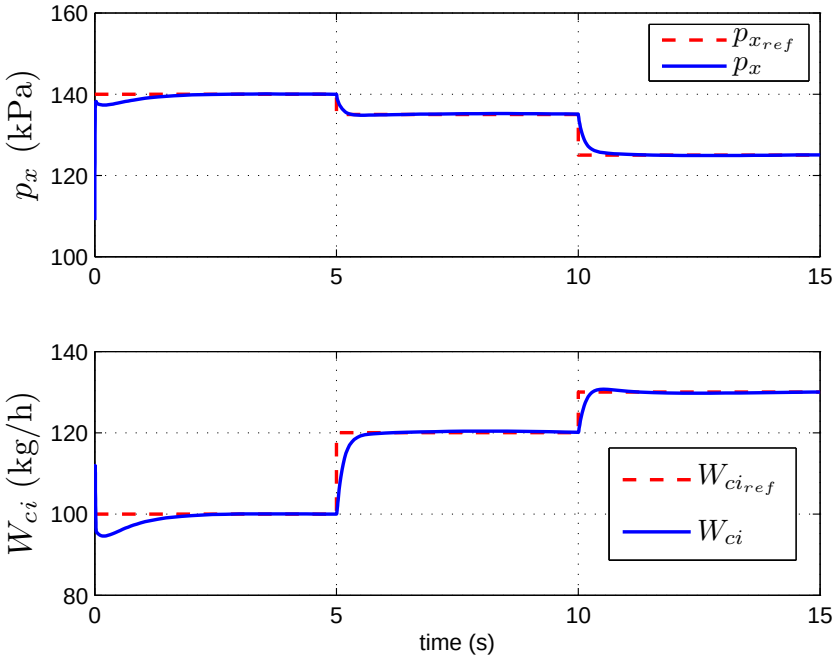

Figure 3.24. Exhaust manifold pressure, compressor air mass flow references and the corresponding system response

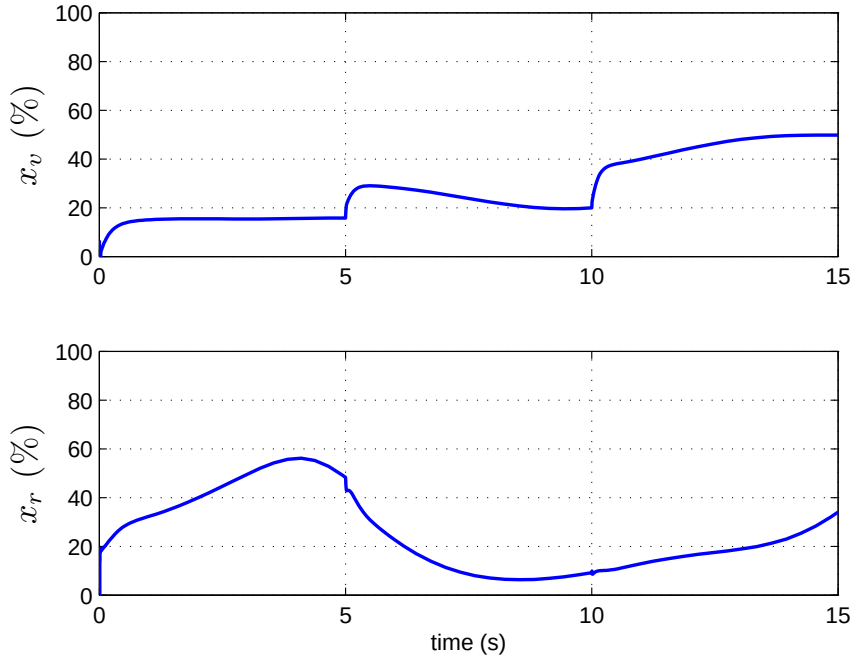

Figure 3.25. Vgt vane and egr valve positions

3.4. Comments

From the simulation results in Sections 3.2 and 3.3, we see that the performance of the gain scheduled controllers are quite well. The considered parameter ranges are wide enough to cover practical applications. The settling time of the system under the the gain scheduled AW-LPV controller of Section 3.3 is a little bit high compared to that of the controller designed in Section 3.2. This is due to the high range of temperature variables included in the second section. To see the importance of taking manifold temperatures as variables, let us use both AW-LPV controllers for the variable manifold temperatures model to track the $p_x - W_{ci}$ references. The fuel flow rate is $W_f = 1+0.8\cos(\mathrm{t})$ (g), $N = 2000+300\sin(\mathrm{t})$ (rpm), $T_i = 320+20\sin(10\mathrm{t})$ (K) and $T_x = 450+50\sin(10\mathrm{t})$ (K). The results are shown in Figure 3.26. Red-color signals are references, blue color are the results using AW-LPV controller designed under the assumption of variable manifold temperatures and the black color signals are results using AW-LPV controller designed under the assumption of constant manifold temperatures. As seen, the second controller is not robust to variable manifold temperatures.

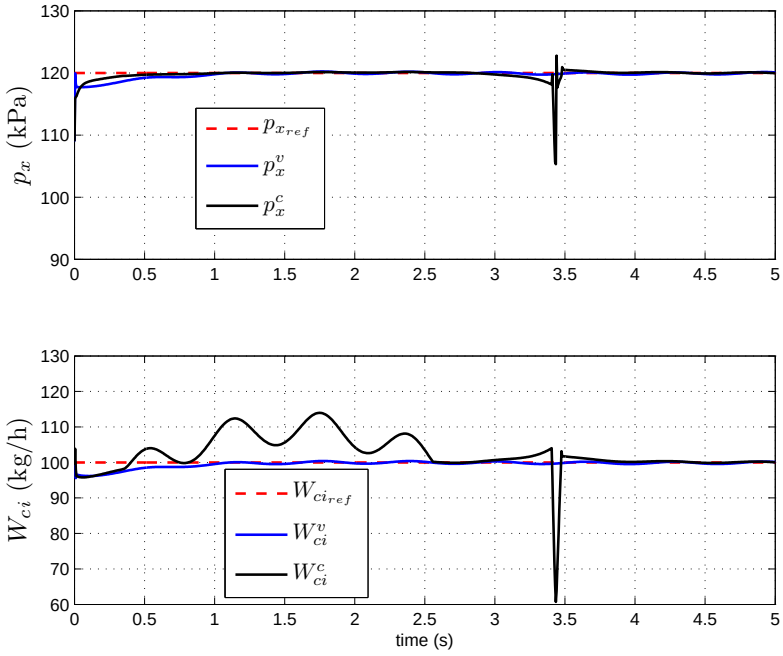

Figure 3.26. Performance of AW-LPV controllers for the variable manifold temperatures model

3.5. Comparison of Gain-Scheduled and H_∞ Controllers

In this section, to appreciate the importance of air path system control using a gain-scheduled approach, we will compare performances of the gain-scheduled controller based on variable manifold temperatures and a H_∞ controller based on a linearized model of the engine around an equilibrium point of the nonlinear engine model. The main external parameters to the system are $N \in [1000, 2500]$ rpm, $T_i \in [300, 350]$ K and $T_x \in [350, 700]$ K. To find an equilibrium point of the system we first choose nominal values of these external parameters. That is, we take $N_{\text{nom}} = 1750$ rpm, $T_{i_{\text{nom}}} = 325$ K and $T_{x_{\text{nom}}} = 525$ K. The equilibrium set point values for the engine inputs (modified inputs) and fuel flow rate are taken as $W_{xt_{\text{eq}}} = 25$ g, $W_{xi_{\text{eq}}} = 10$ g and $W_{f_{\text{eq}}} = 1$ g. The corresponding equilibrium states are determined as $p_{i_{eq}} = 125$ kPa, $p_{x_{eq}} = 133.5$ kPa and $P_{c_{eq}} = 823$ W. The linearized model around the equilibrium

points is

$$\begin{aligned}\dot{\tilde{x}} =& A\tilde{x} + B\tilde{u},\\ \tilde{y} =& C\tilde{x} + D\tilde{u},\end{aligned}$$

where

$$A = \begin{pmatrix} -17.58 & 0 & 453.22 \\ 40.99 & 0 & 0 \\ 0 & 0.18 & -9.09 \end{pmatrix}, B = \begin{pmatrix} 0 & 0 & 15.54 \\ 150.67 & -150.67 & -150.67 \\ 0 & 0.29 & 0 \end{pmatrix},$$

$$C = \begin{pmatrix} 0 & 1 & 0 \\ -3.09 & 0 & 104.95 \end{pmatrix}, D = \begin{pmatrix} 0 & 0 & 0 \\ 0 & 0 & 0 \end{pmatrix},$$

$$\tilde{x} = \begin{pmatrix} p_i - p_{i_{\text{eq}}} \\ p_x - p_{x_{\text{eq}}} \\ P_c - P_{c_{\text{eq}}} \end{pmatrix}, \tilde{u} = \begin{pmatrix} W_f - W_{f_{\text{eq}}} \\ W_{xt} - W_{xt_{\text{eq}}} \\ W_{xi} - W_{xi_{\text{eq}}} \end{pmatrix}, \tilde{y} = \begin{pmatrix} p_x - p_{x_{\text{eq}}} \\ W_{ci} - \dfrac{\eta_c}{c_p T_a} \dfrac{P_{c_{\text{eq}}}}{\left(\dfrac{p_{i_{\text{eq}}}}{p_a}\right)^{\mu} - 1} \end{pmatrix}.$$

For the H_∞ controller, the weight selection is the same as in Section 3.3. The obtained $\mathcal{L}_2$-gain, γ is 1.0664. The controller implementation is the same as before.

Next, we will consider two case studies. In the first case study, we will set the values of main external variables N, T_i and T_x close to their nominal values and track set points for $p_x - W_{ci}$ which are close to their equilibrium values. Then, we will compare the performances of the two controllers. In the second case study, we will choose values of N, T_i and T_x far from their nominal values and track set points for $p_x - W_{ci}$ which are also far from their equilibrium values. Again, we will compare the performance of the two controllers. In comparison figures, the red color signals are the reference signals, the blue color signals are the system response or control inputs with gain-scheduled controller and the green color signals are those corresponding to H_∞ controller.

3.5.1. Case I

In this case study, fuel flow rate, engine speed and manifold temperatures are all sinusoids around their nominal values and $p_x - W_{ci}$ references consist of two steps. The corresponding plots are shown through Figures 3.27 and 3.30.

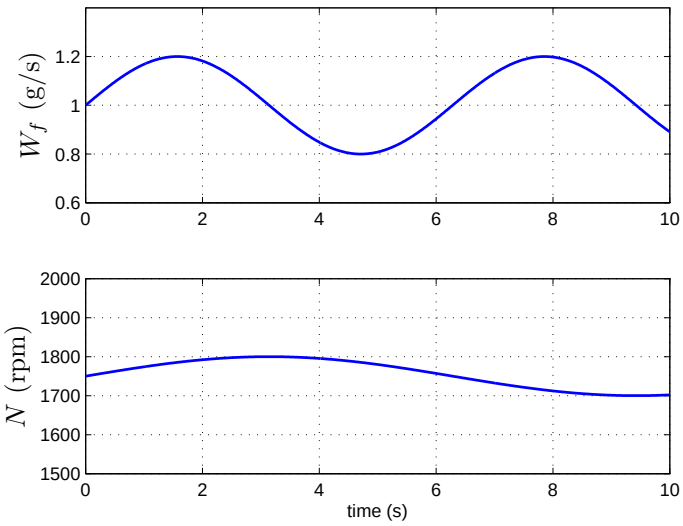

Figure 3.27. Fuel flow rate and engine speed

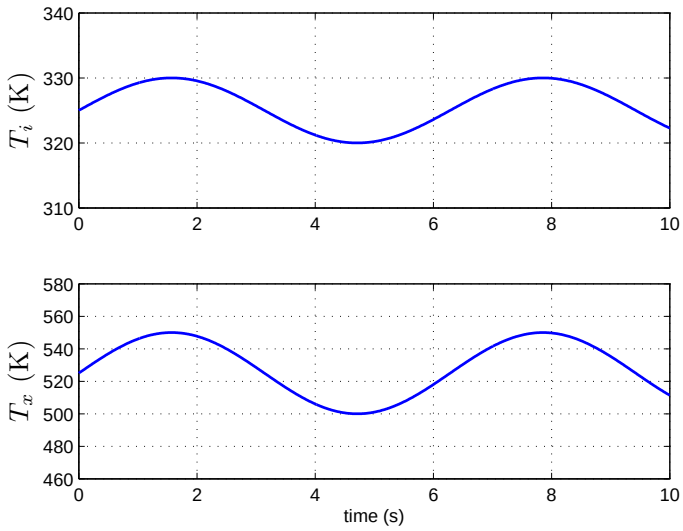

Figure 3.28. Intake and exhaust manifold temperatures

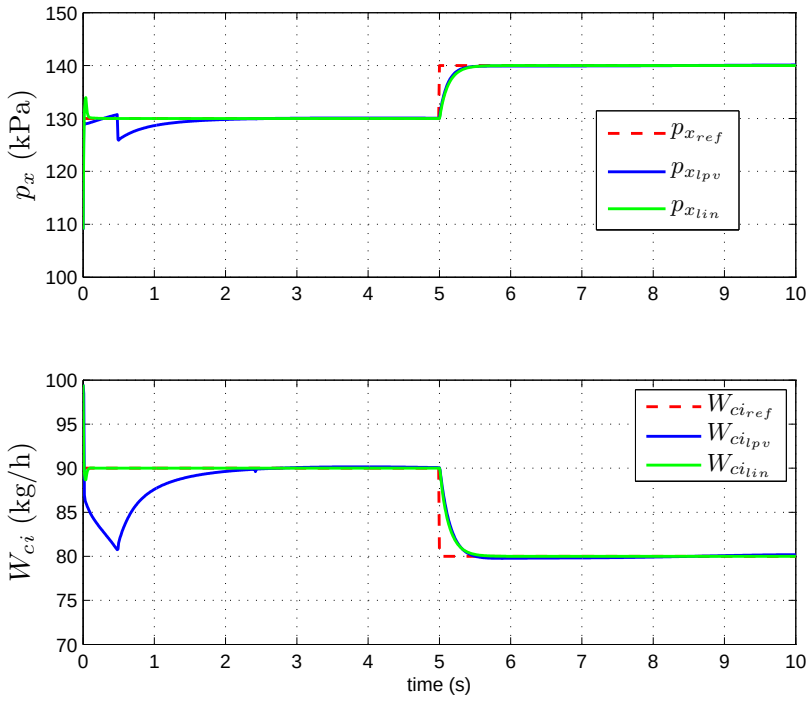

Figure 3.29. Exhaust manifold pressure, compressor air mass flow references and the corresponding system response

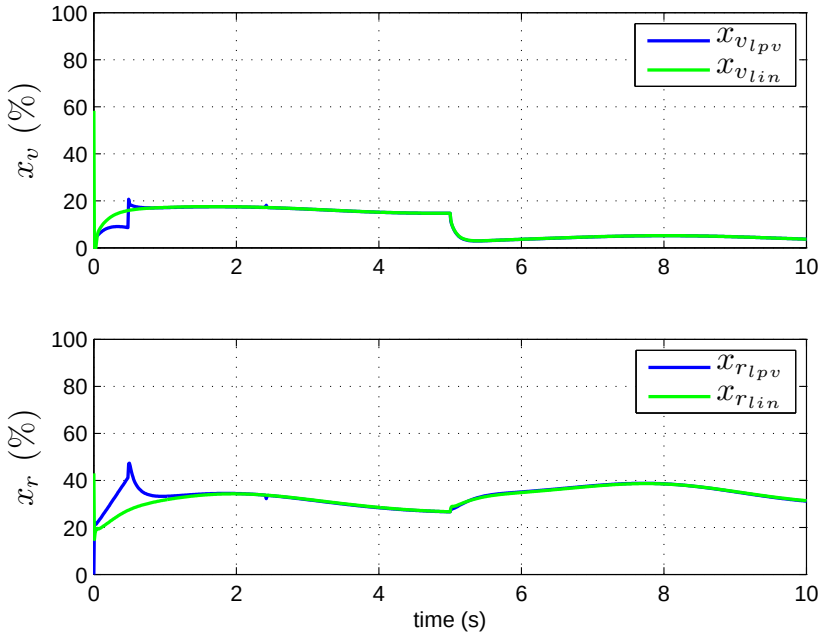

Figure 3.30. Vgt vane and egr valve positions

3.5.2. Case II

In the second case study, fuel flow rate and engine speed are sinusoids, manifold temperatures are steps and $p_x - W_{ci}$ references consist of two steps. The corresponding plots are shown through Figures 3.31 and 3.34.

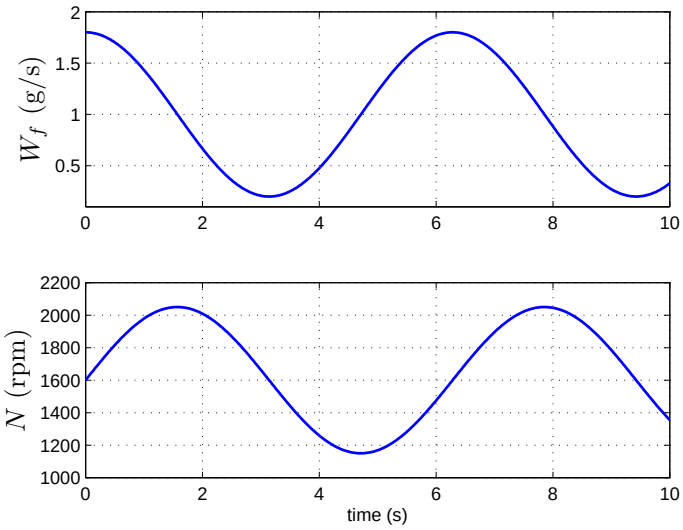

Figure 3.31. Fuel flow rate and engine speed

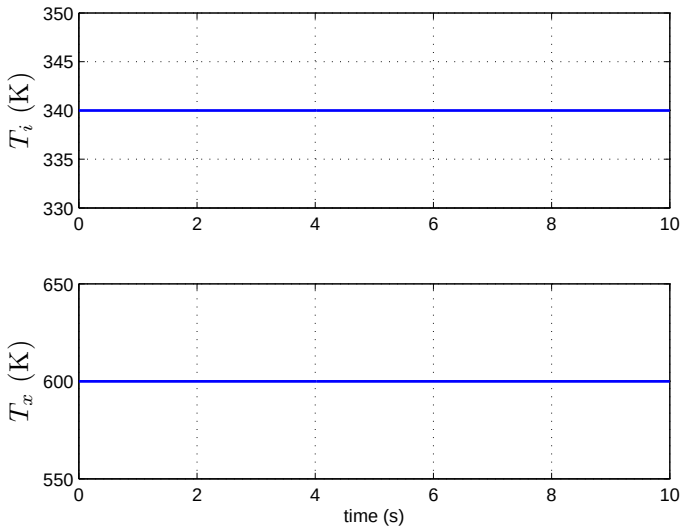

Figure 3.32. Intake and exhaust manifold temperatures

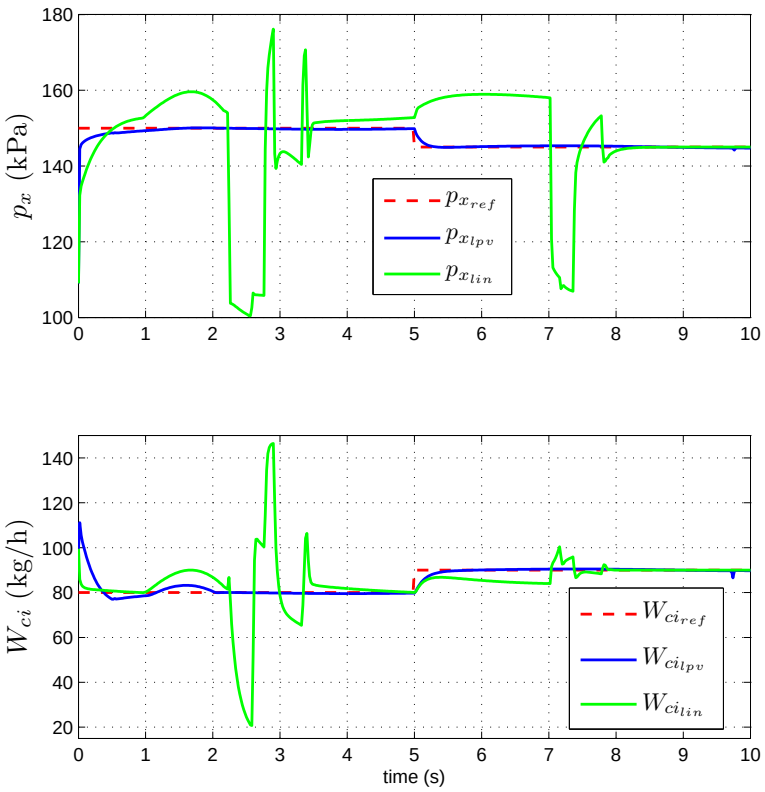

Figure 3.33. Exhaust manifold pressure, compressor air mass flow references and the corresponding system response

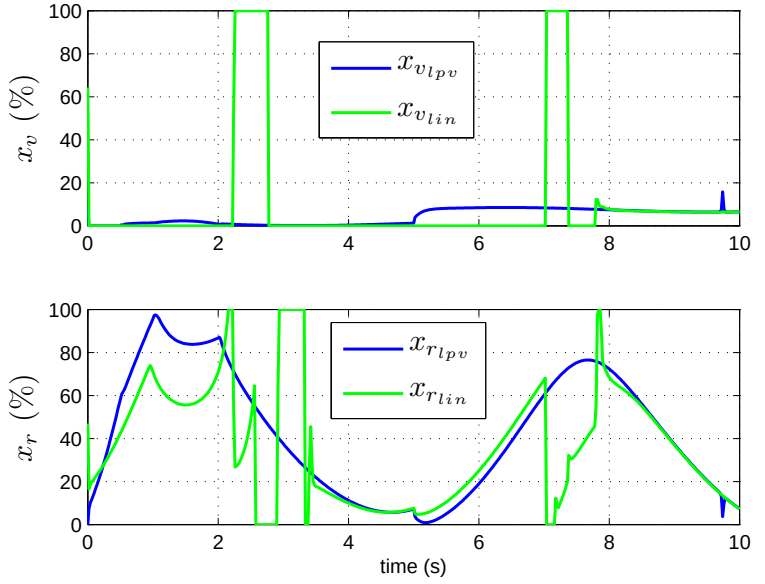

Figure 3.34. Vgt vane and egr valve positions

From the first case study we see that H_∞ controller and gain-scheduled controller produce almost the same results when the main external parameters N, T_i and T_x are around their nominal values and when the tracked outputs are close to their equilibrium values. Interestingly, for the first case study the performance of H_∞ controller is better than that of gain-scheduled controller. The reason for this is that the gain-scheduled controller works in a wide range of operating points and this comes at a cost of performance decrease. On the other hand, the second case study clearly illustrates that H_∞ controller does not work when the parameters N, T_i and T_x are far from their nominal values and/or when the reference set points for the outputs are far from their equilibrium values. As a conclusion, when the wide range of engine operating points is considered, it is very possible that a linear controller will not work. This implies the necessity of gain-scheduled controllers for engine air path control.

4. COMPRESSOR AIR MASS FLOW ESTIMATION VIA AN IDENTIFICATION-BASED ESTIMATION METHOD

In turbocharged diesel engines with EGR, compressor flow is measured by a mass air flow (MAF) sensor, which have limited accuracy and is more expansive than a manifold absolute pressure (MAP) sensor or exhaust manifold pressure sensors. In addition, when the pressure drop across the compressor is close to 1, compressor flow is typically low and the accuracy of MAF is weak. Other conditions affecting the accuracy are oscillations in the engine and back-flow situations. In most control oriented engine applications, compressor flow is a feedback signal and a poor measurement of this signal may result in poor control performance, which in turn, affects the fuel economy. Therefore, from both cost reduction point of view and good quality signal point of view for control problems, accurate estimation of compressor flow is an important task in diesel engine applications.

We consider again the diesel engine model of Chapter 3, where manifold temperatures are considered as time-varying parameters. Taking temperatures variable parameters is important since in estimation problems the underlying model must be accurate as much as possible. The mean-value engine model of the previous chapter is repeated below for the sake of completeness purposes.

$$\dot{p}_i = \left[\frac{R\eta_c}{V_i c_p T_a}\right] T_i \frac{P_c}{\left(\frac{p_i}{p_a}\right)^{\mu} - 1} + \left[\frac{R}{V_i}\right] T_i \tilde{u}_2 - \left[\frac{\eta_v V_d}{120 V_i}\right] N p_i, \tag{4.1a}$$

$$\dot{p}_x = \left[\frac{\eta_v V_d}{120 V_x}\right] \frac{N T_x}{T_i} p_i + \left[\frac{R}{V_x}\right] T_x \tilde{u}_3 - \left[\frac{R}{V_x}\right] T_x \tilde{u}_1 - \left[\frac{R}{V_x}\right] T_x \tilde{u}_2, \tag{4.1b}$$

$$\dot{P}_c = \left[\frac{1}{\tau}\right] P_c + \left[\frac{c_p \eta_t}{\tau}\right] T_x \left(1 - \left(\frac{p_a}{p_x}\right)^{\mu}\right) \tilde{u}_1, \tag{4.1c}$$

where the terms in the square brackets are constants, $\tilde{u}_1 = W_{xt}, \tilde{u}_2 = W_{xi}, \tilde{u}_3 = W_f$ and the terms N, T_i, T_x are interpreted also as inputs.

The structural property of the above model is that although the model is a

nonlinear model, the state variable P_c appears linearly in the equations. In this chapter, we develop a general method to estimate unmeasured states appearing linearly in deterministic nonlinear models and then apply to estimate compressor power. The compressor air mass flow will be estimated indirectly from

$$W_{ci} = \frac{\eta_c}{c_p T_a} \frac{P_c}{\left(\frac{p_i}{p_a}\right)^m u - 1}. \tag{4.2}$$

The developed method is based on a recursive least-squares identification algorithm. The proposed method possesses some superior properties, mainly its simplicity and better estimation performance, compared to other typical estimation methods. The effectiveness of the method is demonstrated on academic-purpose constructed case studies and then applied to diesel engine compressor air mass flow estimation, all with a comparison to the popular extended kalman filter (EKF). Although the method is developed for state estimation, it can be easily modified for time-varying parameter (appearing linearly in the equations) estimation.

The chapter is organized as follows. In Section 1, a general introduction for state estimation methods is given. Section 2 details the developed estimation method including the error analysis. Section 3 demonstrates the application of the method to case studies with a comparison to EKF. Section 4 is devoted to the employment of the developed method to compressor air mass flow in diesel engines and, again, with a comparison to EKF. Finally, the main findings of this chapter are presented in Section 5 of the chapter.

4.1. Introduction

State estimation using measured outputs and inputs is an important problem in engineering applications where the underlying process requires control, monitoring, fault diagnosis, etc. Sometimes it is not possible to measure some states or it is not desirable for cost reduction purposes. For linear systems, this topic has been

extensively studied and has proven useful results especially for control applications such as observer-based control design. Most of engineering models are nonlinear systems and therefore linear methods cannot be applied. For nonlinear systems this topic is neither complete nor successful in contrast to linear systems. In literature, different approaches have been developed based on different tools and taking into account the specific structure of the underlying dynamics.

Among all nonlinear state estimation methods, the celebrated EKF is by far the most popular and dominant approach [47, 48, 49, 50]. In the EKF approach, linearization about the current mean and covariance is performed and a Riccati equation is solved to obtain the estimator gain. The main drawback of the EKF method is that it requires the knowledge of the noisy model. Most of the time this is not known perfectly and the model involves uncertainties. A mismatch may cause biased estimation results or even divergence [51]. In addition, since linearization techniques are employed convergence and speed of convergence are local properties which in turn imply that while the estimation error converges in a given time interval, it may diverge in another one. The speed of the convergence is also dependent on the initial value of the covariance matrix, which is assumed to start the algorithm [52]. The approximation issues of the EKF method are handled in the unscented Kalman filter method but this brings additional computational burden and complication. The application of EKF to deterministic nonlinear systems can be done in two ways. First, by adding a small noise component to the model and then performing state estimation. In this case, one faces the main flaws of the EKF mentioned above. The second way is addition of a fictitious noise component to account for linearization errors, resulting in a tuning problem, which again may not be an easy task.

The second class of approaches to nonlinear state estimation are based on Lyapunov stability results, for example [53]. They produce sufficient conditions (even in global sense) for the existence of observers. Since they are based on Lyapunov theory, there is no constructive procedure and most of time trial and error is done and the method cannot be used practically for higher dimensional and complicated systems.

The third class is called extended linearization, for example as in [54, 55]. In such methods, an operating point is chosen, a function of output is injected to state dynamics to make linearized error dynamics have locally constant eigenvalues. Since the method works locally, a serious improvement is not brought.

The fourth group of methods are based on a Lie-algebraic approach [56, 57]. The nonlinear system is converted to a linear system through a nonlinear state transformation and then linear observer theory is utilized. The main disadvantages of these approaches are that the nonlinear system must satisfy certain conditions and finding the nonlinear transformation is a very difficult task.

Finally, other estimation methods are collected under the generic name "other class of approaches". Monte Carlo [58], neural approximation [59], genetic optimization [60], extended Luenberger-like observer approach [61] are among these approaches. Again each of these has their own advantages and disadvantages.

As a summary, up to now there is no method which outperforms all other ones and is applicable in general. In this chapter, the situation in which the state variables in a deterministic nonlinear system are classified into measured and unmeasured components is studied. It is assumed that measurements are made without noise, and that the unmeasured components appear linearly in the equation:

$$\begin{aligned} \dot{x} =& \mathcal{A}(x_m, u)x_{um} + b(x_m, u) \\ y =& x_m \end{aligned} \tag{4.3}$$

where $x_m \in R^{n_1}$, $x_{um} \in R^{n_2}$ are the measured and unmeasured parts of the state vector $x \in R^{n_1+n_2}$ and $u \in R^m$ and $y \in R^p$ are input and output vectors, respectively. Our interest is in estimating the unmeasured component of the state vector, x_{um}.

The structure in (4.3) is utilized to provide efficient estimation of x_{um} that quickly reduces the error resulting from initial estimates. The procedure has two components. Firstly, the measured state variables are estimated through a linear moving model.

Linear moving model identification is based on the use of orthogonal functions and recursive least-squares (with a variable forgetting factor to track fast parameter changes). Secondly, discretization of unmeasured states is performed and the linear moving model together with the structure of the system are used to recover x_{um} and results in an iterative estimation formula. The developed method is an easy-to-apply method (in contrast to Lyapanov-based or transformation based methods) and is very effective in state estimation and has better performance than EKF, as shown on case studies and on compressor air mass flow estimation. Furthermore, the suggested method can be modified easily for estimation of time-varying parameters appearing linearly in nonlinear systems.

4.2. State Estimation

Using the structure of (4.3), our method is divided into two parts. Firstly, a linear moving model structure is used to approximate the dynamics of x_m. This is needed to account for the influence of the unmeasured x_{um}. Once this approximation is done, the discretization of unmeasured states combined with the linear structure of the equations in x_{um} can be used to recover the unmeasured state vector efficiently. The two steps of state estimation for x_{um} are detailed in the following subsections

4.2.1. Stage 1: Estimation of Measured States by a Linear Moving Model

For the measured states and system inputs the following linear model is assumed in the time interval $kt_s \leq t \leq (k+1)t_s$:

$$\dot{x}_m \cong A_k x_m + B_k u, \tag{4.4}$$

where t_s is the sampling period, A_k and B_k are matrices of appropriate dimensions to be found. Consider the variables $x_m(t)$ and $u(t)$ in the time interval $t_k = kt_s \leq t \leq$

$(k+1)t_s = t_{k+1}$ and let

$$t := kt_s + \eta, \quad x_m(k) := x_m(kt_s), \quad u(k) := u(kt_s),$$

where k=0,1,2..., and $0 \leq \eta \leq t_s$. Next, the variables $x_m(t)$ and $u(t)$ within $t_k \leq t \leq t_{k+1}$ are approximated by r orthogonal functions (which are introduced in Appendix B) as

$$x_m(t) \cong \sum_{i=0}^{r-1} x_{m_i}^{(k)} \phi_i(t) = x_m^{(k)} \phi$$
$$u(t) \cong \sum_{i=0}^{r-1} u_i^{(k)} \phi_i(t) = u^{(k)} \phi,$$

where $x_m^{(k)} := [x_{m_0}^{(k)}, \cdots, x_{m_{r-1}}^{(k)}] \in \mathbb{R}^{n_1 \times r}$ and $u^{(k)} := [u_0^{(k)}, \cdots, u_{r-1}^{(k)}] \in \mathbb{R}^{m \times r}$ are the coefficient matrices and $\phi = [\phi_0(t)\, \phi_2(t), \cdots, \phi_{r-1}(t)]^T$. Integrating (4.4) from $t = t_k$ to $t = t_{k+1}$ and using the integral property of orthogonal functions results in

$$x_m^{(k)} - [x_m(k)\ 0 \cdots 0] \cong A_k x_m^{(k)} O + B_k u^{(k)} O, \tag{4.5}$$

where O is the operational matrix (of integration) for the corresponding orthogonal set of functions used. In the estimation by orthogonal functions, only the first term of the expansion coefficients, $x_{m_0}^{(k)}$ and $u_0^{(k)}$, is used, taking the remaining coefficients as 0 within $t_k \leq t \leq t_{k+1}$. Then,

$$x_{m_0}^{(k)} \cong \frac{x_m(k+1) + x_m(k)}{2}, \quad u_0^{(k)} \cong \frac{u(k+1) + u(k)}{2}$$

and (4.5) becomes

$$x_m(k+1) - x_m(k) \cong b_0 \Big[A_k \big(x_m(k) + x_m(k+1) \big) + B_k \big(u(k) + u(k+1) \big) \Big], \tag{4.6}$$

where b_0 is the (1,1) entry of O. Now, (4.6) can be written as

$$x_m^T(k+1) - x_m^T(k) \cong b_0 \left[x_m^T(k) + x_m^T(k+1) \quad u^T(k) + u^T(k+1) \right] \begin{bmatrix} A_k^T \\ B_k^T \end{bmatrix}. \qquad (4.7)$$

Defining

$$\begin{aligned} y(k+1) :=& x_m^T(k+1) - x_m^T(k), \\ \varphi(k+1) :=& b_0 \begin{bmatrix} x_m(k) + x_m(k+1) \\ u(k) + u(k+1) \end{bmatrix}, \\ \theta(k+1) :=& \begin{bmatrix} A_k^T \\ B_k^T \end{bmatrix}, \end{aligned}$$

(4.7) can be written more compactly as

$$y(k+1) \cong \varphi^T(k+1)\theta(k+1).$$

In estimating input-output data by a set of orthogonal functions, any kind of orthogonal functions can be used since it is well known in the literature, for example [62], that their performance is very close to each other. In addition, note that since estimation is done in time intervals with a length equal to sampling period, it is sufficient to use the first element of the orthogonal function vector. Using more than one component yields negligible improvement.

Matrices A_k, B_k will be determined for each time interval $[t_k, t_{k+1}]$ and therefore they change with time. The corresponding model in (4.4) is called a "linear moving model". In determining the moving coefficients at each sample time, a recursive least squres algorithm for time varying parameters can be used [63, 64, 65, 66]. Here, the algorithm of [63] is used, where a Gauss-Newton variable forgetting factor is used in the recursive least squares. It has good estimation properties for fast time-varying

parameters. The algorithm is given as follows. Consider

$$\theta(n+1) = \theta(n) + k(n+1)\left[y(n+1) - \theta^T(n)\varphi(n+1)\right],$$

where $\theta(n+1)$ is the parameter vector to be estimated, $\varphi(n+1)$ is the measured data vector, $k(n+1)$ is the gain vector and $y(n+1)$ is measured output at time step $n+1$. Updating of $k(n+1)$ is done based on the following algorithm.

$$\begin{aligned}
k(n+1) =& \frac{P(n)\varphi(n+1)}{\lambda(n+1) + \varphi^T(n+1)P(n)\varphi(n+1)},\\
P(n+1) =& \frac{1}{\lambda(n+1)}\left[P(n) - k(n+1)\varphi^T(n+1)P(n)\right],\\
z(n+1) =& (1-\alpha)z(n) + \alpha r^T(n)\varphi(n+1)\varphi^T(n+1)r(n),\\
\lambda(n+1) =& \lambda(n) + \alpha\frac{r^T(n)\varphi(n+1)e(n+1)}{z(n+1)},\\
M(n+1) =& \frac{1}{\lambda(n+1)}\Big[\big(I - k(n+1)\varphi^T(n+1)\big)M(n)\\
&+ \big(I - \varphi(n+1)k^T(n+1)\big) + k(n+1)k^T(n+1) - P(n+1)\Big],\\
r(n+1) =& \left[I - k(n+1)\varphi^T(n+1)\right]r(n) + M(n+1)\varphi(n+1)e(n+1),
\end{aligned}$$

where $e(n+1) = y(n+1) - \theta^T(n)\varphi(n+1)$ and α is called the convergence rate. The initial choices are suggested as follows: $P(0) \simeq \delta I, M(0) \simeq \delta I$ with $\delta \gg 10^4$, $\theta(0) = 0, z(0) \gg 10^4, k(0) = 0$. Finally, $0 < \alpha < 0.2$, $0.5 < \lambda(0) < 0.9$. To use the above algorithm for cases of multi-outputs, the algorithm is applied for each output component to compute the corresponding column of the parameter matrix.

4.2.2. Stage 2: Discretization of Unmeasured States

The state equations of the system given by (4.3) can be decomposed as

$$\dot{x}_m = \mathcal{A}_m(x_m, u)x_{um} + b_m(x_m, u) \tag{4.8a}$$

$$\dot{x}_{um} = \mathcal{A}_{um}(x_m, u)x_{um} + b_{um}(x_m, u), \tag{4.8b}$$

where $\mathcal{A}_m(x_m, u)$, $\mathcal{A}_{um}(x_m, u)$ are $n_1 \times n_2$ and $n_2 \times n_2$ matrices, respectively. On the other hand, from Section 4.2.1,

$$\dot{x}_m \cong A_k x_m + B_k u \text{ over } t \in [t_k, t_{k+1}]. \tag{4.9}$$

From (4.8a) and (4.9),

$$\mathcal{A}_m(x_m, u)x_{um} = A_k x_m + B_k u - b_m(x_m, u) + e_{id}(t) \text{ over } t \in [t_k, t_{k+1}], \tag{4.10}$$

where $e_{id}(t)$ is the error due to identification at time t. Next, evaluate (4.10) at times t_k, t_{k+1}. For $t = t_k$,

$$\mathcal{A}_m(x_m(t_k), u(t_k))x_{um}(t_k) = A_k x_m(t_k) + B_k u(t_k) - b_m(x_m(t_k), u(t_k)) + e_{id}(t_k),$$

or more compactly

$$\mathcal{A}_m(k)x_{um}(k) = A_k x_m(k) + B_k u(k) - b_m(k) + e_{id}(k), \tag{4.11}$$

where A_k, B_k are values of the moving matrices at t_k. where A_k, B_k are values of the moving matrices at t_k. Similarly, for $t = t_{k+1}$,

$$\mathcal{A}_m(k+1)x_{um}(k+1) = A_{k+1} x_m(k+1) + B_{k+1} u(k+1) - b_m(k+1) + e_{id}(k+1). \tag{4.12}$$

Next, discretize the expression of x_{um} given by (4.8b) using the forward-difference method

$$x_{um}(k+1) = (t_s \mathcal{A}_{um}(k) + I)x_{um}(k) + t_s b_{um}(k) + e_{disc}(k+1), \tag{4.13}$$

where $e_{disc}(k+1)$ is the error at time t_{k+1} due to the discretization process. After a rearrangement, equations (4.11), (4.12) and (4.13) can be written as

$$\begin{bmatrix} 0 \\ \mathcal{A}_m(k+1) \\ I \end{bmatrix} x_{um}(k+1) = \begin{bmatrix} A_k x_m(k) + B_k u(k) - b_m(k) \\ A_{k+1} x_m(k+1) + B_{k+1} u(k+1) - b_m(k+1) \\ t_s b_{um}(k) \end{bmatrix} + \begin{bmatrix} -\mathcal{A}_m(k) \\ 0 \\ t_s \mathcal{A}_{um}(k) + I \end{bmatrix} x_{um}(k) + \begin{bmatrix} e_{id}(k) \\ e_{id}(k+1) \\ e_{disc}(k+1) \end{bmatrix}. \tag{4.14}$$

Defining

$$\widetilde{A}(k+1) := \begin{bmatrix} 0 \\ \mathcal{A}_m(k+1) \\ I \end{bmatrix}, \; h(k+1) := \begin{bmatrix} A_k x_m(k) + B_k u(k) - b_m(k) \\ A_{k+1} x_m(k+1) + B_{k+1} u(k+1) - b_m(k+1) \\ t_s b_{um}(k) \end{bmatrix}$$

$$H(k) := \begin{bmatrix} -\mathcal{A}_m(k) \\ 0 \\ t_s \mathcal{A}_{um}(k) + I \end{bmatrix}, \; e(k+1) := \begin{bmatrix} e_{id}(k) \\ e_{id}(k+1) \\ e_{disc}(k+1) \end{bmatrix},$$

(4.14) becomes

$$\widetilde{A}(k+1) x_{um}(k+1) = h(k+1) + H(k) x_{um}(k) + e(k+1). \tag{4.15}$$

Clearly, the matrix $\widetilde{A}(k+1)$ has full-column rank and hence the solution of (4.15) is

$$x_{um}(k+1) = \left[\widetilde{A}^T(k+1)\widetilde{A}(k+1)\right]^{-1} \big(\widetilde{A}^T(k+1) h(k+1) + \widetilde{A}^T(k+1) H(k) x_{um}(k) + \mathcal{A}_m^T(k+1) e_{id}(k+1) + e_{disc}(k+1) \big). \tag{4.16}$$

4.2.3. Error Analysis

In (4.16), the initial condition $x_{um}(0)$ is not known and therefore the combined effect of an incorrect initial condition, the identification and discretization errors on estimation is not clear at this step. It is necessary to determine a set of conditions which will guarantee that the effect of any initial condition will die out and the other errors will be bounded as time goes to infinity. Firstly, for a more compact notation let

$$\begin{aligned} S_{dis}(k+1) :=& [\widetilde{A}^T(k+1)\widetilde{A}(k+1)]^{-1}, \\ v(k+1) :=& S_{dis}(k+1)\widetilde{A}^T(k+1)h(k+1), \\ Q(k+1) :=& S_{dis}(k+1)\widetilde{A}^T(k+1)H(k), \\ S_{id}(k+1) :=& S_{dis}(k+1)\mathcal{A}_m^T(k+1). \end{aligned}$$

Then, (4.16) can be written as

$$\begin{aligned} x_{um}(k+1) =& v(k+1) + Q(k+1)x_{um}(k) \\ &+ S_{id}(k+1)e_{id}(k+1) + S_{dis}(k+1)e_{disc}(k+1). \end{aligned} \tag{4.17}$$

For future use, for $n > m$ define

$$\prod_{i=n}^{m} K_i := K_n K_{n-1} \cdots K_{m+1} K_m$$

Assume that $x_{um}(0) = x_{um_0}$. Then, after a simple algebra,

$$\begin{aligned} x_{um}(k+1) = v(k+1) + \sum_{i=1}^{k} \prod_{j=k+1}^{i+1} Q(j)v(i) + \prod_{j=k+1}^{1} Q(j)x_{um_0} + \sum_{i=1}^{k} \prod_{j=k+1}^{i+1} Q(j)S_{id}(i)e_{id}(i) \\ + S_{id}(k+1)e_{id}(k+1) + \sum_{i=1}^{k} \prod_{j=k+1}^{i+1} Q(j)S_{disc}(i)e_{disc}(i) + S_{disc}(k+1)e_{disc}(k+1). \end{aligned}$$

Next, define the residual term

$$R(k+1) := R_{ic}(k+1) + R_{id}(k+1) + R_{disc}(k+1),$$

where

$$R_{ic}(k+1) := \prod_{j=k+1}^{1} Q(j) x_{um_0}, \tag{4.18a}$$

$$R_{id}(k+1) := \sum_{i=1}^{k} \prod_{j=k+1}^{i+1} Q(j) S_{id}(i) e_{id}(i) + S_{id}(k+1) e_{id}(k+1), \tag{4.18b}$$

$$R_{disc}(k+1) := \sum_{i=1}^{k} \prod_{j=k+1}^{i+1} Q(j) S_{disc}(i) e_{disc}(i) + S_{disc}(k+1) e_{disc}(k+1). \tag{4.18c}$$

Now note that for all time steps,

$$||R(k+1)||_* \leq ||R_{ic}(k+1)||_* + ||R_{id}(k+1)||_* + ||R_{disc}(k+1)||_*,$$

where $||\cdot||_*$ is any vector norm on $\mathbb{R}^{n_2}$. Next, each of these errors is analyzed.

4.2.3.1. Bound Analysis of R_{ic}. Consider $||R_{ic}(k+1)||_*$,

$$\begin{aligned} ||R_{ic}(k+1)||_* &= \left|\left| \prod_{j=k+1}^{1} Q(j) x_{um_0} \right|\right|_* \\ &\leq \left|\left| \prod_{j=k+1}^{1} Q(j) \right|\right|_{i*} ||x_{um_0}||_* \\ &\leq \prod_{j=1}^{k+1} ||Q(j)||_{i*} ||x_{um_0}||_*, \end{aligned} \tag{4.19}$$

where $||\cdot||_{i*}$ is the corresponding induced-norm, namely,

$$||Q(j)||_{i*} := \sup_{z \neq 0} \frac{||Q(j)z||_*}{||z||_*}, \quad \forall j \geq 1.$$

At this point, the following assumption is made:

Assumption 4.1: *There exists* $n_* > 0$ *such that*

$$\beta := \sup_{j>n_*} ||Q(j)||_{i*} < 1.$$

Then, from (4.19),

$$||R_{ic}(k+1)||_* \xrightarrow{k\to\infty} 0. \tag{4.20}$$

Hence, with Assumption 1 the effect of any initial condition on estimation dies out as time goes to infinity.

4.2.3.2. Bound Analysis of R_{id}. Next, the error due to identification is considered:

$$||R_{id}(k+1)||_* = \left|\left|\sum_{i=1}^{k}\prod_{j=k+1}^{i+1} Q(j)S_{id}(i)e_{id}(i) + S_{id}(k+1)e_{id}(k+1)\right|\right|_* .$$

For the error associated with recursive-least squares algorithm, define

$$\rho := \sup_{i>n_*} ||e_{id}(i)||_* , \tag{4.21a}$$

$$\gamma := \sup_{i>n_*} ||S_{id}(i)||_{i*} . \tag{4.21b}$$

Then,

$$\begin{aligned} ||R_{id}(k+1)||_* &\le \left|\left|\sum_{i=1}^{n_*}\prod_{j=n_*+1}^{i+1} Q(j)S_{id}(i)e_{id}(i)\right|\right|_* \\ &\quad + \rho\sum_{i=n_*+1}^{k}\beta^{k-i+1}\,||S_{id}(i)||_{i*} + \rho\,||S_{id}(k+1)||_{i*} \\ &\le \left|\left|\sum_{i=1}^{n_*}\prod_{j=n_*+1}^{i+1} Q(j)S_{id}(i)e_{id}(i)\right|\right|_* + \rho\gamma\sum_{i=n_*+1}^{k}\beta^{k-i+1} + \rho\gamma. \end{aligned}$$

Here, it is assumed that $k > n_*$ since the interest will be in the limiting behavior of $||R_{id}(k+1)||_*$. The limiting behavior is

$$\lim_{k\to\infty} ||R_{id}(k+1)||_* \leq \left|\left|\sum_{i=1}^{n_*} \prod_{j=n_*+1}^{i+1} Q(j) S_{id}(i) e_{id}(i)\right|\right|_* + \frac{\rho\gamma}{1-\beta}. \tag{4.22}$$

Hence, the error due to identification remains bounded as time goes to infinity. Note that here we simply assumed that (4.21a) and (4.21b) hold, which is practically the case for our algorithm.

4.2.3.3. Bound Analysis of R_{disc}. Finally, consider $R_{disc}(k+1)$. It is known that [67]

$$||e_{disc}(k+1)||_* = \frac{t_s^2}{2} ||\ddot{x}_{um}(\tau)||_* \text{ for some } \tau \in (t_k, t_{k+1}).$$

Define

$$\delta := \frac{t_s^2}{2} \sup_{t>0} ||\ddot{x}_{um}(t)||_* \tag{4.23a}$$

$$\eta := \sup_{i>n_*} ||S_{disc}(i)||_{i*} \tag{4.23b}$$

Then,

$$\sup_{i>n_*} ||e_{disc}(i)||_* \leq \delta \tag{4.24}$$

and using Assumption 1, (4.18c), (4.23b) and (4.24),

$$\begin{aligned} ||R_{disc}(k+1)||_* &\leq \left|\left|\sum_{i=1}^{n_*} \prod_{j=n_*+1}^{i+1} Q(j) S_{disc}(i) e_{disc}(i)\right|\right|_* \\ &\quad + \left|\left|\sum_{i=n_*+1}^{k} \prod_{j=k+1}^{i+1} Q(j) S_{disc}(i) e_{disc}(i)\right|\right|_* + ||S_{dics}(k+1) e_{disc}(k+1)||_* \\ &\leq \left|\left|\sum_{i=1}^{n_*} \prod_{j=n_*+1}^{i+1} Q(j) S_{disc}(i) e_{disc}(i)\right|\right|_* + \delta\eta \sum_{i=n_*+1}^{k} \beta^{k-i+1} + \delta\eta. \end{aligned}$$

Hence,

$$\lim_{k\to\infty} ||R_{disc}(k+1)||_* \leq \left|\left|\sum_{i=1}^{n_*}\prod_{j=n_*+1}^{i+1} Q(j)S_{disc}(i)e_{disc}(i)\right|\right|_* + \frac{\delta\eta}{1-\beta}. \tag{4.25}$$

Therefore, error propagation associated with discretization part is also bounded. The condition (4.23a) is implicity assumed to be satisfied.

4.2.3.4. Total Error Bound. Combining (4.20), (4.22) and (4.25), the asymptotic total error bound becomes

$$\begin{aligned}\lim_{k\to\infty} ||R(k+1)||_* \leq &\left|\left|\sum_{i=1}^{n_*}\prod_{j=n_*+1}^{i+1} Q(j)S_{id}(i)e_{id}(i)\right|\right|_* \\ &+ \left|\left|\sum_{i=1}^{n_*}\prod_{j=n_*+1}^{i+1} Q(j)S_{disc}(i)e_{disc}(i)\right|\right|_* + \frac{1}{1-\beta}(\gamma\rho+\delta\eta).\end{aligned}$$

4.2.4. Remarks

(i) If $\mathcal{A}_m(x_m,u)$ has full column-rank for all (x_m,u), then there is no need to use the discretization part and in this case, using (4.10),

$$x_{um}(k) = [\mathcal{A}_m^T(k)\mathcal{A}_m(k)]^{-1}\mathcal{A}_m^T(k)\big(A_k x_m(k) + B_k u(k) - b_m(k) + e_{id}(k)\big). \tag{4.26}$$

For such a case, any assumption is not needed and note that there is no possibility of error propagation due to identification errors of the previous steps (since there is no x_{um} term on right-hand side). Assuming in addition that entries of $\mathcal{A}_m(k)$ are finite for all k,

$$\begin{aligned}||R_{id}(k+1)||_* &= \left|\left|[\mathcal{A}_m^T(k)\mathcal{A}_m(k)]^{-1}\mathcal{A}_m(k)^T(k)e_{id}(k)\right|\right|_* \\ &\leq \rho\left|\left|[\mathcal{A}_m^T(k)\mathcal{A}_m(k)]^{-1}\mathcal{A}_m^T(k)\right|\right|_{i*}, \quad \forall k \geq n_*.\end{aligned}$$

One more point to notice is that if the right-hand side of (4.8a) contains unknown parameters to be estimated, which appear also linearly, and the augmented matrix of unmeasured states and parameters is full-rank, then a joint state and parameter estimation can be achieved very easily. More precisely, assume that

$$\dot{x}_m = \mathcal{A}^a_m(x_m, u)x^a_{um} + b_m(x_m, u),$$

where x^a_{um} is the augmented vector containing the unmeasured states and the unknown time-varying parameters and $\mathcal{A}^a_m$ is the associated augmented matrix. If $\mathcal{A}^a_m(x_m, u)$ is always full-rank, then the solution x^a_{um} is given by (4.26) in which $\mathcal{A}_m(x_m, u)$ should be replaced by $\mathcal{A}^a_m(x_m, u)$.

(ii) In case of linear time-invariant systems, the matrices Q, S_{id} and S_{disc} are constant matrices.

(iii) In general, $Q,\ S_{id}, S_{disc}$ are functions of measured states and inputs. A verification of Assumption 1 can be done as follows. If the input u is known beforehand or is from a controller, then the known input or the designed control law can be applied off-line to the system model by considering the guessed $x_{um}(0)$. If Assumption 1 holds, then it can be sure that the effect of a wrong initial condition on estimation will die out with time.

(iv) In finite dimensional normed spaces, all norms are equivalent (see Appendix A.3). I.e., convergence with respect to one norm implies convergence with respect to other norms. Hence, in checking Assumption 1, it is enough to to choose an induced matrix norm such that it will result in an n_*. Furthermore, the expressions of scaled matrices Q, S_{id}, S_{disc} contain the term $[\widetilde{A}^T(k+1)\widetilde{A}(k+1)]^{-1}$ and hence their entries are divided by the determinant of $[\widetilde{A}^T(k+1)\widetilde{A}(k+1)]$, most of the time resulting in their norms to be small. This, in turn, reduces the effect of propagation of identification and discretization errors on estimation, as demonstrated on the following case studies.

4.3. Case Studies

In this section, the developed method is applied to three academic-purpose constructed nonlinear models and results are compared with EKF for a set of initial guesses for the state to be estimated. Small additive measurement and process noises are considered. As induced matrix norm (for the verification of Assumption 1), the spectral norm is used, which is defined as the square-root of the maximum eigenvalue of $Q(t)^T Q(t)$:

$$||Q(t)||_{i2} = \sqrt{\lambda_{max}\left(Q(t)^T Q(t)\right)}.$$

In all case studies, the following initializations/settings required for recursive least-squares algorithm or EKF are used:

$$\alpha = 0.01,\ \lambda(0) = 0.75,\ P = M = 10^5 I,\ z = 10^5,\ r = 0,\ k = 0,\ \theta = 0.$$

Additionally, in each case study, small Gaussian process noise (v) and observation errors (w) are added. All noise terms are independent with variance 10^{-8}. In the comparison figures of the following case studies, the signal in blue color is the real signal (x_{i_r}), the signal in black color is the estimated signal by EKF (x_{i_k}) and the red-color signal is the the one estimated by the proposed method (x_{i_p}).

4.3.1. Example 1

As a first example, consider

$$\begin{aligned} \dot{x}_1 &= \left(\frac{0.6 + 0.5\sin x_1}{2 + \cos x_1}\right)^2 x_2 + v_1 \\ \dot{x}_2 &= \cos(x_1) x_2 + v_2 \end{aligned} \tag{4.27}$$

where $x_{um} = x_2$, $x_m = x_1 + w_1$ and $x_1(0) = 6$, $x_2(0) = 1$. Assumption 1 is not needed in this example since $\mathcal{A}(x_1)$ is full column-rank for all values of x_1. Figure 4.1 shows comparison results with EKF for different initial guesses for x_2. The performance of EKF is poor (especially when the initial guess is very far from the true value).

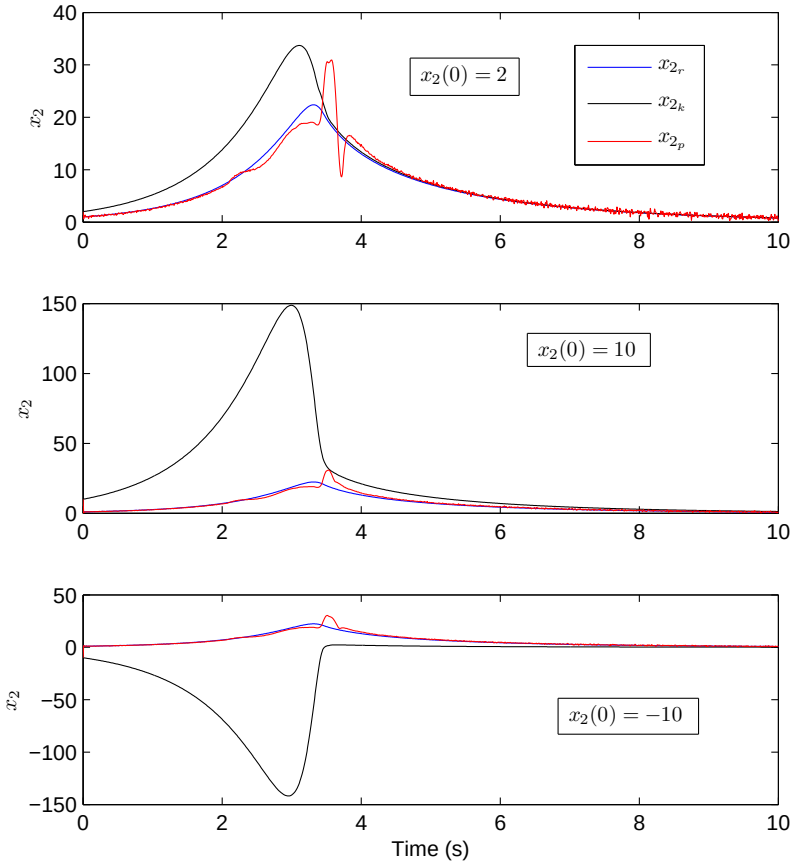

Figure 4.1. x_2 and estimates for it.

4.3.2. Example 2

The next example is

$$\begin{aligned}
\dot{x}_1 &= x_1 e^{-0.25x_1^3} x_2 - 0.5\cos x_3 + v_1 \\
\dot{x}_2 &= \sin(2x_1)x_2 + v_2 \\
\dot{x}_3 &= \log(1 + x_3^2)x_1^3 + v_3
\end{aligned}$$

where $x_{um} = x_2$, $x_m = [x_1 + w_1 \;\; x_3 + w_2]^T$ and $x_1(0) = 1$, $x_2(0) = 2$, $x_3(0) = -5$. $\mathcal{A}(x_1)$ may not be full-column rank and hence an off-line checking of Assumption 1 is necessary for the guessed initial value of $x_2(0)$. Figures (4.2, 4.3) show the verification of the assumption and the comparison results with EKF, respectively. As seen, the performance of the proposed method is clearly superior to EKF even for initial guesses considerably different than the initial true value of x_2.

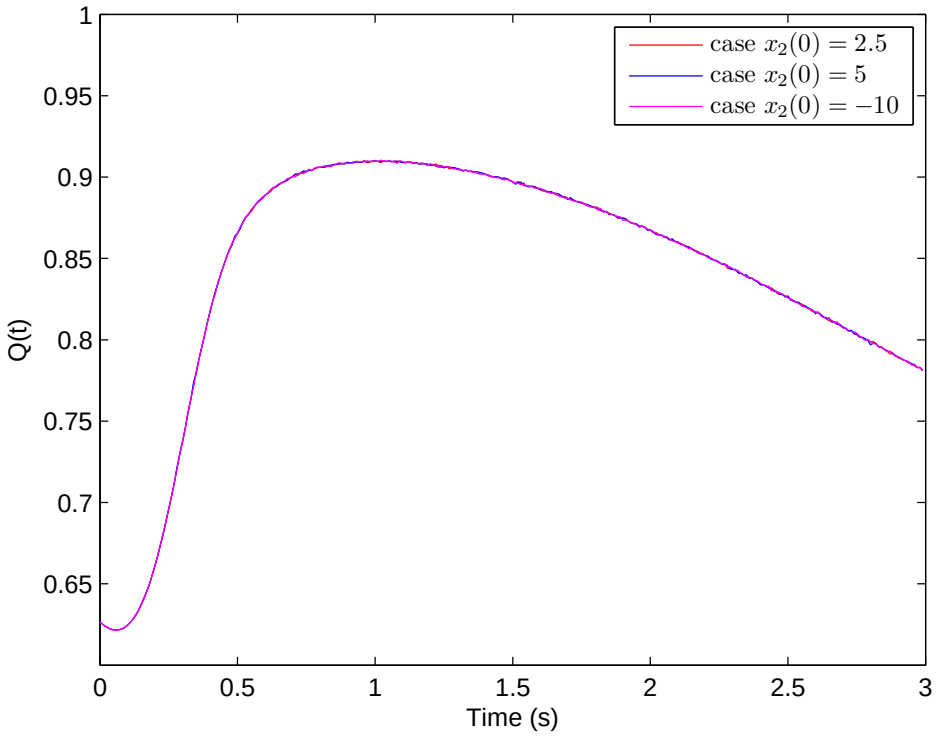

Figure 4.2. Off-line verification of Assumption 1

4.3.3. Example 3

As a last example, consider

$$\dot{x}_1 = -0.32x_1^2 + 0.1x_2 + v_1$$
$$\dot{x}_2 = 0.16x_1^2 + v_2$$

where $x_{um} = x_2$, $x_m = x_1 + w_1$ and $x_1(0) = 3$, $x_2(0) = 4.5$. In this example, $\mathcal{A}(x_m)$ is constant and for verification of Assumption 1, an off-line check is not needed. A simple

calculation gives $Q(t) = 0.99$. Therefore, the proposed method can be used. The results are shown in Figure 4.4. As seen, when the guessed initial condition is chosen more far away from the correct value, the speed of convergence of EKF decreases seriously.

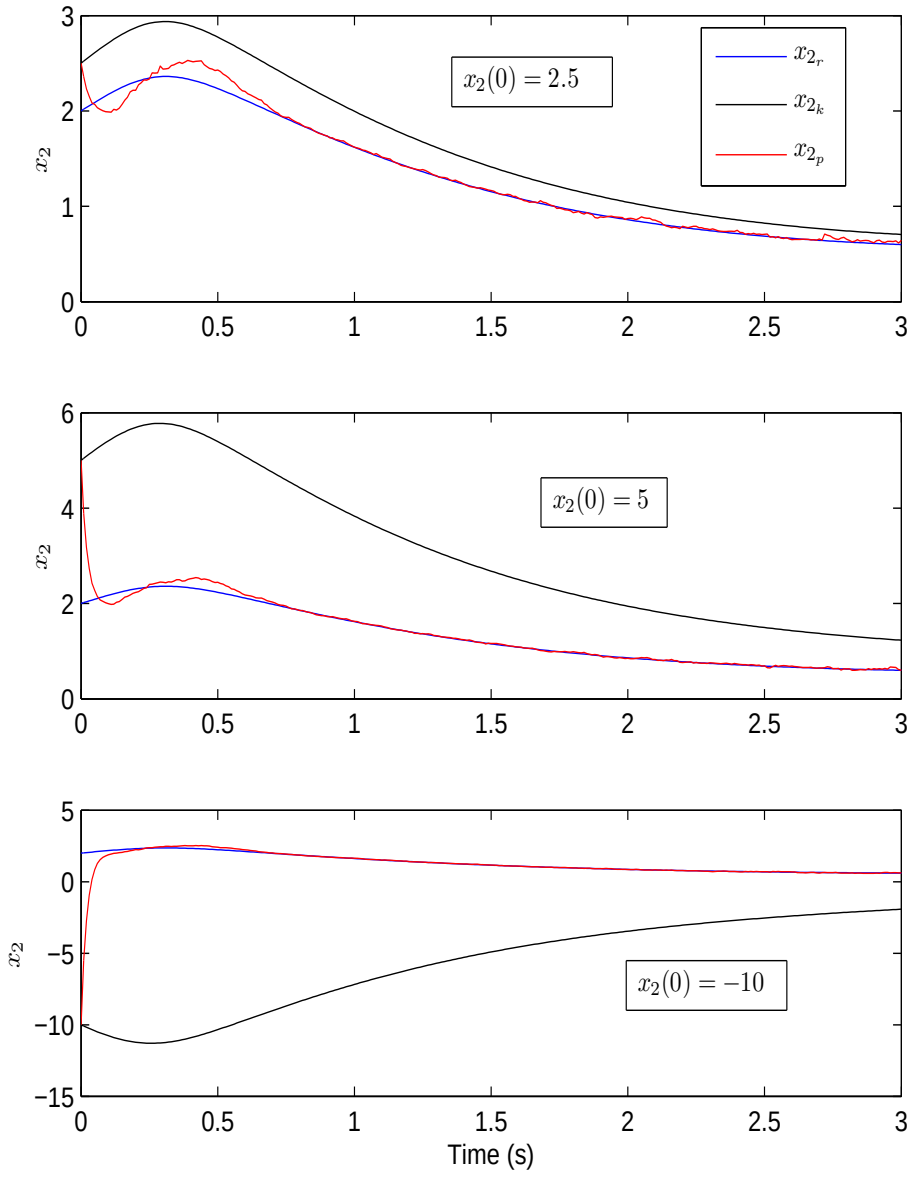

Figure 4.3. x_2 and estimates for it

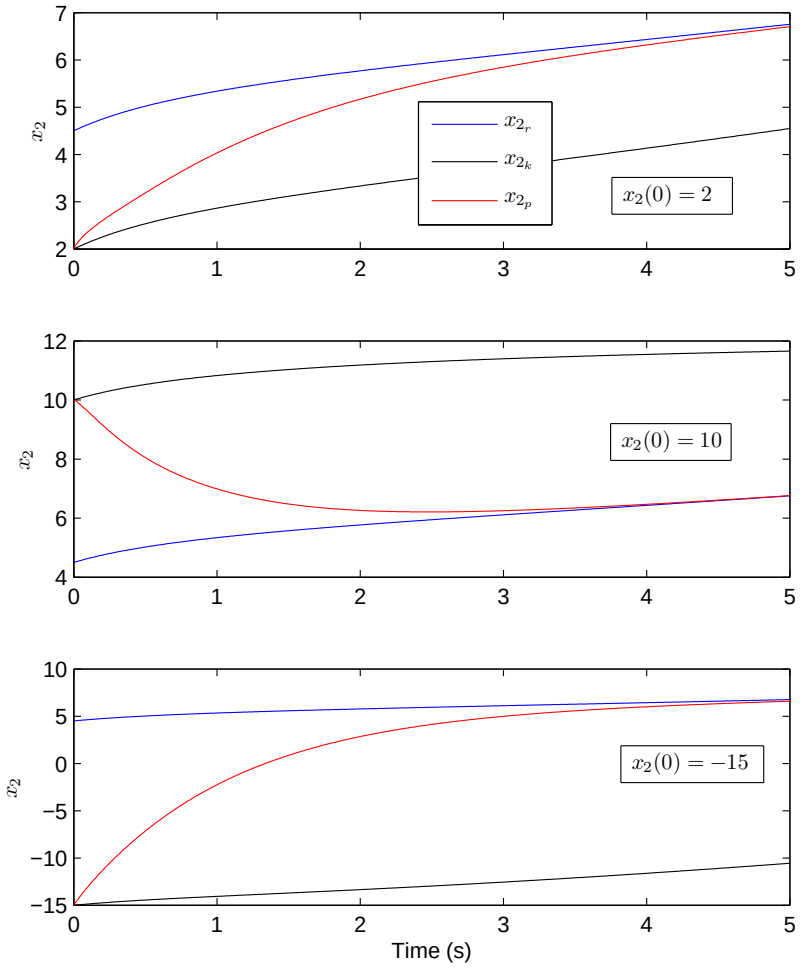

Figure 4.4. x_2 and estimates for it

4.4. Application to Diesel Engine Compressor Air Mass Flow Estimation

The application of the method with a comparison to EKF is shown in the following two case studies, where

$$\alpha = 0.01,\ \lambda(0) = 0.75,\ P = M = 10^5 I,\ z = 10^5,\ r = 0,\ k = 0,\ \theta = 0.$$

Additionally, in each case study, small Gaussian process (v) and observation noise (w) are added (for both methods). In the first case, process and measurement noise terms are independent with variances 10^{-10} and 10^{-4}, respectively; the orders being compatible with the orders of input and output signals. For the second case study,

the variances of process and measurement noises are 10^{-12} and 10^{-4}. Note also that the coefficient of P_c in (4.1a), $(R\eta_c T_i)/(V_i c_p T a)$, is always positive and hence the first remark mentioned in the previous section applies in this case.

4.4.1. Case I

The corresponding input, parameter signals and estimation results are shown through Figures 4.5 and 4.8. In the estimation comparison figures, the signal in blue color is the real signal (x_r), the signal in black color is the estimated signal by EKF (x_k) and the red-color signal is the the one estimated by the proposed method (x_p).

In the simulations, the true initail conditions are $p_i(0) = 103$ kPa, $p_x(0) = 109$ kPa and $P_c(0) = 250$ W. The assumed initial condition for P_c in both the developed method and EKF is 600 W.

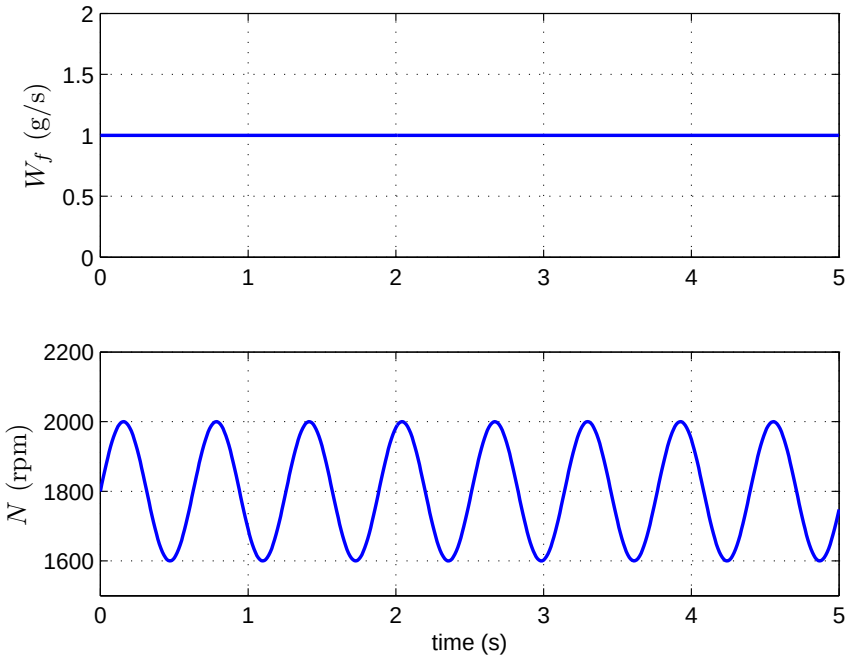

Figure 4.5. Fuel flow rate and engine speed

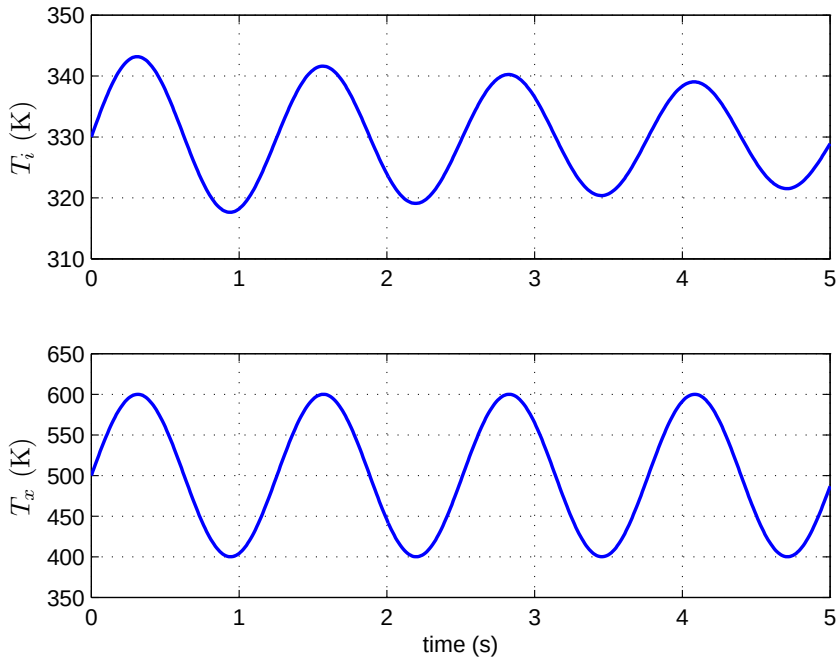

Figure 4.6. Intake and exhaust manifold temperatures

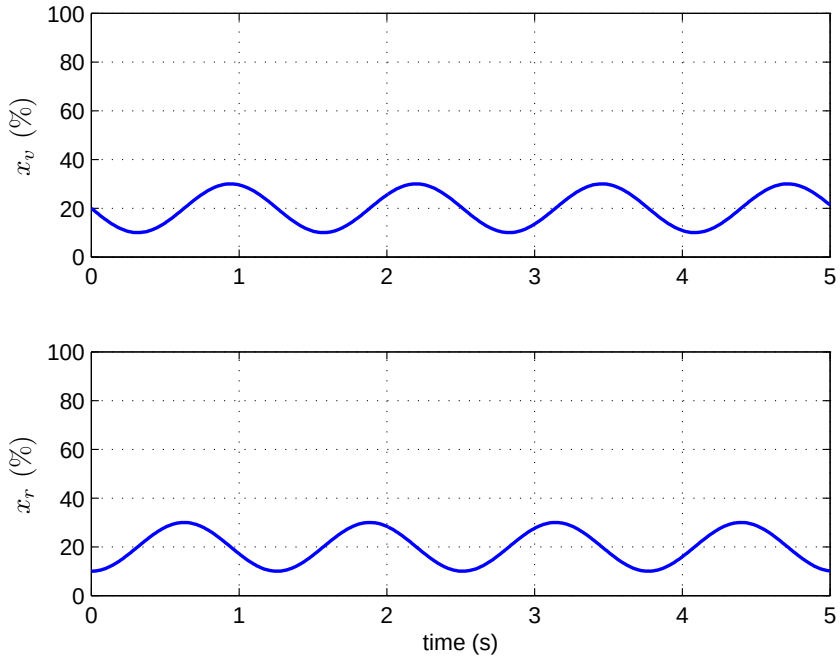

Figure 4.7. Vgt vane and egr valve position

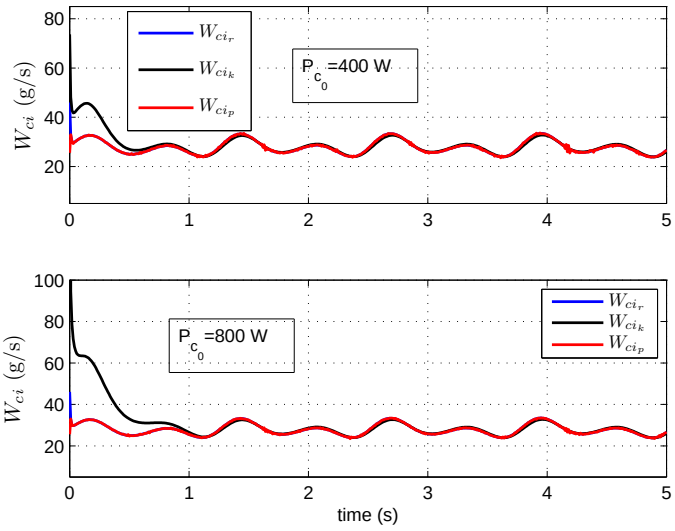

Figure 4.8. Compressor air mass flow and its estimations.

4.4.2. Case II

The initial conditions are the same as before. The corresponding input, parameter signals and estimation results are shown through Figures 4.9 and 4.12.

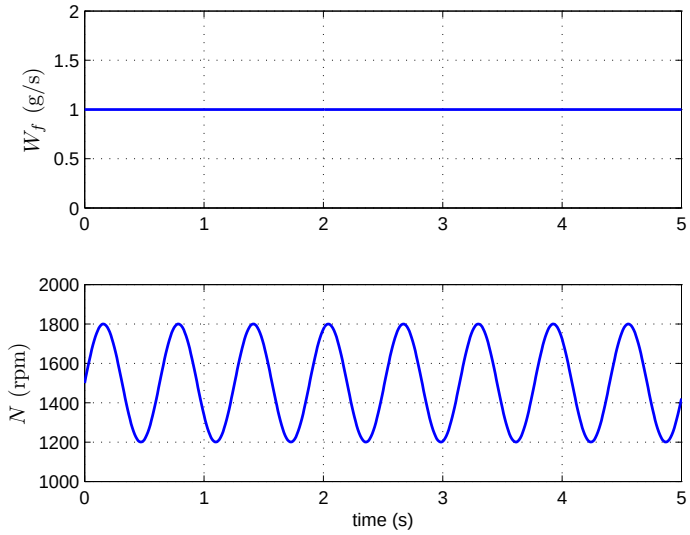

Figure 4.9. Fuel flow rate and engine speed

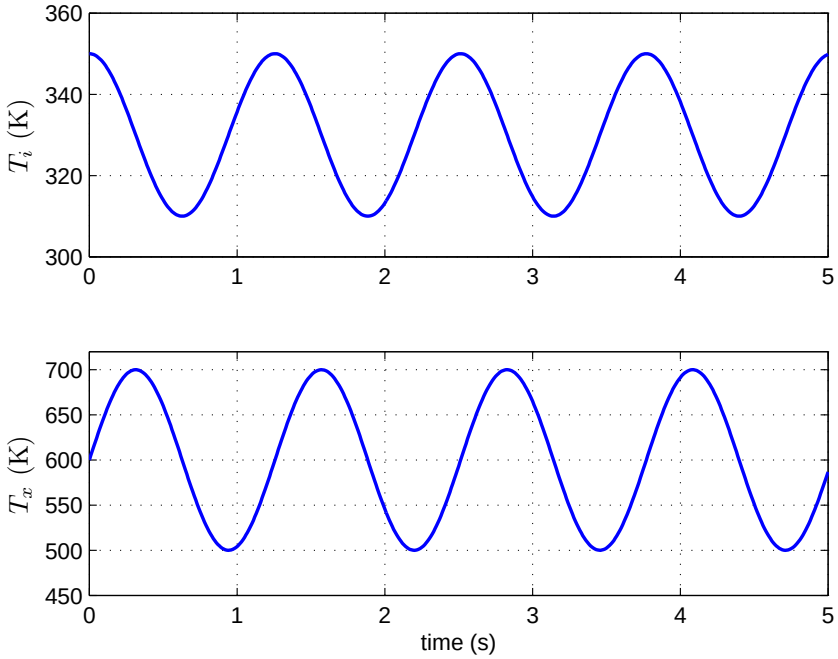

Figure 4.10. Intake and exhaust manifold temperatures

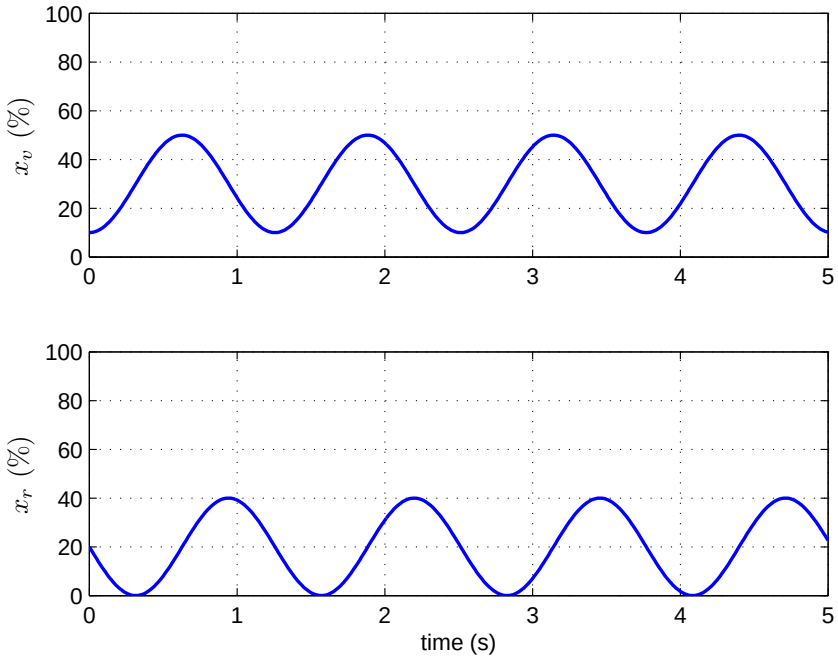

Figure 4.11. Vgt vane and egr valve position

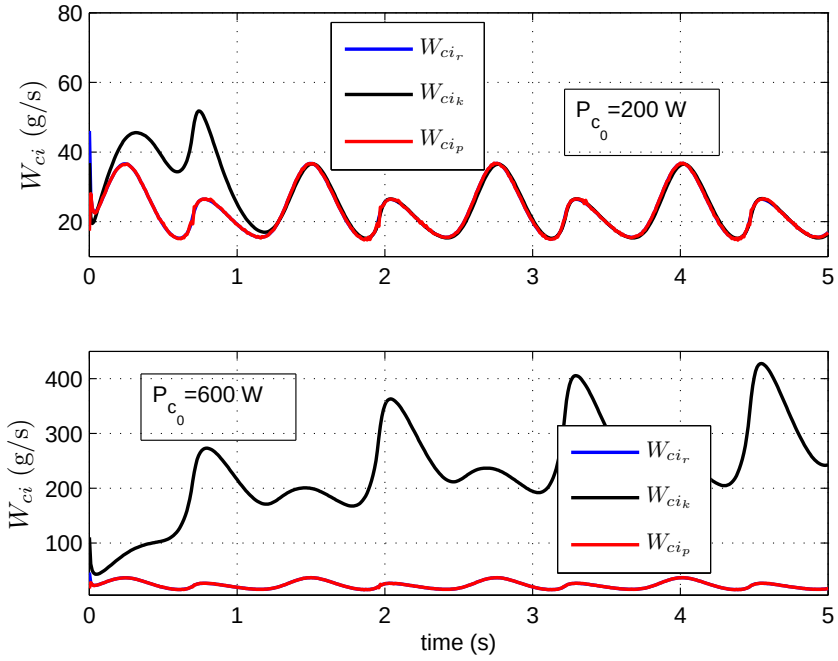

Figure 4.12. Compressor air mass flow and its estimations

4.5. Comments

In this chapter, an identification based, on-line state estimation method for deterministic nonlinear dynamical systems where unmeasured states appear linearly is developed and then it is applied to estimate compressor air mass flow in diesel engines, which can be problematic and hence its estimation important in the situations mentioned before. The method consists of two stages. In the first stage, a linear moving model is identified for measured states and for that purpose orthogonal functions are used. In the second stage, a forward-difference method is applied to the unmeasured state dynamics and together with the results of the first stage, a discrete-time formulation of the unmeasured states is derived. An error analysis of the method was discussed with the associated error bounds. One of the striking properties of the method is its easiness of application. In contrast to the methods discussed in the Introduction, no injection of a function of the output (as is the case for extended linearization methods) or a transformation of the dynamics (as in Lie-algebraic methods) is required. Since there is no constructive procedure involved (as in the case of Lyapunov-based methods), no trial-error is reqired. As shown through three examples and diesel engine

compressor air mass flow estimation, the proposed method outperforms EKF. EKF results are poor since EKF uses linearization at each time step and this causes a slow convergence or divergence which may be worser when initial guesses are far from the true initial values. In contrast to EKF, the proposed method is robust to wrong initial guesses for the state(s) to be estimated. Since the developed method is for deterministic systems, in comparison with EKF, small additive process and measurement noises are used. In case of a high measurement noise, an on-line noise filtering process can be incorporated to improve the results.

In air compressor mass flow estimation, the results from the first case study shows that the effects of wrong initial conditions, linearization errors and guessed variances cause EKF to have an initial poor estimate but later on converging to true results. On the other hand, in the second case study for the second wrong initial condition, EKF is not able to be convergent. In contrast, the estimation results with the proposed method are very satisfactory in both cases.

5. LPV-BASED COMPRESSOR AIR MASS FLOW ESTIMATION

Although the identification-based method presented in the previous chapter gave us satisfactory results, the method is not an asymptotically convergent method; rather it gives results which are optimal in the sense of least-squares. In this chapter, we construct an asymptotically convergent observer for the estimation of compressor air mass flow using the previous mean-value engine model and the LPV-based state estimation method presented in [34] for affine LPV systems.

As a first task, the mean-value engine model is transformed into an equivalent model with affine parameter dependence. Since the designed estimator has asymptotic convergence nature, it gives better results. Of course, such a comparison is meaningful when both methods are applicable on the same system and it is important to keep in mind that there may be situations where the LPV-based state estimation is not applicable. I.e., there may be some systems for which the identification-based method works but the LPV-based method to be presented here may not be applicable.

The chapter is organized as follows. In Section 1, affine linear parameter-varying systems and the observer design procedure of [34] are shortly summarized. In Section 2, the used diesel engine model is re-introduced and its transformation to an affine parameter-dependent form is given. Simulation results are given in Section 3. Finally, we conclude with the main findings of this work in Section 4 of the chapter.

5.1. LPV-Systems and Scheduled Observer Design

In this section, we will first define the necessary concepts and then summarize the observer design method presented in [34].

5.1.1. General Concepts

As mentioned before, linear parameter-varying systems are in the following form

$$\begin{aligned} \dot{x} =& \mathcal{A}(\rho)x + \mathcal{B}(\rho)u, \\ y =& \mathcal{C}(\rho)x + \mathcal{D}(\rho)u, \end{aligned} \tag{5.1}$$

where $x \in R^n, u \in R^m, y \in R^p$ are the state, input and measured outputs, respectively. The system matrices are depending on a measurable parameter vector $\rho \in R^r$. If parameter vector ρ includes a state, then the underlying model is called a quasi-LPV model. One class of LPV systems is affine parameter-dependent LPV systems, which we define next.

Definition 5.1. *System (5.1) is said to be an affine parameter-dependent LPV system if*

$$\begin{aligned} A(\rho) =& A_0 + \sum_{i=1}^{r} \rho_i A_i, \;\; B(\rho) = B_0 + \sum_{i=1}^{r} \rho_i B_i, \\ C(\rho) =& C_0 + \sum_{i=1}^{r} \rho_i C_i, \;\; D(\rho) = D_0 + \sum_{i=1}^{r} \rho_i D_i, \end{aligned}$$

where $\rho = [\rho_1 \, \rho_2 \, \cdots \rho_r]^T$.

In the design of scheduled observer for state estimation, we will use the concept of affine quadratic stability (AQS). Therefore, next this concept is defined.

Definition 5.2. *The linear parameter-dependent system*

$$\dot{\xi} = A(\rho)\xi$$

is said to be affinely quadratically stable if there exists $r + 1$ *matrices* $P_0, P_1, \cdots, P_r$

such that

$$P(\rho) := P_0 + \sum_{i=1}^{r} \rho_i P_i \succ 0$$
$$\Omega(\rho, \dot{\rho}) := A(\rho)^T P(\rho) + P(\rho)A(\rho) + P(\dot{\rho}) - P_0 \prec 0$$

Note that for a system to be affinely quadratically stable affinely parameter-dependence is not required.

5.1.2. Scheduled Observer Design

In this part, we present the scheduled observer design method of [34]. For details, the reader is referred to [34]. Consider, the system

$$\begin{aligned} \dot{x} &= \mathcal{A}(\rho)x + \mathcal{B}(\rho)u \\ y &= \mathcal{C}x, \end{aligned} \tag{5.2}$$

where

- the parameter-dependent system matrices are affine in the parameter vector.
- C is full row-rank.
- each parameter $\rho_i(t)$ is measurable, $\rho_i(t) \in [\underline{\rho}_i, \overline{\rho}_i]$ and $\underline{\rho}_i < 0, \overline{\rho}_i > 0$.
- $\dot{\rho}_i \in [\underline{\nu}_i, \overline{\nu}_i]$.

Note that the conditions $\underline{\rho}_i < 0$, $\overline{\rho}_i > 0$ are not restrictive in the third assumption since they can be achieved by a change of variable. The parameter vector and its derivative remain in the hyper-rectangles with 2^r vertices as defined below.

$$\mathcal{S} := \{(s_1, s_2, \cdots, s_r) : s_i \in \{\underline{\rho}_i, \overline{\rho}_i\}\}$$
$$\mathcal{T} := \{(\tau_1, \tau_2, \cdots, \tau_r) : \tau_i \in \{\underline{\tau}_i, \overline{\tau}_i\}\}$$

The structure of the full-order observer is assumed to be of

$$\begin{aligned}\dot{\eta}(t) =& H\left(\rho(t)\right)\eta(t) + L\left(\rho(t)\right)y(t) + J\left(\rho(t)\right)u(t),\\ \hat{x}(t) =& \eta(t) + My(t),\end{aligned} \tag{5.3}$$

where $\eta \in R^n$ and $\hat{x} \in R^n$ is the estimate of the state vector. The matrix M and parameter dependent matrices are matrices to be determined so that the estimation error converges to zero asymptotically. Defining

$$e := \hat{x} - x, \quad T := I_n - MC$$

error dynamics becomes

$$\dot{e} = H(\rho)e + \big(H(\rho)T + L(\rho)C - TA(\rho)\big)x + \big(J(\rho) - TB(\rho)\big)u. \tag{5.4}$$

The observer design problem is reduced to the determination of the parameter dependent observer matrices $H(\rho), L(\rho), J(\rho)$ and the matrix M such that (5.4) is stable regardless of the initial conditions $x(0), \eta(0)$, control input u and the parameter vector ρ with the specified ranges. Next, the determination of these matrices is considered.

5.1.2.1. Interpolation Algorithm. The parameter-dependent observer state-space matrices are obtained by an interpolation algorithm on the parameter vector. The containment of the parameter vector $\rho(t)$ in a hyper rectangle box with 2^r vertices $\mathcal{S}$ implies that $H(\rho), J(\rho)$ and $L(\rho)$ are contained in the matrix polytopes $R^{n\times n}, R^{n\times m}$ and $R^{n\times p}$, respectively, with the associated vertices

$$\begin{aligned}\widehat{H} :=& \{\widehat{H}_0, \widehat{H}_1, \cdots, \widehat{H}_{2^r-1}\},\\ \widehat{L} :=& \{\widehat{L}_0, \widehat{L}_1, \cdots, \widehat{L}_{2^r-1}\},\\ \widehat{J} :=& \{\widehat{J}_0, \widehat{J}_1, \cdots, \widehat{J}_{2^r-1}\}.\end{aligned}$$

Note that each corner $\widehat{H}_i$ of $\widehat{H}$,$\widehat{L}_i$ of $\widehat{L}$ and $\widehat{J}_i$ of $\widehat{J}$ is a matrix and corresponds to a corner of $\mathcal{S}$. The next task is to determine this correspondence. To that end, let $(a_r^i\, a_{r-1}^i \cdots a_2^i\, a_1^i)$ be the binary representation of the index i, $0 \leq i \leq 2^r - 1$, with a_1 being the last significant and a_r the most significant bit. Then, the parameter box corner $(\hat{s}_1, \hat{s}_2, \cdots, \hat{s}_r)$ of $\mathcal{S}$ corresponding to $\widehat{H}_i, \widehat{L}_i, \widehat{J}_i$ is

$$\hat{s}_j = \begin{cases} \underline{\rho}_j, & \text{if } a_j^i = 0 \\ \overline{\rho}_j, & \text{if } a_j^i = 1 \end{cases}$$

The interpolated observer matrices are given as

$$H(\rho) = \sum_{i=0}^{2^r-1} \pi_i(\rho) \widehat{H}_i, \tag{5.5a}$$

$$L(\rho) = \sum_{i=0}^{2^r-1} \pi_i(\rho) \widehat{L}_i, \tag{5.5b}$$

$$J(\rho) = \sum_{i=0}^{2^r-1} \pi_i(\rho) \widehat{J}_i, \tag{5.5c}$$

where the interpolation function $\pi_i(\rho)$ is given by

$$\pi_i(\rho) = \prod_{j=1}^{r} \frac{\alpha_{ij}\rho_j + \beta_{ij}}{\underline{\rho}_j - \overline{\rho}_j}, \tag{5.6}$$

where

$$\alpha_{ij} = \begin{cases} 1, & \text{if } a_j^i = 0 \\ 0, & \text{if } a_j^i = 1 \end{cases}, \quad \beta_{ij} = \begin{cases} -\overline{\rho}_j, & \text{if } a_j^i = 0 \\ \underline{\rho}_j, & \text{if } a_j^i = 1 \end{cases}$$

After a simple algebra, it can be shown that the interpolation functions satisfy the following properties.

- $0 \leq \pi_i(\rho) \leq 1$ for all $i = 1, 2, \cdots, 2^r - 1$.
- $\sum_{i=1}^{2^{r-1}} \pi_i(\rho) = 1$.

5.1.2.2. Observer Design Procedure. In this section, the parameter-dependent observer construction procedure is given. Using (5.5-5.6), we get the following equivalent system of equations.

$$H(\rho) = H_0 + \sum_{i=1}^{r} \rho_i H_i + \sum_{i=1,j>i}^{r} \rho_i \rho_j H_{r+i+j-2} + \cdots + \prod_{i=1}^{r} \rho_i H_{2^{r-1}}, \tag{5.7a}$$

$$L(\rho) = L_0 + \sum_{i=1}^{r} \rho_i L_i + \sum_{i=1,j>i}^{r} \rho_i \rho_j L_{r+i+j-2} + \cdots + \prod_{i=1}^{r} \rho_i L_{2^{r-1}}, \tag{5.7b}$$

$$J(\rho) = J_0 + \sum_{i=1}^{r} \rho_i J_i + \sum_{i=1,j>i}^{r} \rho_i \rho_j J_{r+i+j-2} + \cdots + \prod_{i=1}^{r} \rho_i J_{2^{r-1}}. \tag{5.7c}$$

Note that although the system has affine structure, the interpolated observer matrices are nonlinear functions of the parameters.

Proposition 5.1. *([34]) System (5.3) is a scheduled observer for the system (5.2) if the following conditions are met.*

$$\dot{\xi} = H(\rho)\xi \quad \textit{has AQS.} \tag{5.8a}$$

$$H(\rho)T + L(\rho)C - TA(\rho) = 0 \tag{5.8b}$$

$$T = I_n - MC \tag{5.8c}$$

$$J(\rho) = TB(\rho) \tag{5.8d}$$

Now, the aim is to express the the conditions of Proposition 1 as a LMI feasibility problem. Note that (5.8b) is a Sylvester equation with non-constant matrices. The resolution of this equation gives

$$H(\rho) = -K(\rho)C + TA(\rho) \tag{5.9a}$$

$$L(\rho) = K(\rho) + H(\rho)M, \tag{5.9b}$$

where $K(\rho)$ is an arbitrary parameter-dependent matrix. For this matrix, the same

structure as for the matrices $H(\rho), L(\rho)$ and $J(\rho)$ is chosen

$$K(\rho) = K_0 + \sum_{i=1}^{r} \rho_i K_i + \sum_{i=1, j>i}^{r} \rho_i \rho_j K_{r+i+j-2} + \cdots + \prod_{i=1}^{r} \rho_i H_{2^{r-1}}. \tag{5.10}$$

From (5.7,5.9) and (5.10), we get

$$H_i = -K_i C + T A_i \qquad \text{for } i = 0, 1, \cdots, r \tag{5.11a}$$

$$H_i = -K_i C \qquad \text{for } i = r+1, r+2, \cdots, 2^r - 1 \tag{5.11b}$$

$$L_i = K_i + H_i M \qquad \text{for } i = 0, 1, \cdots, 2^r - 1 \tag{5.11c}$$

$$J_i = T B_i \qquad \text{for } i = 0, 1, \cdots, r \tag{5.11d}$$

$$J_i = 0 \qquad \text{for } i = r+1, r+2, \cdots, 2^r - 1. \tag{5.11e}$$

Inserting (5.9a) into (5.8a) and using (5.8c, 5.10) gives a relation involving unknown matrices $K_0, K_1, \cdots, K_{2^r-1}$ and M. Hence, the problem of observer design reduces to determination of those matrices such that (5.8a) has AQS. The next theorem gives the conditions under which AQS holds and the expressions for the unknown matrices to be determined.

Theorem 5.1. *([34]) System (5.3) is a scheduled observer for the system (5.2) if there exist matrices $V, \mathcal{Q}$ and symmetric matrices $P_0, P_1, \cdots, P_r$ such that the following LMI condition*

$$\begin{bmatrix} -(V + V^T) & W(s) + P(s) & V^T \\ W^T(s) + P(s) & -P(s) + P(\tau) - P_0 & 0 \\ V & 0 & -P(s) \end{bmatrix} \prec 0$$

$$\text{for all } (s, \tau) \in \mathcal{S} \times \mathcal{T} \tag{5.12}$$

is feasible, where $W(\rho) = \mathcal{Q}\Phi(\rho) + V^T A(\rho)$, where

$$\Phi(\rho) = C \begin{bmatrix} I & \rho_1 I & \cdots & \rho_r I & \rho_1\rho_2 I & \rho_1\rho_3 I & \cdots & \rho_1\rho_r I & \cdots & \left(\prod_{i=1}^{r} \rho_i\right) I & A^T(\rho) I \end{bmatrix}^T$$

and

$$P(\rho) = P_0 + \rho_1 P_1 + \cdots + P_r \rho_r.$$

Then,

$$\mathcal{K} = \begin{bmatrix} -K_0 & -K_1 & \cdots & -K_{2^r-1} & -M \end{bmatrix} = V^{-T}\mathcal{Q}.$$

After determination of K_i and M, H_i, L_i and J_i can be computed from (5.11a)-(5.11e).

5.2. Application to Diesel Engine Compressor Air Mass Flow Estimation

Considering the same diesel engine model of the previous chapters, we have the following equivalent system.

$$\dot{p}_i = k_1 \rho_1 P_c + \tilde{\tilde{u}}_1, \tag{5.13a}$$

$$\dot{p}_x = k_2 \rho_2 p_i + \tilde{\tilde{u}}_2, \tag{5.13b}$$

$$\dot{P}_c = k_3 P_c + \tilde{\tilde{u}}_3, \tag{5.13c}$$

where

$$k_1 = \frac{R\eta_c}{c_p T_a V_i},\ k_2 = \frac{\eta_v V_d}{120 V_x},\ k_3 = -\frac{1}{\tau},$$
$$\tilde{\tilde{u}}_1 = \frac{RT_i}{V_i}\left(W_{xi} - W_{ie}\right),\ \tilde{\tilde{u}}_2 = \frac{RT_x}{V_x}\left(W_f - W_{xi} - W_{xt}\right),\ \tilde{\tilde{u}}_3 = \frac{W_{xt} c_p T_x \eta_t}{\tau}\left(1 - \left(\frac{p_a}{p_x}\right)^{\mu}\right)$$

and the scheduling parameters are

$$\rho_1 = \frac{T_i}{\left(\frac{p_i}{p_a}\right)^{\mu} - 1},\ \rho_2 = \frac{T_x N}{T_i}.$$

The measured variables are the states $p_i, p_x,$ the engine inputs x_v, x_r, W_f and the external exogenous parameters T_i, T_x and N. Note that W_{xi}, W_{xt} and W_{ie} are functions of the above measured variables and therefore we are able to define the transformed inputs $\tilde{\tilde{u}}_1$ and $\tilde{\tilde{u}}_2$. The model (5.13) will be called a "transformed diesel engine model" and is affine in the parameters ρ_1 and ρ_2. The aim is first to estimate the state P_c and then determine the compressor air mass flow from the estimated compressor power via the relation

$$W_{ci} = \frac{\eta_c}{c_p T a} \frac{P_c}{\left(\frac{p_i}{p_a}\right)^{\mu} - 1}.$$

The last task is the determination of the ranges for the scheduling parameters and for their rates of variation. We assume that $p_i \in [100,\ 160]$ kPa, $T_i \in [300,\ 350]$ K, $T_x \in [350,\ 700]$ K and $N \in [500,\ 3500]$ rpm. This results in $\rho_1 \in [2,\ 153] \times 10^3$ and $\rho_2 \in [0.5,\ 8.2] \times 10^3$. Finally,

$$\rho_1 = \frac{T_i}{\left(\frac{p_i}{p_a}\right)^{\mu} - 1} \Rightarrow \dot{\rho}_1 = \frac{\dot{T}_i \left(\left(\frac{p_i}{p_a}\right)^{\mu} - 1 \right) - T_i \mu \frac{p_i^{\mu-1}}{p_a^{\mu}} \dot{p}_i}{\left(\left(\frac{p_i}{p_a}\right)^{\mu} - 1 \right)^2},$$

$$\rho_2 = \frac{T_x N}{T_i} \Rightarrow \dot{\rho}_2 = \frac{\left(\dot{N} T_x + N \dot{T}_x\right) T_i - \dot{T}_i \left(N T_x\right)}{T_i^2}.$$

Letting $\dot{p}_i \in [-100,\ 100]$ kPa/s, $\dot{T}_i, \dot{T}_x \in [-10,\ 10]$ K and $\dot{N} \in [-500, 500]$ rpm/s gives $\dot{\rho}_1 \in [-1.93,\ 1.93] \times 10^7$ and $\dot{\rho}_2 \in [-1.77,\ 1.77] \times 10^3$. For the application of the method, we need a change of variables. Defining

$$\rho_1 = \widetilde{\rho}_1 + 77.5 \times 10^3,\ \rho_2 = \widetilde{\rho}_2 + 4.35 \times 10^3,$$

we have $\widetilde{\rho}_1 \in [-75.5,\ 75.5] \times 10^3$ and $\widetilde{\rho}_2 \in [-3.85,\ 3.85] \times 10^3$. Finally, $\dot{\widetilde{\rho}}_i = \dot{\rho}_i$, $i = 1, 2$ gives $\dot{\widetilde{\rho}}_1 \in [-1.93,\ 1.93] \times 10^7$ and $\dot{\widetilde{\rho}}_2 \in [-1.77,\ 1.77] \times 10^3$. In computing the ranges

of the scheduling parameters and their rates of variation we use the toolbox INTLAB [69] which is used for interval related computations and optimizations.

5.3. Simulations

Figure 5.1 summaries the working principle of observer schematically for compressor air mass flow estimation. For the transformed system (5.13), the parameter-

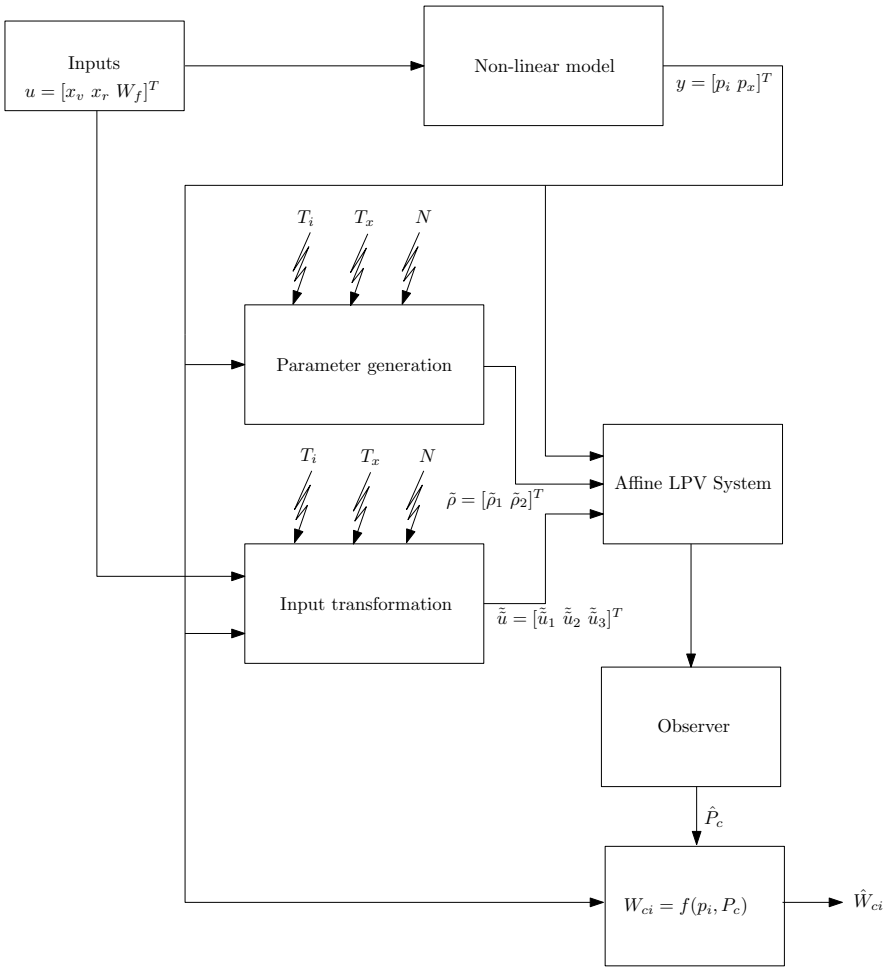

Figure 5.1. Working principle of observer

dependent system matrices are

$$A(\rho) = \begin{bmatrix} 0 & 0 & k_1(\widetilde{\rho}_1 + 77.5 \times 10^3) \\ k_2(\widetilde{\rho}_2 + 4.35 \times 10^3) & 0 & 0 \\ 0 & 0 & k_3 \end{bmatrix}, \; B(\rho) = \begin{bmatrix} 1 & 0 & 0 \\ 0 & 1 & 0 \\ 0 & 0 & 1 \end{bmatrix}.$$

Since we are estimating compressor power based on real time measurement of manifold pressures, we have

$$C = \begin{bmatrix} 1 & 0 & 0 \\ 0 & 1 & 0 \end{bmatrix}.$$

The parameter dependent Lyapunov matrix $P(\rho)$ to be determined is

$$P(\widetilde{\rho}) = P_0 + \widetilde{\rho}_1 P_1 + \widetilde{\rho}_2 P_2,$$

and the matrix Φ is

$$\Phi(\widetilde{\rho}) = \begin{bmatrix} C^T & \widetilde{\rho}_1 C^T & \widetilde{\rho}_2 C^T & \widetilde{\rho}_1 \widetilde{\rho}_2 C^T & C^T A(\widetilde{\rho})^T \end{bmatrix}^T.$$

Next, we consider the same case studies of Chapter 4 (the same inputs and T_i, T_x, N values) and a comparison with EKF.

5.3.1. Case I

The corresponding input, parameter signals and estimation results are shown through Figures 5.2 and 5.5. In the estimation comparison figures, the signal in blue color is the real signal (x_r), the signal in black color is the estimated signal by EKF (x_k) and the red-color signal is the one estimated by the proposed LPV-based method (x_{lpv}).

5.3.2. Case II

The corresponding input, parameter signals and estimation results are shown through Figures 5.6 and 5.9.

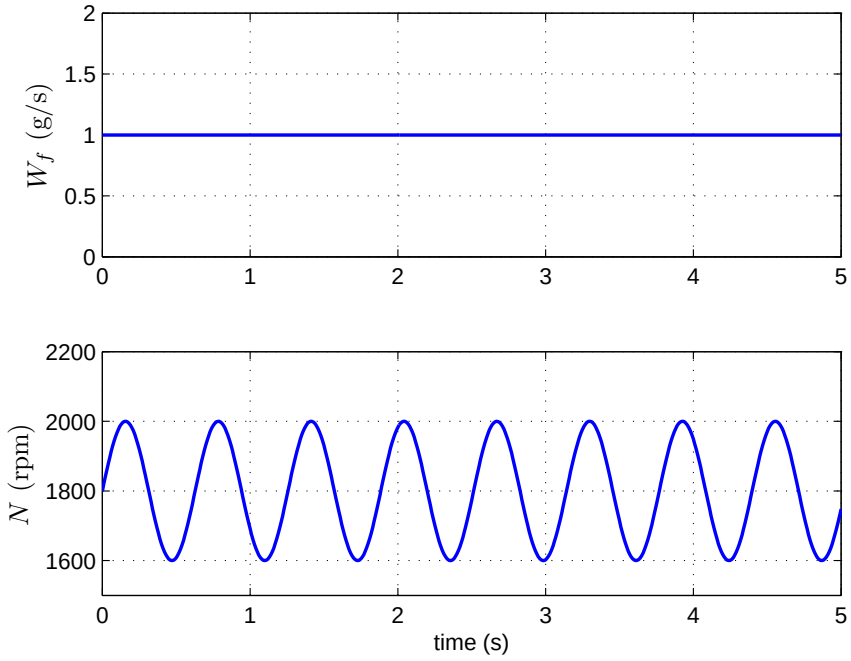

Figure 5.2. Fuel flow rate and engine speed

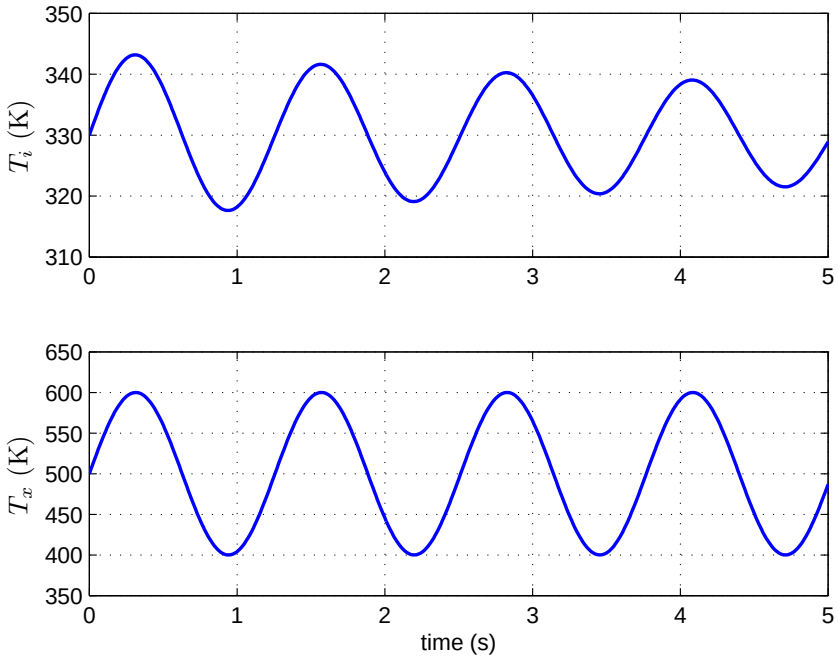

Figure 5.3. Intake and exhaust manifold temperatures

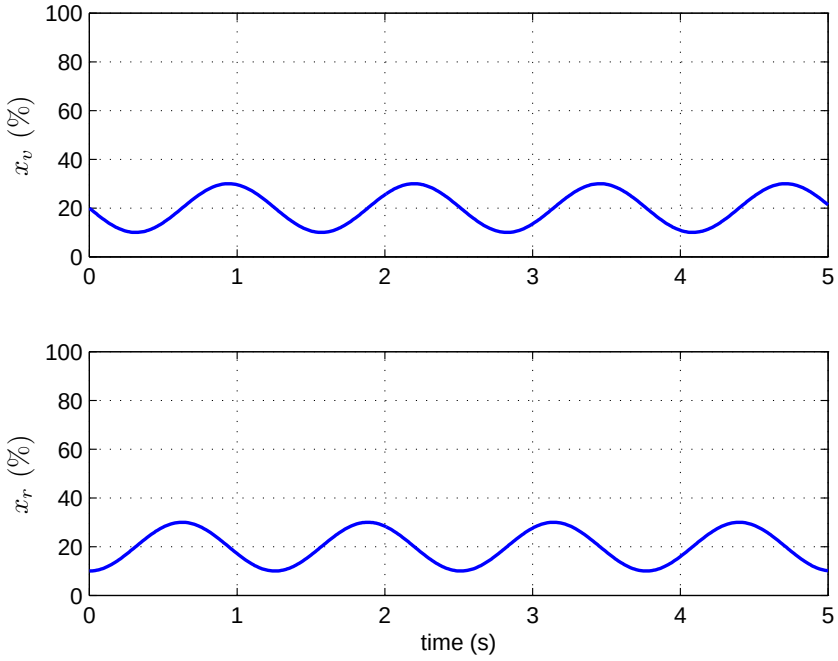

Figure 5.4. Vgt vane and egr valve position

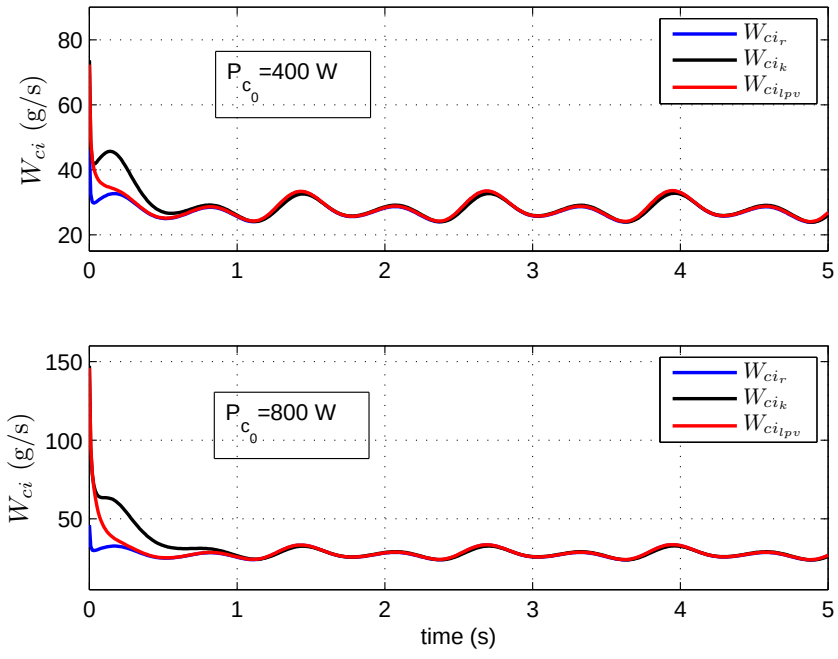

Figure 5.5. Compressor air mass flow and its estimations.

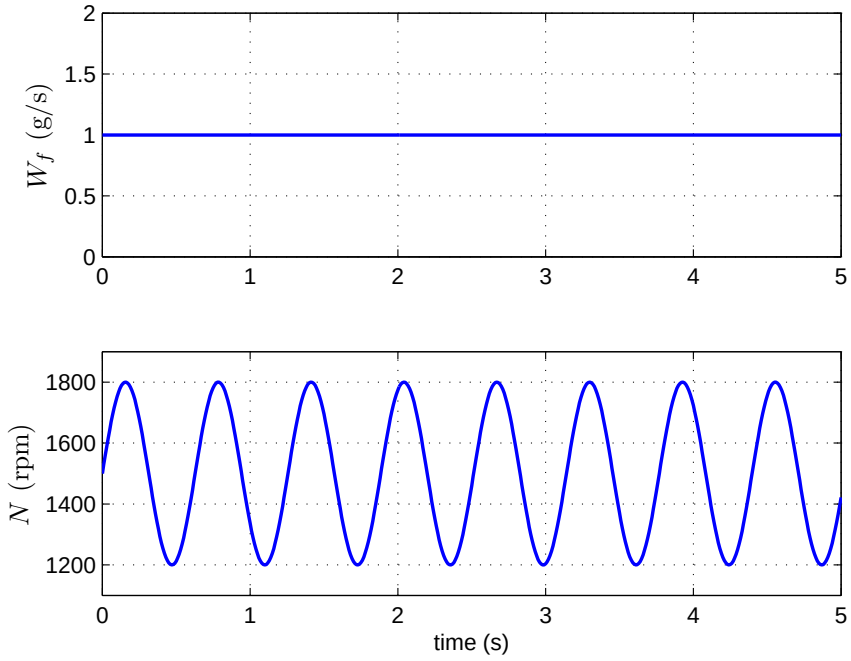

Figure 5.6. Fuel flow rate and engine speed

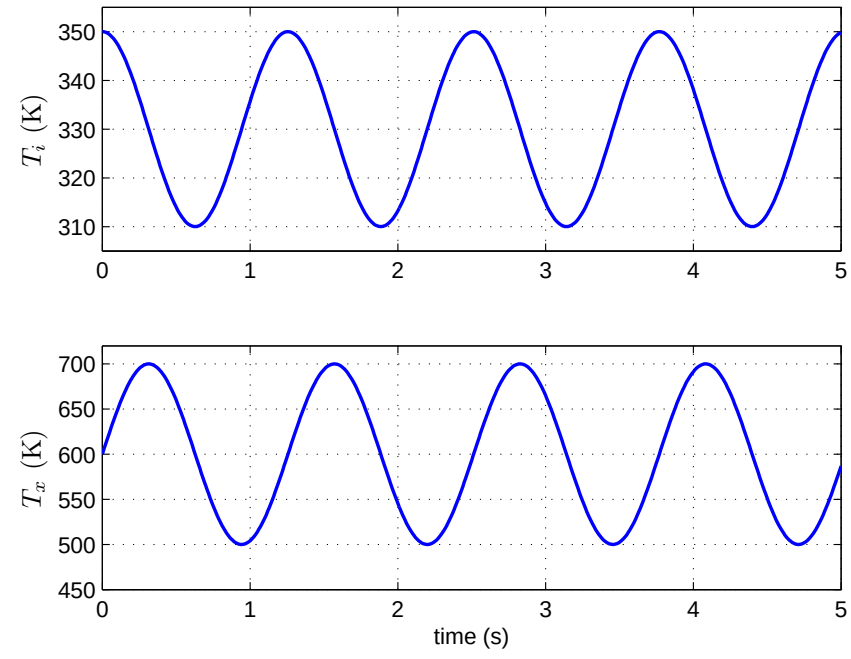

Figure 5.7. Intake and exhaust manifold temperatures.

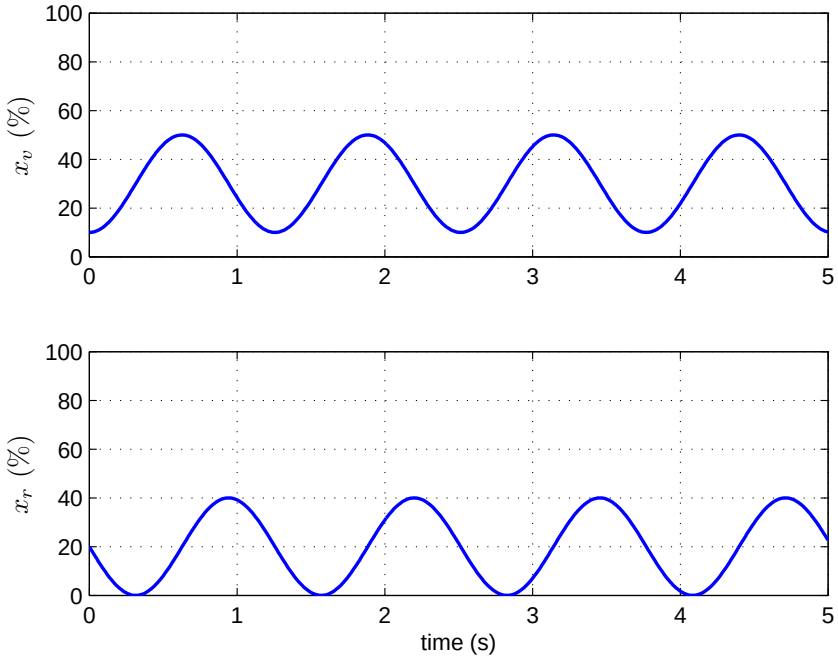

Figure 5.8. Vgt vane and egr valve position

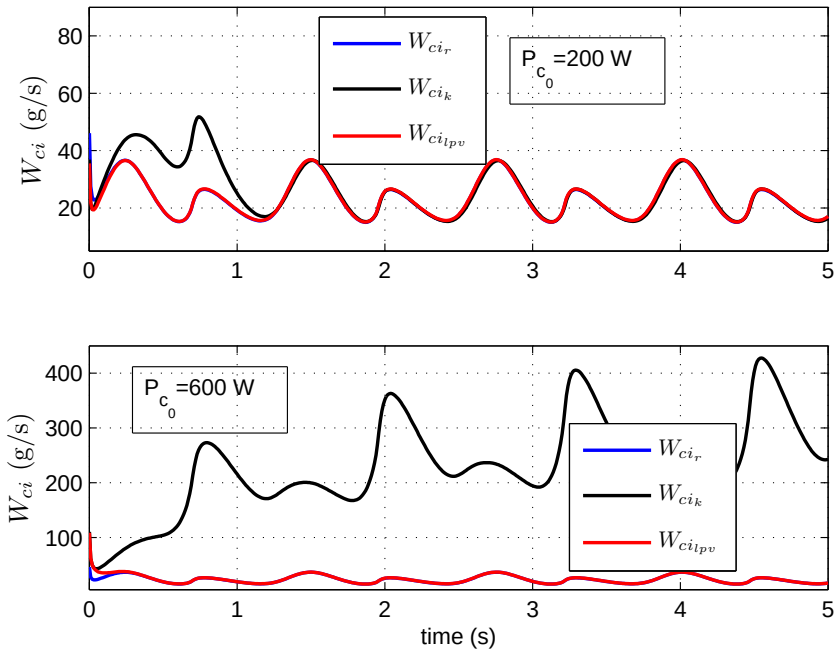

Figure 5.9. Compressor air mass flow and its estimations

5.4. Comments

Observer design for nonlinear systems is in general a difficult task. In this chapter, we considered a nonlinear mean-value diesel engine model and, without any simplification on it, we transformed the model to an equivalent affine parameter-dependent system and then applied the observer design method of [34]. Based on the measurements of manifold pressures and engine inputs, compressor power was estimated and then compressor flow was estimated from the estimated compressor power. An accurate estimation of compressor air mass flow is an important task both for removal of the expensive MAF sensor (which is, also, not accurate in some situations as mentioned) when cost is a consideration and achievement of a good quality signal when it is used as a feedback variable in control applications. The performance of the designed asymptotic observer was shown through simulations with comparisons to EKF to demonstrate cases where EKF may show poor performance and hence not useful in compressor air mass flow estimations.

6. CONCLUSIONS AND FUTURE WORK

In this thesis, we considered the separate problems of controlling the air path system and compressor air mass flow estimation in diesel engines. To summarize:

- As a control problem we dealt with to regulate the air path system in diesel engines by controlling the exhaust manifold pressure and compressor air mass flow using a linear parameter-varying approach by considering a general nonlinear, mean-value engine model used extensively in the literature. The control strategy is such that no simplifications on engine model is done or no operating point is chosen and even manifold temperatures are considered as time-varying parameters. In this regard, the presented control strategy is very general, in contrast to the existing other control strategies in the literature using the same model.
- Two different estimation methods were given to estimate compressor air mass flow which may be difficult and/or unreliable to measure in certain situations.
  (i) The first estimation method is a developed general state estimation method to be used in state/parameter estimation in nonlinear models where the state or parameter to be estimated appears linearly in the system dynamics. The case for state estimation was given and the parameter estimation case can be developed with a slight modification. The method was based on a combination of fitting a linear moving model to the measured states and inputs and using the discretization of the unmeasured states. This results in an iterative formula. The method was successfully applied to some case studies and then used for compressor air mass flow estimations. All results were compared with EKF to see the performance of the method.
  (ii) The second estimation approach was a state estimation method for affinely parameter-dependent systems developed by [34]. For the application of this method, the nonlinear engine model was transformed into an equivalent affinely parameter-dependent form. The main advantage of this second approach is that it is an asymptotic observer. Again the method was applied for diesel engine compressor air mass flow estimation, with a comparison to

EKF. The results were even better than using the first estimation method since the second method is of asymptotic convergence. However, the first estimation method may be used in some estimation schemes where the second cannot be used.

As a future work, in the control part we considered volumetric, turbine and compressor efficiencies as some optimal constant values. A further improvement may be modeling of these variables and then considering them as additional time-varying parameters. A second way may be interpreting them as uncertain parameters and then apply a control approach for partly measured LPV systems [70].

As to the future work in the estimation part, it is well-known that it is expensive and difficult to measure exhaust manifold quantities like pressure, temperature or the flow W_{xt} since the soot in the exhaust can quickly cover the sensors and make the measurements unreliable. Development of new joint state-parameter estimation methods is necessary in order to estimate these exhaust quantities.

APPENDIX A: Basic Terminology

A.1. Signal Norms

Before defining signal norms, it will be better first to give the definition of a "signal" and a "norm". A "signal" $u(t)$ is a function from the nonnegative real numbers, R_+, to R^m. Let V be a vector space. Simply, a norm, $\|\cdot\|$, is a function from the vector space V to R_+ satisfying the following properties for each $u, v \in V$:

(i) $\|u\| \geq 0$ and $\|u\| = 0 \Leftrightarrow u = 0$
(ii) $\|u + v\| \leq \|u\| + \|v\|$
(iii) $\|\alpha u| = |\alpha|\|u\| \ \forall \alpha \in R$

A signal norm is a norm and is one of the ways to measure its size. Among many signal norms, here we will be interested in the *2-norm* which is defined as follows:

$$\|u\|_2 := \left(\int_0^\infty u(t)^T u(t) dt\right)^{\frac{1}{2}} = \left(\frac{1}{2\pi}\int_0^\infty \hat{u}(jw)^* \hat{u}(jw) dw\right)^{\frac{1}{2}}, \tag{A.1a}$$

where $\hat{u}(jw)$ is the Laplace transformation of $u(t)$. The second equality is known as "Parseval's Relation".

A.2. Linear Matrix Inequalities

Linear matrix inequalities are expressions encountered in convex optimization problems, which define convex constraints. For $x = (x_1\, x_2\, \cdots x_n)^T \in R^n$, a LMI in x is an expression of the form

$$\text{LMI(x)} := A_0 + \sum_{i=1}^{n} x_i A_i \succ 0 \tag{A.2}$$

where $A_0, A_1, \cdots, A_n$ are symmetric matrices in S^n, the set of symmetric matrices, and $\succ$ means positive definiteness. Although we have defined a LMI for $\succ$, it is possible to have the forms $\succeq, \prec$ and $\preceq$.

The LMI (A.2) defines a convex constraint on the decision variable x. That is, the set $\{x \in R^n : \text{LMI(x)} \succ 0\}$ is a convex set. A system of LMIs given by $\text{LMI}^{(1)}(x) \succ 0$, $\text{LMI}^{(2)}(x) \succ 0$, $\cdots, \text{LMI}^{(k)}(x) \succ 0$ can be expressed as the single LMI

$$\textbf{diag}\left(\text{LMI}^{(1)}(x),\ \text{LMI}^{(2)}(x),\ \cdots, \text{LMI}^{(k)}(x)\right) \succ 0.$$

In the literature, the encountered forms of LMIs are not in the form given by (A.2) which involves scalar decision variables, rather they involve matrices as the decision variables. As an example, consider

$$A^T P + PA \succ 0,$$

where $A \in R^{n \times n}$ is a given matrix and $P = P^T$ is the matrix variable. This problem can be easily converted to the form (A.2). Expressions of LMIs involving matrices as decisions variables can save a lot of space and in addition parsers of LMI solvers (like Yalmip parser used for Sedumi solver) can be used for LMIs in this condensed form.

The LMI problems given by the main form (A.2) or other forms reducible to this main form are called LMI feasibility problems and the solution set is called the *feasibility set*. It is also possible to have convex optimization problems involving as their constraints LMIs. In particular, the *linear objective minimization problem*

$$\text{minimize } c^T x \text{ subject to LMI(x)} \succ 0$$

is such an example. Both LMI feasibility problems and optimization problems involving a convex objective function with LMIs as their constraints are examples of convex optimization problems. Here, convexity has the important consequence that such problems

can be solved numerically with a guarantee of finding the solution if it exists. Efficient numerical algorithms (like interior-point methods) exist in the literature to solve such problems.

Many control system analysis and design problems (especially those which are based on Lyapunov analysis and design), estimation-identification problems, structural design, matrix scaling problems, etc involve LMIs. In the control part of this thesis, LMIs were used for synthesis of gain scheduled controllers. A short list of other applications involving LMIs can be given as follows [71]:

- matrix scaling problems, e.g., minimizing condition number by diagonal scaling
- quadratic stability and performance analysis of Lyapunov based control algorithms
- multi-criterion LQR/LQG
- inverse problem of optimal control
- synthesis of Lur'e-type Lyapunov functions for nonlinear systems
- optimal system realization
- weighted interpolation problems

Next, we consider an example involving LMIs.

A.2.1. Stability Example

Consider the dynamical system

$$\dot{x} = Ax,$$

whose stability is equivalent to the existence of a matrix $P = P^T$ such that

$$A^T P + PA \prec 0,$$
$$P \succ 0.$$

The stability analysis can be extended to linear time-variant (LTV) systems. Consider the system

$$\dot{x} = A(t)x, \tag{A.3}$$

where $A(t)$ varies in the convex envelope of a set of linear time-invariant (LTI) systems:

$$A(t) \in \mathbf{Co}\{A_1, A_2, \cdots, A_N\} := \left\{ \sum_{i=1}^{N} \alpha_i A_i : \alpha_i \geq 0, \sum_{i=1}^{N} \alpha_i = 1 \right\}.$$

A sufficient condition for the stability of (A.3) is the existence of a matrix $P = P^T$ such that the following systems of LMIs are satisfied:

$$A_i^T P + P A_i \prec 0,$$
$$P \succ 0.$$

A.3. Equivalence of Norms on Finite Dimensional Vector Spaces

Let $\|u\|_a$ and $\|u\|_b$ be two norms defined on a finite dimensional vector space V. We say that $\|u\|_a$ and $\|u\|_b$ are equivalent norms on V if there exist $\alpha, \beta \geq 0$ such that

$$\alpha \|u\|_a \leq \|u\|_b \leq \beta \|u\|_a$$

The importance of equivalent norms is that the convergence of a sequence defined on V with respect to one norm implies the convergence with respect to the other.

APPENDIX B: Orthogonal Functions

We will introduce orthogonal functions briefly here . For detailed information on this topic, the reader is referred to [68].

Definition B.1. *A set of functions* $S = \{\phi_k(t) : k = 0, 1, 2, \cdots, r-1\}$*, is said to be orthogonal in the interval* $[a, b]$ *if*

$$\int_a^b \phi_i(t)\phi_j(t)dt = K \tag{B.1}$$

where $K = 0$ *if* $i \neq j$ *and non-zero for* $i = j$*.*

One of the important properties of orthogonal functions is their integral property. The orthogonal functions in the set S satisfy the following integral property

$$\int_{t_0}^t \phi(\tau)d\tau \cong O\phi(t) \tag{B.2}$$

where $\phi = [\phi_0(t), \phi_1(t), \cdots, \phi_{r-1}(t)]^T$ and O is known as operational matrix (of integration). Examples of orthogonal functions are

- Fourier series
- Shifted Jacobi polynomials
- Shifted Chebyshev polynomials
- Shifted Legendre polynomials.

In this work, we use the shifted Legendre polynomials (in $[0, t_f]$), which are obtained from the recursive formula [68]

$$\phi_{n+1} = \frac{2n+1}{n+1}\left(\frac{2t}{t_f} - 1\right)\phi_n(t) - \frac{n}{n+1}\phi_{n-1}(t), \ n \geq 1, \tag{B.3}$$

with $\phi_0 = 1,\ \ \phi_1(t) = \dfrac{2t}{t_f} - 1$. The corresponding operational matrix is given as

$$O = t_f \begin{bmatrix} 1 & 1 & 0 & 0 & \cdots & \cdots & \cdots & 0 & 0 & 0 \\ -\frac{1}{3} & 0 & \frac{1}{3} & 0 & \cdots & \cdots & \cdots & 0 & 0 & 0 \\ 0 & -\frac{1}{5} & 0 & \frac{1}{5} & \cdots & \cdots & \cdots & 0 & 0 & 0 \\ \vdots & & & & \ddots & & & & \vdots & \vdots \\ \vdots & & & & \ddots & \ddots & & & \vdots & \vdots \\ \vdots & & & & \ddots & \ddots & \ddots & & \vdots & \vdots \\ \vdots & & & & & \ddots & \ddots & & & \\ 0 & 0 & 0 & 0 & & & & 0 & \dfrac{1}{2r-5} & 0 \\ 0 & 0 & 0 & 0 & \cdots & \cdots & & \dfrac{-1}{2r-3} & 0 & \dfrac{1}{2r-3} \\ 0 & 0 & 0 & 0 & \cdots & \cdots & & 0 & \dfrac{-1}{2r-1} & 0 \end{bmatrix}$$

APPENDIX C: Linear Fractional Transformations

Consider the complex matrix M appropriately partitioned as

$$P = \begin{pmatrix} P_{11} & P_{12} \\ P_{21} & P_{22} \end{pmatrix} \in \mathbb{C}^{(q_1+q_2)\times(r_1+r_2)}$$

and let $\Delta_l \in \mathbb{C}^{(r_2\times q_2)}$ and $\Delta_u \in \mathbb{C}^{(r_1\times q_1)}$. Then, the lower fractional transformation of P with respect to Δ_l is defined as

$$\mathcal{F}_l(P, \Delta_l) := P_{11} + P_{12}\Delta_l \left(I - P_{22}\Delta_l\right)^{-1} P_{21} \tag{C.1}$$

provided that the inverse $(I - P_{22}\Delta_l)^{-1}$ exists. Similarly, the upper fractional transformation of P with respect to Δ_u is defined as

$$\mathcal{F}_u(\Delta_u, P) := P_{22} + P_{21}\Delta_u \left(I - P_{11}\Delta_u\right)^{-1} P_{12} \tag{C.2}$$

provided that $(I - P_{11}\Delta_u)^{-1}$ exists.

APPENDIX D: Diesel Engine Model Parameters

Table D.1. Engine Model Parameters [23]

Symmbol	Value	Unit	Description
V_i	6×10^{-3}	m^3	intake manifold volume
V_x	1×10^{-3}	m^3	exhaust manifold volume
V_d	2×10^{-3}	m^3	displacement volume
c_p	1014.4	J/kg/K	specific heat at constant pressure
c_v	727.4	J/kg/K	specific heat at constant volume
R	287	J/kg/K	gas constant ($R = c_p - c_v$)
p_a	99.2	kPa	ambient pressure
T_a	302	K	ambient temperature
p_{ref}	101.3	kPa	reference pressure
T_{ref}	298	K	reference temperature
γ	1.3936	-	specific heat ratio $\left(\gamma = \frac{c_p}{c_v}\right)$

APPENDIX E: Self Conditioned Controller Design for Anti-Windup

Most real engineering systems involve actuators which are input bounded. When the real process input is different than the desired control output, inadequacy of control state variables may deteriorate the controller performance. In [45], in order to restore this inadequacy of sate variables, auxiliary reference inputs called "realizable references" are used. In this part, we determine realizable references for a LPV controller. For details, refer to [45].

Assume that the equations of a LPV controller without AW protection are

$$\begin{aligned}
\dot{x}_c =& A_c x_c + B_{p_c} p_c + B_c e, \\
q_c =& C_{q_c} x_c + D_{q_c p_c} p_c + D_{q_c e} e, \\
u =& C_u x_c + D_{u p_c} p_c + D_{ue} e, \\
p_c =& \Delta_c q_c,
\end{aligned}$$

where $e = y - w$ is the difference between measured and reference signals. The corresponding equations when a realizable reference w_r is used as input are

$$\dot{x}_c^r = A_c x_c^r + B_{p_c} p_c^r + B_c e_r, \tag{E.1a}$$

$$q_c^r = C_{q_c} x_c^r + D_{q_c p_c} p_c^r + D_{q_c e} e_r, \tag{E.1b}$$

$$u_r = C_u x_c^r + D_{u p_c} p_c^r + D_{ue} e_r, \tag{E.1c}$$

$$p_c^r = \Delta_c q_c^r, \tag{E.1d}$$

where $e_r = y - w_r$ and x_c^r, u_r, p_c^r and q_c^r are the variables corresponding to w_r, respectively. Let $D_{q_c e} = D_1, D_{ue} = D_2$ and assume that D_2 is invertible (which is the case in

this thesis). The control input u is assumed to be

$$u = C_u x_c^r + D_{up_c} p_c^r + D_2 e. \tag{E.2}$$

and that $u = u_r$. Using (E.1c) and (E.2) and the expressions for e, e_r, we get

$$w_r = w + D_2^{-1}\left(u_r - u\right). \tag{E.3}$$

Using (E.1), e_r and (E.3), we obtain

$$\dot{x}_c^r = A_c x_c^r + B_{p_c} p_c^r + B_c e + B_c D_2^{-1} e_u, \tag{E.4a}$$

$$q_c^r = C_{q_c} x_c^r + D_{q_c p_c} p_c^r + D_{q_c e} e_r, \tag{E.4b}$$

$$u = C_u x_c^r + D_{up_c} p_c^r + D_{ue} e_r, \tag{E.4c}$$

$$p_c^r = \Delta_c q_c^r, \tag{E.4d}$$

$$u_r = \mathrm{sat}(u), \tag{E.4e}$$

where "sat" denotes the actuator saturation effect. The AW-LPV Controller (a.k.a. Self Conditioned Controller) represented by E.4 is shown in Figure E.1.

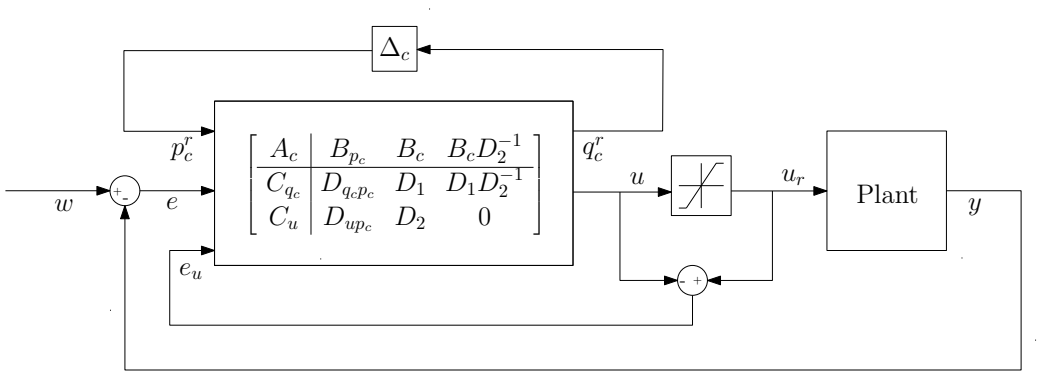

Figure E.1. LPV control with AW protection

REFERENCES

1. Ferguson, C.R. and A.T. Kirkpatric, *Internal Combustion Engines: Applied Thermosciences*, Second edition, Jonh Wiley and Sons. Inc., 2000.

2. Davis, S.C., S.W. Diegel and R.G. Boundy, *Transportation Energy Data Book*, Edition 27, ORNL-6981, 2008.

3. Wei, X., *Advanced LPV Techniques for Diesel Engines*, Ph.D. thesis, Johannes Kepler University, 2006.

4. Kraushaar, J.J and R. A. Ristinen, *Energy and the Environment*, Second edition, New York: John Wiley & Sons, Inc. ISBN 978-0471739890, 1998.

5. Guzzella L. and C. H. Onder, *Introduction to Modeling and Control of Internal Combustion EngineSystems*, Springer, Berlin, 2004.

6. U.S. Environmental Protection Agency, "Final Regulations for Revisions to the Federal Test Procedure for Emissions From Motor Vehicles, *Federal Register*, Vol. 61, No. 205, pp. 5482-5486, October 22, 1996.

7. U.S. Environmental Protection Agency, "*Control of Air Pollution From New Motor Vehicles: Tier 2 Motor Vehicle Emissions Standards and Gasoline Sulfur Control Requirements*, Federal Register, Vol. 65, No. 28, pp. 80-86, February 10, 2000.

8. European Standards: DieselNet, *Emissions Standards, European Union, Cars and Light Trucks*, web site: www.dieselnet.com/standards/eu/ld.php.

9. *Motor Trend Magazine*, http://images.motortrend.com/roadtests/coupes /112_0605_vtg_16z+porsche_vtg_turbocharger+cutaway.jpg, 2010.

10. Stefanopoulou, A. G., I. Kolmanovsky and J. S. Freudenberg, "Control of variable geometry turbocharged diesel engines for reduced emissions", *IEEE Transactions*

on Control Systems Technology, Vol. 8, Issue 4, pp. 733-745, 2000.

11. Yuanwang D., Z. Meilin, X. Dong and C. Xiaobei, "An Analysis for Effect of Cetane Number on Exhaust Emissions from Engine with the Neural Network", *Fuel*, Vol. 81, Issue 15, pp. 1963-1970, 2003.

12. Durna A., M. Lapuertab and F.J. Rodrguez ,"Neural Networks Estimation of Diesel Particulate Matter Composition from Transesterified Waste Oils Blends", *Fuel*, Vol. 84, Issue 16, pp. 2080-2085, 2005.

13. Lucas A., M. Duran, M. Carmona and M. Lapuerta, "Modeling Diesel Particulate Emissions with Neural Networks", *Fuel*, Vol. 80, Issue 4, pp. 539-548, 2001.

14. Hafner M., M. Schler, O. Nelles and R. Iserman, "Fast Neural Networks for Diesel Engine Control Design", *Control Eng. Pract*, Vol. 8, Issue 11, pp. 1211-1221, 2000.

15. Tan Y. and M. Saif ,"Neural Networks-Based Nonlinear Dynamic Modeling for Automotive Engines", *Neurocomputing 30*, pp. 129-142, 2000.

16. Roskilly A. P., E. Mesbahi, G. Armstrong and P. N. Pappas,"On-line Adaptive Modelling of Diesel engines", *Transactions - Institute of Marine Engineers*, Vol. 109, Issue 4, pp. 313-324, 1997.

17. Kao M. and J.J. Moskwa, "Nonlinear Diesel Engine Control and Cylinder Presure Observation", *ASME Winter Annual Meeting, Advanced Automotive Technologies*, DSC-Vol.52, pp. 187-198, 1993.

18. Rajamani R.,"Control of a Variable-Geometry Turbocharged and Wastegated Diesel Engine", *Proc. of IMechE. Part D, Journal of Automobile Engineering*, Vol. 219, pp. 1361-1368, 2005.

19. Linoa P., B. Maione and A. Rizzoa ,"Nonlinear Modelling and Control of a Common Rail Injection System for Diesel Engines", *Applied Mathematical Modelling*, Vol. 31, Issue 9, pp. 1770-1784, 2007.

20. Plianos A., A. Achir, R. Stobart, H. Chafouk and N. Langlois, "Optimal Nonlinear Control of a Diesel Engine Air-Path System Using VGT/EGR Actuation", *European Control Conference*, Kos, Greece, 2007.

21. Wei X. and L.D. Re, "Gain scheduled H_∞ Control for Air Path Systems of Diesel Engines Using LPV Techniques", *IEEE Transactions on Control Systems Technology*, Vol. 15, pp. 406-415, 2007.

22. Song, Q. and K. M. Grigoriadis, "Diesel Engine Speed Regulation Using Linear Parameter Varying Control", *Procedings of the American Control Conference*, Denver, Colorado, USA, 2003.

23. Jung M. and K. Glover, "Calibratable Linear Parameter-Varying Control of a Turbocharged Diesel Engine", *IEEE Transactions on control Ssystems Technology*, Vol. 14, No. 1, pp. 45-61, 2006.

24. Wang, J., "Air Fraction Estimation for Multiple Combustion Mode Diesel Engines with Dual-Loop EGR Systems", *Control Engineering Practice*, Vol. 16, Issue 12, pp. 1479-1486, 2008.

25. Brahma, A., D. Upadhyay, A. Serrani and G. Rizzoni, "Modeling, Identification and State estimation of Diesel Engine Torque and NO_x Dynamics in Response to Fuel Quantity and Timing Excitations", *Proceeding of the 2004 American Control Conference*, Boston, Massachusetts, June 30 -July 2, 2004.

26. Zweiri, Y. H. and L. D. Seneviratne, "Diesel Engine Indicated and Load Torque Estimation Using a Nonlinear Observer", *IMechE, Part D: J. Automobile Engineering*, Vol. 220, pp. 775-785, 2006.

27. Zweiri, Y. H., "Diesel Engine Indicated Torque Estimation Based on Artificial Neural Networks ", *International Journal of Intelligent Systems and Technologies*, Vol. 1, pp. 233-239, 2006.

28. Desantes, J. M., J. Galindo, C. Guardiola and V. Dolz., "Air Mass Flow Estimation in Turbocharged Diesel Engines from in-Cylinder Pressure Measurement", *Experimental Thermal and Fluid Science*, Vol. 34, Issue 1, pp. 37-47, 2010.

29. Jankovic, M., M. Jankovic and I.V. Kolmanovsky, "Constructive Lyapunov Control Design for Turbocharged Diesel Engines", *IEEE Transactions on Control Systems Technology*, Vol. 8, No. 2, pp. 288-299, 2000.

30. Plianos, A., A. Achir, R. Stobart, N. Langlois and H. Chafouk, "Dynamic Feedback Linearization Based Control Synthesis of the Turbocharged Diesel engine", *Proceedings of the 2007 American Control Conference*, USA, July 11-13, 2007.

31. Dabo, M., N. Langlois and H. Chafouk, "Asymptotic Tracking Applied to the Control of a Turbocharged Diesel Engine", *Proceedings of the UKACC International Conference on Control*, 2008.

32. Wahlstrom, J., *Control of EGR and VGT for Emission Control and Pumping Work Minimization in Diesel Engines*, Phd. Thesis, Linköping University, 2009.

33. Scherer, C. W. and S. Weiland, *Linear Matrix Inequalities in Control*, Mechanical Engineering Systems and Control Group, Delft University of Technology, 2005.

34. Bara, G. I., J. Daafouz, Z. Kratz and J. Ragot, "Parameter-Dependent State observer Design for Affine LPV systems", *International Journal of Control*, Vol. 74, No. 16, pp. 1601-1611, 2001.

35. Christen, U., K. J. Vantine and N. Collings, "Event-Based Mean Value Modeling of DI Diesel Engines for Controller Design", *Society of Automotive Engineers*, 2001.

36. Zhou K. and J. C. Doyle, *Essentials of Robust Control*, Prentice Hall, New Jersey, 1997.

37. Hecker, S., A. Varga and J. F. Magni, "Enhanced LFR-toolbox for Matlab", *Aerospace Science and Technology*, Vol. 9, Issue 2, pp. 173-180, 2005.

38. Megretski, A. and A. Rantzer, "System Analysis via Integral Quadratic Constraints", *IEEE Transactions on Automatic Control*, Vol. 42, No. 6, pp. 819-830, June 1997.

39. Scherer, C. W., "Mixed Control and Linear Parameter-Varying Control with Full Block Scalings", in S.-I. Niculescu and L. El Ghaoui (eds.), A*dvances in Linear Matrix Inequality Methods in Control*, pp. 187-207, SIAM, 1999.

40. Apkarian, P. and R. J. Adams, "Advanced Gain-Scheduling Techniques for Uncertain Systems", *IEEE Transactions on Control Systems Technology*, Vol. 6, No. 1, pp. 21-32, 1998.

41. Wu, F., *Control of Linear Parameter-Varying Systems*, Ph.D. Dissertation, Univ. of California, Berkeley, 1995.

42. Skelton, R. E., T. Iwasaki and K. Grigoriadis, "A Unified Algebraic Approach to Linear Control Design", *Automatica*, Vol. 39, Issue 11, pp. 2014-2016, November 2003.

43. Gahinet, P. and P. Apkarian, "A Linear Matrix Inequality Approach to H_∞ Control", *Int. J. Robust Nonlinear Control*, Vol. 4, Issue 4, pp. 421-448, 1994.

44. Huang, Y. and A. Jadbabaie, "Nonlinear H_∞ Control: An Enhanced Quasi-LPV Approach", *Proceedings of the IFAC World Congress*, Beijing, China, 1999.

45. Hanus R., M. Kinnaert and J. L. Henrotte, "Conditioning Technique, a General Anti-Windup and Bumpless Transfer Method", *Automatica*, Vol. 23, No. 6, pp. 729-739, 1987.

46. Kolmanovsky, I., P. Moraal, M.van Nieuwstadt and A. Stefanopoulou, "Issues in Modeling and Control of Intake Flow in Variable Geometry Turbocharged Diesel Engines", *Proc. 18th IFIP Conferance on System Modeling Optimization*, Detroit, MI, July, 1997.

47. Gelb A., J. F. Kasper, R. A. Nash, C.F. Price C. F. and A. Sutherland, *Applied Optimal Estimation*, Cambridge, MA: MIT Press, 1974.

48. Garcia, R. A., M. I. Troparevsky and A. J. L Mancilla, "An Observer for Nonlinear Noisy Systems", *Lat. Am. Appl. Res.* 2000, Vol. 30, Issue 2, 1987.

49. Maybeck, P. S., *Stochastic Models, Estimation and Control*, London Academic Press, 1982.

50. Lewis, F. L., *Optimal estimation*, New York: Wiley, 1986.

51. Ljung, L.,"Asymptotic Behavior of the Extended Kalman Filter as a Parameter Estimator for Linear Systems", *IEEE Trans. Autom. Control*, Vol. 24, Issue 1, pp. 36-50, 1979.

52. Biagiola, S.I. and J. L. Figueroa, "State Estimation in Nonlinear Processes. Application to pH Process Control", I*nd. Eng. Chem. Res*, Vol. 41, pp. 4777-4785, 2002.

53. Kou, S. R., D. L. Elliott and T. J. Tarn, "Exponential Observers for Nonlinear Dynamic Systems", *Information and Control*, Vol. 29, pp. 393-428, 1975.

54. Baumann, W. T. and W. J. Rugh, "Feedback Control of Nonlinear Systems by Extended Linearization: The Multi-Input Case", *Proc. 7th Int. Symp. Math. Theory Networks Syst.*, Stockholm, Sweden, 1985.

55. Baumann, W. T. and W. J. Rugh, "Feedback Control of Nonlinear Systems by Extended Linearization", *IEEE Transactions on Automatic Control*, Vol. AC-31, pp. 40-46, Jan. 1986.

56. Zeitz, M., "The Extended Luenberger Observer for Nonlinear Systems", *Systems and Control Letters*, Vol. 9, pp. 149-156, 1987.

57. Keller, H., "Nonlinear Observer Design by Transformation into a Generalized Ob-

server Canonical Form", *International Journal of Control*, Vol. 46, No 6, pp. 1915-1930, 1987.

58. Arulampalam, S., S. Maskell, N. Gordon and T. Clapp, "A Tutorial on Particle Filters for on-line Nonlinear/non-Gaussian Bayesian tracking", *IEEE Transactions on Signal Processing*, Vol. 50, pp. 174-188, 2002.

59. Scardovi, L., M. Baglietto and T. Parisini, "Active State Estimation for Nonlinear Systems: A Neural Approximation Approach", *IEEE Transactions on Neural Networks*, Vol. 18, No. 4, pp. 1172-1184, July 2007.

60. Garrido S., L. Moreno and C. Balaguer, "State Estimation for Nonlinear Systems Using Restricted Genetic Optimization", *Lecture Notes In Computer Science*, Springer Berlin / Heidelberg, Vol. 1415, pp. 758-767, 1998.

61. Zhu, G. and L. Saydy, "An Extended Luenberger-Like Observer and its Application to Target Tracking", *AIAA Guidance, Navigation, and Control Conference and Exhibit*, San Francisco, California, August 15-18, 2005.

62. Pachecoa, R. P. and V. Steffen, "On the Identification of Nonlinear Mechanical Systems Using Orthogonal Functions", *International Journal of nonlinear Mechanics*, Vol. 39, Issue 7, pp. 1147-1159, 2004.

63. Song, S., J. S. Lim, S. Baek and K. M. Sung, "Gauss Newton Variable Forgetting Factor Recursive Least-Squares for Time-Varying Parameter Tracking", *Electronics Letters*, Vol. 36, No. 11, pp. 988-990, 2000.

64. Paleologu, C., J. Benesty and S. Ciochina, "A Robust Variable Forgetting Factor Recursive Least-Squares Algorithm for System Identification", *IEEE Signal Processing Letters*, Vol. 15, Issue 3, pp. 597-600, 2008.

65. Leung, S.H. and C. F. So, "Gradient-Based Variable Forgetting Factor RLS Algorithm in Time-Varying Environments", *IEEE Transactions on Signal Processing*,

Vol. 53, No. 8, pp. 3141-3150, 2005.

66. Yazdi, H. S., M. S. Yazdi and M. R. Mohammadi, "A Novel Forgetting Factor Recursive Least Square Algorithm Applied to the Human Motion Analysis", *International Journal of Applied Mathematics and Computer Sciences*, 5:2, pp. 128-135, 2009.

67. Quarterino A., Sacco R. and Saleri F. *"Numerical Mathematics"*, Texts in Applied Mathematics 37, Springer, 2000.

68. Datta, K.B. and B.M. Mohan, *Orthogonal Functions in System and Control*, Advanced Series in Electrical and Computer Engineering, World Scientific, Jun 1995.

69. Rump, S.M., *INTLAB - INTerval LABoratory*, In Tibor Csendes, editor, Developments in Reliable Computing, Kluwer Academic Publishers, Dordrecht, pp: 77-104, 1999.

70. Köse, İ. E. and F. Jabbari, "Control of LPV Systems with Partly-Measured Parameters, *IEEE Transactions on Automatic Control*, Vol. 44, No.3, pp. 658-664, 1999.

71. Boyd, S., L. E. Ghaoui, E. Feron and V. Balakrishnan, *Linear Matrix Inequalities in System and Control Theory*, Society for Industrial and Applied Mathematics (SIAM), Vol. 15, 1994.